UNIVERSITÀ
DEGLI STUDI
DI PADOVA

Università degli Studi di Padova

Dipartimento di Scienze Farmaceutiche

SCUOLA DI DOTTORATO DI RICERCA IN SCIENZE MOLECOLARI

INDIRIZZO IN SCIENZE FARMACEUTICHE

CICLO XXIV

SYNTHESIS AND BIOLOGICAL EVALUATION OF TECHNETIUM(III)-BASED RADIOPHARMACEUTICALS

Direttore della Scuola : Ch.mo Prof. Maurizio Casarin

Coordinatore d'indirizzo: Ch.ma Prof. Adriana Chilin

Supervisore :Ch.ma Prof. Maria Grazia Ferlin

Co-Supervisore: Dr. Cristina Bolzati.

Dottorando: Dr. Nicola Salvarese

CONTENTS

ABSTRACT

Development of new ^{99m}Tc and $^{186/188}$Re radiopharmaceuticals still remain an interesting research topic because of their almost ideal nuclear properties. ^{99m}Tc is the radioisotope of election for SPECT-imaging (E_γ=140 keV, $t_{1/2}$=6.02 h), while $^{186/188}$Re are radionuclides with an important therapeutic potential (^{186}Re: E_{β^-}=1.07 MeV, E_γ=137 keV, $t_{1/2}$=90.6 h; ^{188}Re: E_{β^-}=2.12 MeV, E_γ=155 keV, $t_{1/2}$=17 h). Compounds of both Tc and Re in the 3+ oxidation state are well known, however, the chemistry of Tc(III) and Re(III) applied to Nuclear Medicine is still relatively unexplored.

This study reports the synthesis and evaluation of a new class of stable, mixed hexacoordinated [^{99m}Tc^{III}(PS)$_2$(L)] complexes, where PS is a phosphinothiolate, and L is a dithiocarbamate. The asymmetric structure potentially allow a fine tuning of the biological and pharmacokinetical behavior of the final compounds through appropriate chemical modifications of the ligands; derivatizations of L can also be conjugated with a biologically active molecule in order to obtain target-specific radiolabeled compounds. A series of model complexes where M=Re,^{99g}Tc and PS=(diphenylphosphino)ethanethiolate (PS2) or 2-(diisopropylphosphino)ethanethiolate (PSiso) were firstly prepared and characterized. Then, four analogues ^{99m}Tc-radiolabeled complexes are prepared and biologically evaluated.

RIASSUNTO

Lo sviluppo di nuovi radiofarmaci a base di Tecnezio-99m e Renio-186/188 è ancora un campo attuale di ricerca, viste le caratteristiche ideali che questi radionuclidi presentano per l'*imaging* Medico Nucleare e per la Radioterapia.

Lo stato di ossidazione 3+ rappresenta uno dei più comuni e stabili stati di ossidazione del Renio e del Tecnezio. Tuttavia la chimica del Tc(III) e del Re(III) applicata alla Medicina Nucleare continua ad essere poco esplorata. Ciò è dovuto al fatto che la preparazione di tali complessi è generalmente condotta in solventi non acquosi e di conseguenza difficilmente applicabile alla produzione di radiofarmaci in condizioni idonee alla somministrazione nell'uomo. Gli unici esempi di agenti utilizzati in pratica clinica sono il ^{99m}Tc-Teboroxime (un complesso della classe BATO che era utilizzato per l'*imaging* cardiaco), e il complesso $[^{99m}Tc(HIDA)_2]^-$, tutt'oggi utilizzato per l'*imaging* della funzionalità epatobiliare (HIDA Scan).

Questo studio presenta la sintesi e la caratterizzazione di una nuova classe di composti del tecnezio e del renio allo stato di ossidazione III, aventi formula generale $[M^{III}(PS)_2(L)]$, dove PS = fosfinotiolato e L = ditiocarbammato.

E' stato effettuato dapprima uno studio a livello "macroscopico", di sintesi e caratterizzazione di complessi con gli isotopi $^{185/187}$Re e ^{99g}Tc.

Quindi, quattro analoghi radiocomplessi a base di ^{99m}Tc sono stati preparati e valutati nella loro stabilità e nel comportamento biodistributivo in ratti Sprague-Dawley sani.

1. INTRODUCTION

1.1 WHAT IS NUCLEAR MEDICINE?[1-4]

Nuclear medicine is branch of medicine and medical imaging that uses radionuclides and relies on the process of radioactive decay in the diagnosis and treatment of disease (radiotheraphy).

Diagnosis. The diagnostic part of the Nuclear Medicine (Diagnostic Nuclear Medicine) provides efficient techniques which represent important tools for Molecular Imaging. Molecular Imaging is a discipline that weds molecular biology and *in vivo* imaging: it allows the visualization of cellular function and the follow-up of molecular processes in living organisms, without perturbing them. Molecular imaging uses probes, most commonly known as *tracers*, to image tissues, organs or biochemical/physiological pathways. Tracers chemically interact with their surroundings, therefore the image is altered according to molecular changes occurring within the area of interest. This process is significantly different from other imaging methods, such as X-ray Imaging, Ultrasounds or Magnetic Resonance Imaging, which principally image differences in qualities such as density or water content. Molecular Imaging shows the physiological function of the system being investigated as opposed to traditional imaging, which displays only anatomical images. This ability to image fine molecular changes opens up an incredible number of stimulating possibilities for medical application, including early detection and treatment of disease, assessment the disease status and follow-up of the effect of a therapeutic treatment and basic pharmaceutical development. Thus, it is very easy to see that the potentialities of this field are several, particularly in medical diagnosis and treatment. Diagnostic Nuclear Medicine offers some of the most effective and powerful molecular imaging solutions and modalities. As mentioned above, it uses tracers containing a radionuclide γ- or β^+-emitter (*radiotracers*) whose radiation can be externally detected. Diagnostic Nuclear Medicine procedures involve systemically administration of a radiotracer at a very low concentration (nanomolar to

picomolar range), which is enough to get the radiation detected and, on the other hand, to avoid any pharmacological effect. The radiotracer is biodistributed depending on his physicochemical an biological characteristics, and the detector measures the activity from various organs and displays information in the form of images. While γ-emitters are used in the technique called SPECT (Single Photon Emission Computed Tomography), β^+-emitters are used for PET (Positron Emission Tomography). Both of them are well-established clinical imaging modalities that offer high-quality sensitivity in deep tissues. In SPECT, γ emissions directly from the radioisotopes are collected in a so-called gamma camera, which enables to reconstruct a picture of where the γ-rays originated (Figure 1A). The same thing basically happens in the PET modality (Figure 1B), but with an crucial difference: as the radioisotope undergoes decay, it emits a positrons that travel for a short distance and collide with electrons (their respective antiparticles); the annihilation process produces a pair of 511 keV γ-photons that move in almost the opposite direction (180°) to each other. As soon as they arrive at the circular array of detectors the photons are registered by PET and it is possible to determine their source along a straight line of coincidence. These coincidences are forwarded to the image processing unit to generate PET images via mathematical reconstruction procedures.

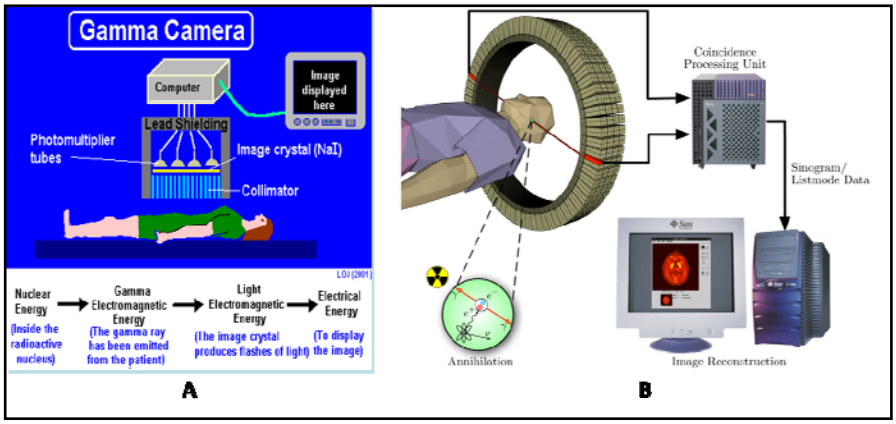

Figure 1: Scheme of a SPECT (A) and PET (B) acquisition process.

Therapy. Therapeutic Nuclear Medicine uses low penetration radiation (α, β and Auger electrons) to destroy diseased tissues, such as tumor tissues. The radiation mainly produces ionization of water molecules, generating highly reactive species that reacts with

biomolecules, eventually producing cell death. Therapeutic doses of radiation can be delivered to sites of disease in three ways: external beam irradiation, implantable *seeds* or systemic administration. The first form is the traditional and most common form of radiotherapy, and utilizes an external-generated radiation beam (kV or MV X-rays or MeV electron), which is pointed at a particular part of the body. Implantable *seeds*, which are radiation sources physically placed at the tumor site, are used in *brachytherapy*; it is only useful for the treatment of surgically accessible tumor mass. Systemic administration requires the use of therapeutic radiopharmaceuticals, which are molecules designed to deliver the therapeutic doses of ionizing radiation to specific diseased sites (a definition of "radiopharmaceutical" is given further below). Ideally, therapeutic radiopharmaceuticals should localize at the diseased site in sufficient concentration to deliver a cytotoxic radiation dose to the tumor cells, and clear rapidly from the blood and other normal organs to minimize radiation damage to normal tissues: this is why therapeutic agents used in radiotherapy often belong to the target-specific class (*vide infra*) and this is why their development is very challenging. With this features, therapy based on systemic-administered radiopharmaceuticals allows the treatment of multifocal or metastatic cancer. A wide variety of radionuclides are available for effective treatment of different tumor sizes. High energy β-emitters as ^{90}Y, ^{188}Re, ^{186}Re and ^{131}I have been intensively studied[5], but even low energy β-emitters, such as ^{177}Lu, ^{47}Sc, ^{67}Cu, ^{117}Sb, ^{117m}Sn, ^{167}Tm, ^{197}Hg, ^{195m}Pt and ^{199}Au, have been proposed for targeted radionuclide therapy of single tumor cells and micrometastases[6, 7].

Most of the radioisotopes actually used or proposed in Nuclear Medicine are metals, because they generally possess suitable nuclear properties, and for this reason basic research in this fields involve coordination chemistry. Many review articles on medical applications of radiometals are available, some of them have been already cited, and most of them cover specific aspects of metal complexes used in Nuclear Medicine including detailed structural data, labeling procedures and protocols, biodistribution data, etc.

On the other hand, the intent of this chapter is to get the reader just into some important notions necessary to understand what is the field this PhD project is focused on. For this reason, the following paragraphs briefly define what is a radiotracer and, in accordance to

the subject of this work, present an short overview of Technetium and Rhenium complexes used in (or proposed for) application in Nuclear Medicine.

1.2 RADIOPHARMACEUTICALS: DEFINITION AND CLASSIFICATION

Radiopharmaceuticals are pharmaceuticals combined with elemental radionuclides; could be coordination compounds (complexes in which the metal isotope is radioactive), organic small molecules (the radioisotope is part of the structure and covalently bound), simple inorganic compounds or salts. More rarely, they could be macromolecules such as peptides, monoclonal antibodies or fragments of them, which are labeled with a radionuclide. Although several important nonmetallic radionuclides (^{18}F, ^{11}C, ^{13}N, ^{15}O, ^{124}I, etc.) are widely used, metallic radionuclides are of particular interest for radiopharmaceutical development, because of their wider range of nuclear properties (half-life, decay characteristics, etc.), rich coordination chemistry, and easy availability. A perfect example of this statement is the huge success of ^{99m}Tc complexes for diagnostic purposes[1-4, 8], as discussed below.

Hence, a radiopharmaceutical is basically composed of two parts: the radionuclide and the non-radioactive part of the molecule, which many authors call “pharmaceutical”, even though this is somehow improper because not always it is a pharmaceutical in the strict sense of the word. Depending on the radionuclide emission characteristics, radiopharmaceuticals can be divided into two primary classes: diagnostics and therapeutics. They can also be classified according to their pharmacokinetical and pharmacodynamical properties, but the literature is not always consistent about this. Anyway, three commonly recognized categories of radiopharmaceuticals are:

1) the *essential radiotracers*, also known as *“metal-essential”* because basically all of them are metal complexes, whose biodistribution depends primarily on their physicochemical properties such as charge, size and lipophilicity; examples of this class of compounds are given further below;
2) the *metabolic markers*, which are able to integrate into specific metabolic pathways; the most famous examples of this class of compounds are ^{18}FDG and labeled fatty acids and they will not be discussed here;

3) the *target-specific radiopharmaceuticals*, whose biodistribution is determined by receptor binding or other biochemical interactions, by virtue of the chemical conjugation with molecular vectors such as a pharmacophore, a peptide, or even a protein, an antibody or an antibody fragment; nowadays, the direction of research in Nuclear Medicine has been mainly shifted towards the development of this type of compounds. The design of a target-specific radiotracer depends on many factors among which there are the chosen radionuclide and the characteristics of the molecular vector, and some examples are given further below.

1.3 TECHNETIUM AND ^{99m}Tc-BASED RADIOPHARMACEUTICALS

1.3.1 Technetium

More than 80% of the radiotracers used in diagnostic nuclear medicine are ^{99m}Tc-complexes or ^{99m}Tc-labeled biomolecules (pharmacophores, receptor ligands, small peptides and monoclonal antibodies or fragment of them). The great growth of Nuclear Medicine in the last three decades is, in large part, attributed to the successful development of ^{99m}Tc-based radiopharmaceuticals (both blood flow radiotracers and target-specific radiotracers). This is principally due to its ideal nuclear properties: pure monochromatic 140 keV γ-emission with 89% abundance, which is optimum for imaging with gamma cameras, and a 6 hour half-life, which is long enough to allow the centralized radiotracer preparation, distribution to local hospitals, administration and collection of clinically useful images, yet it is short enough to minimize the absorbed radiation dose to the patient. Furthermore, the rapid growth in this field over the last four decades is also attributable to the commercial availability of both ^{99}Mo/^{99m}Tc generators and kits (see below) for the routine preparation of ^{99m}Tc radiotracers in hospitals or centralized radiopharmacies. ^{99m}Tc is a generator-produced isotope from the decay of ^{99}Mo, a fission product of ^{235}U with a half-life of 2.78 days. In a typical ^{99}Mo/^{99m}Tc generator (Figure 2), $^{99}MoO_4^{2-}$ is absorbed to an alumina column and $^{99m}TcO_4^-$ is formed by the decay of ^{99}Mo. $^{99m}TcO_4^-$ is then eluted as sodium salt from the

column with saline. In 1959, Brookhaven National Laboratory developed the first $^{99}Mo/^{99m}Tc$ generator, which is an historical milestone in the field of Nuclear Medicine[9].

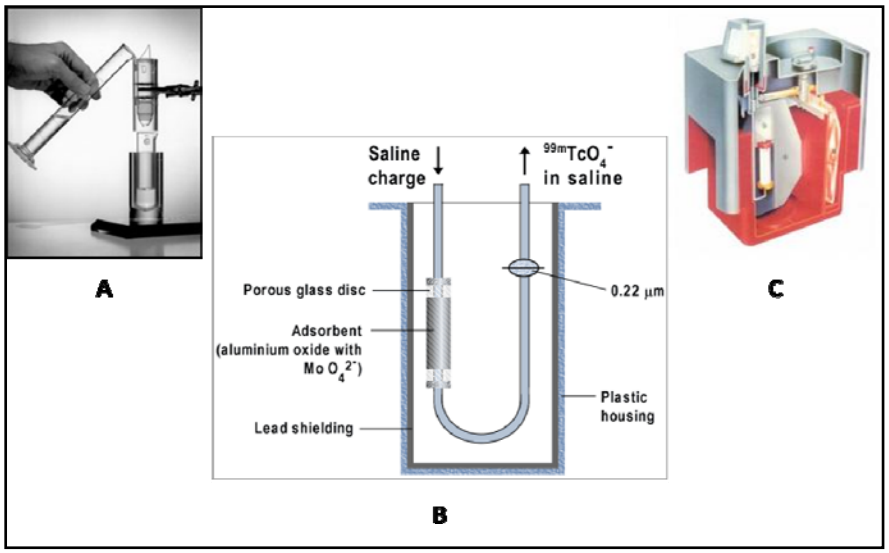

Figure 2: The ^{99m}Tc generator: A) an "homemade" version; B) scheme of a modern generator; C) section of the Elumatic III® generator by Iba.

1.3.2 Technetium complexes used as tracers in Diagnostic Nuclear Medicine[1-4, 8, 10-20].

Technetium is the element 43 of the Periodic Table (group 7, second row of the transition metals). It is an man-made element, hence the name derived from the Greek *τεχνητος*, literally meaning artificial. It has 21 isotopes, all of them are radioactive.

A number of recent, excellent review articles and book chapters cover the main aspects of technetium chemistry and radiopharmaceuticals developed in the last 25 years[1, 10-19]. Furthermore, an exhaustive review present an overview of the literature production until April 2009 relative to the most frequently ^{99m}Tc-labeled peptides under preclinical or clinical evaluation, along with an in-depth discussion of the most important aspects of the chemistry and the drug-designing involved in the evaluation of receptor-based ^{99m}Tc-tracers radiopharmaceutical[20]. In addition, IAEA (International Atomic Energy Agency) constantly provides publications about radiopharmaceuticals, including of course the ^{99m}Tc-based ones. They are obtainable on-line, free-of-charge, (www.iaea.org/publications).

One of the most important characteristics of technetium is its diverse redox chemistry: it has nine accessible oxidation states, each of them is characterized by its own coordination

chemistry, generating a large chemical diversity. Table 1 lists the oxidation states with some examples and the relative coordination geometry. Some oxidation states are particularly stabilized in frames called *cores*, in which the metal is strongly bound to an atom or a ligand to form a single unit with distinctive electronic and chemical characteristics.

Table 1

Oxidation State	Example	Geometry	Coordination Number
+7 (d^0)	$[TcH_9]^{2-}$ $[TcO_4]^-$	Tricrapt trigonal prismatic Tetrahedral	9 4
+6 (d^1)	$[TcO_4]^{2-}$	Tetrahedral	4
+5 (d^2)	$Tc[(diars)_2Cl_4]^+$ $[TcN(S_2CNEt_2)_2]$ $[TcN(Ph_2PCH_2CH_2S)_2]$	Dodecahedral Squared pyramid Trigonal bipyramid	8 5 5
+4 (d^3)	$[TcCl_6]^{2-}$	Octahedral	6
+3 (d^4)	$[TcCl(CDO)_3BCH_3]$	Octahedral	7
+2 (d^5)	$Tc[(diars)_2]$	Octahedral	6
+1 (d^6)	$[Tc(CNC(CH_3)_3)_6]^+$	Octahedral	6
0 (d^7)	$[Tc_2(CO)_{10}]^-$	Octahedral	6
-1 (d^8)	$[Tc(CO)_5]^-$	n.d.	5

The coordination chemistry of certain cores, such as $[Tc{=}O]^{3+}$ (oxotechentium(V)), $[TcO_2]^+$ (dioxotechentium(V)), $[Tc{\equiv}N]^{2+}$ (nitridotechnetium(V)), and $[Tc(NPh)]^{2+}$ (phenilimidotechnetium(V)) have proven to be very useful in radiopharmaceutical development and for this reason their coordination chemistry has been extensively studied; investigations have been improved by the use of the longer-lived, weak β-emitter isotope ^{99g}Tc (E_{β^-} = 292 keV, half-life = 2.12 x 10^5 yr), which is an isomer of ^{99m}Tc. In fact, it is not possible to structural characterize ^{99m}Tc-complexes since the amount of material that can be synthesized is very low (picomoles to nanomoles per preparation), because the ionizing and penetrating γ-radiation limits manipulations in adequate amount. This is a common issue in radiochemistry, and "cold" isotopes (or "less radioactive" as in the case of ^{99g}Tc) are used to prepare the corresponding complexes which are commonly taken as references for structural studies. Comparison between the well-characterized "cold" model and the

corresponding labeled compound is carried out by chromatography (HPLC): only in case the two species have the same retention time, they could be consider identical.

The first technetium radiopharmaceutical was the pertechnetate anion, $[^{99m}TcO_4]_2^-$, directly obtained as sodium salt in saline solution from the generator, which is used since 1961 for diagnosis of thyroid disease, based on the principle that the pertechnetate anion would behave similarly to iodide. The biodistribution and targeting ability thus depended solely on the size, and charge of the complex. This was the first of a series of the so-called "*technetium essential*", or first generation agents. Another given definition of first generation technetium radiopharmaceuticals is that they are simple ^{99m}Tc-labeled species that could measure basic physiological functions by means of non-substrate specific mechanisms. A number of such compounds were successfully developed principally for the imaging of liver, kidney, bones, heart and brain. Examples of technetium essential agents for imaging of the renal and hepatobilary excretion are the complexes with derivatives of aminoacetic acids. These ligands form negatively charged complexes with technetium, whose excretion pathway can readily be controlled by modifications of the molecular structure of the ligand. Thus, the highly hydrophilic technetium complex with DTPA (diethylenetriamine pentaacetic acid, Figure 3A) is excreted via the renal system, while the more lipophilic HIDA (N-(2,6-diethylacetanilido)iminodiacetic acid, Figure 3B) derivative is excreted *via* the hepatobiliary tract and is used for liver scintigraphy. The exact structure of these complexes is still unknown, despite many investigations and much speculation have been done. Studies carried over with ^{99g}Tc level evidenced some dimeric products, which contain the metal atoms in the oxidation states III, IV or V[21]. However, most probably the biologically active species have other, monomeric structures, since the concentration of generator-eluted ^{99m}Tc (about 10^{-10} mol/l) is too low for the formation of significant amounts of dimeric products. Despite the uncertainty of the structures of the ^{99m}Tc-DTPA and ^{99m}Tc-HIDA derivatives, they are in regular radiodiagnostic use and have been a commercial success for decades (Technescan® and HIDA-Scan®).

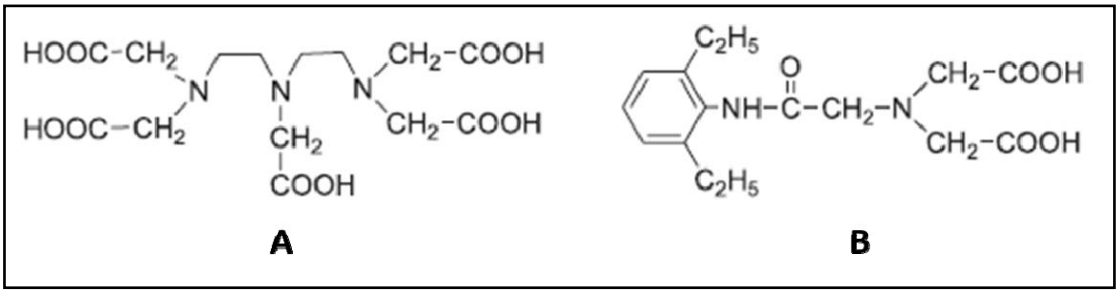

Figure 3: DTPA and HIDA ligands

Complexes of ^{99m}Tc with phosphonate ligands are widely used as diagnostic agents for the imaging of metastatic diseases in bones and bone infarction infections. One examples of routinely used tracers are the complexes with the ligands methylenediphosphonate (MDP), hydroxymethylenediphosphonate (HMDP), 1-hydroxyethylenediphosphonate (HEDP) and 1-hydroxy-4-aminobutylidene-1,1-diphosphonate (ABP) are in routine use. The exact chemical structures of these complexes is still unknown too, even though they are highly effective bone-imaging agents. The presence of uncoordinated phosphonate oxygen atoms allows a mechanism for absorption of the complexes on the surface of newly formed hydroxyapatite. With respect to this fact, such ^{99m}Tc complexes can act as ligands for exposed Ca^{2+} ions on the freshly formed hydroxylapatite during the formation of the mineral components of bone tissue. Many efforts have been done to understand the exact structure of technetium-phosphonates complexes, without obtaining conclusive results. Anyway, it appears quite sure that various polymeric compounds are formed depending on the pH and the concentration of ligands. The polymeric $[^{99g}Tc(OH)(MDP)]_\infty$ (Figure 4) is the only complexes which was isolated and characterized by X-ray crystallography. The compound was prepared by a ligand exchange procedure from the complex $[^{99g}Tc^{IV}Br_6]^{2-}$[22, 23].

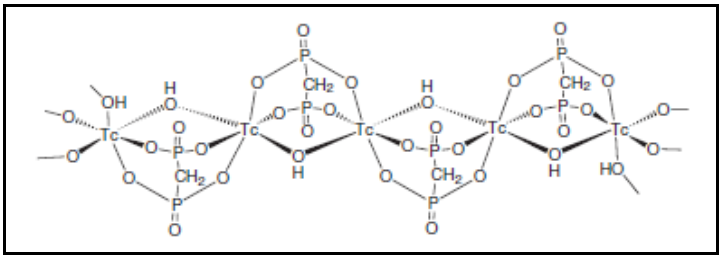

Figure 4: polymeric $[^{99g}Tc(OH)(MDP)]_\infty$ complex.

Second generation ^{99m}Tc radiopharmaceuticals mainly consisted of agents designed to analyze the perfusion in heart, brain or kidneys. Their development was based on rational studies involving structural characterizations (NMR spectroscopy, mass spectrometry, X-ray diffraction) of the corresponding ^{99g}Tc compounds, and evaluation of structural-activity relationships underlying the pharmacokinetical and biological behavior of the ^{99m}Tc agents, especially the *in vivo* localization. This does not means that the second generation tracers are target-specific, but they represent examples of *designed metal essential radiopharmaceuticals*. Early studies about structure-activity relationships suggested monocationic technetium complexes to be promising candidates for myocardial uptake. This was supported by studies on technetium(III) complexes with chelating bisphosphines and bisarsines. Complexes of the type $[TcCl_2(diars)_2]^+$ or $[TcCl_2(DMPE)_2]^+$ (diars = 1,2-bis(dimethylarsino)benzene; DMPE = 1,2-bis(dimethylphosphino)ethane) showed promising heart-uptake result in animal studies, but heart images in humans were poor and the retention rate of the complexes in the myocardium was low, which was assigned to a rapid reduction of the redox-labile compounds in the myocardial cells[(24)]. More successful were attempts with isocyanide complexes of Tc(I). Homoleptic, cationic complexes of the composition $[Tc(L)_6]^+$ are kinetically and redox stable. The d^6 electronic configuration avoids dissociative ligand loss or ligand transchelations in biological systems. The biological properties of such complexes have been optimized for heart uptake versus blood and organ clearance: an optimum was found when methoxyisobutylisocyanide (MIBI) was used as ligand[(25)] (Figure 5A). $[^{99m}Tc(MIBI)_6]^+$ (^{99m}Tc-sestamibi, Cardiolite®) is not uptaken by the myocytes *via* the Na^+/K^+ channels. The cation complex diffuses across the membranes, then it is retained in the cells by enzymatic cleavage of the ether functionalities. The success of ^{99m}Tc-sestamibi inspired the development of a number of other monocationic complexes with ether functionalities, such as the dioxotechnetium(V) $[^{99m}TcO_2(tetrofosmin)_2]^+$ (tetrofosmin = 1,2-bis[bis(2-ethoxyethyl)phosphinoethane), commercially known as Myoview®[(19)], which is largely used for myocardial imaging together with Cardiolite® (Figure 5B). In addition to the cationic complexes, some neutral compounds show significant myocardial uptake. One of them is the seven-coordinate technetium(III) chlatrochelate ($[^{99m}TcCl(CDO)\text{-}(CDOH)_2BMe]$, or ^{99m}Tc-teboroxime, Cardiotec®, Figure 5C), which belong to the BATO class (Boronic Acid Technetium Complexes) because three dioxime ligands are

connected by a boronic acid moiety. BATO complexes such as ^{99m}Tc-teboroxime can be considered as cationic complexes in their physiologically active form, because they readily exchange the anionic chloro ligand for a neutral aquo one (H_2O)[26]. Another neutral complex is the nitridotechnetium(V) ^{99m}Tc-NOET ([^{99m}Tc(N)(NOET)$_2$], NOET = N-ethyl-*N*-ethoxydithiocarbamate), Figure 5D)[27], which displayed an high hart uptake with a first pass hart extraction higher than that of Cardiolite® and Tetrofosmin®. Despite this, it has not become an approved radiotracer for myocardial perfusion imaging in patients. One more very interesting nitridotechnetium(V) complex, which actually is cationic, is ^{99m}Tc-DBODC5 ([^{99m}Tc(N)(PNP5)(DBODC)]$^+$, where PNP5 = *N*,*N*-bis[2-(bis(3-methoxypropyl)phosphino)ethyl]ethoxyethylamine) DBODC = *N*,*N*-bis(ethoxyethyl)dithiocarbamate), Figure 5E), developed by the same group of ^{99m}Tc-NOET[28]. Like the latter compound, this tracer has a nitrido core and a dithiocarbamate as a ligand, along with a neutral aminodiphosphine forming an asymmetrical cationic complex which displays a high hart uptake and a very fast and considerable liver clearance making it a tracer superior to Cardiolite® and Tetrofosmin®. Recent subcellular distribution studies have shown that it accumulates into mitochondria as a result of the interaction with the negative membrane potential, and this most likely is the reason of the high and persistent hart uptake[29]. ^{99m}Tc-DBODC5 is currently under clinical evaluation.

Besides cardiovascular imaging, brain imaging has become a major goal of ^{99m}Tc coordination chemistry. Second generation brain imaging tracers are used for perfusion imaging, while few recently developed third generation tracers are useful for the labeling of central nervous system (CNS) receptor ligands (*vide infra*). Brain perfusion imaging agents must penetrate the intact blood brain barrier by passive diffusion, so they basically be small (low molecular weight), neutral and lipophilic molecules. Furthermore, they preferably should undergo a trapping mechanism, such as protonation in the slightly more acidic brain tissue, or metabolic processes like ester hydrolysis or partial degradation in the brain. Generally, these phenomena help the retention of the compound in the brain tissue, avoiding the washout due to back-perfusion through the blood brain barrier. The latter two mechanisms are mainly used in the successfully tested brain imaging agents which are shown in Figure 6. All of them are five-coordinate oxotechnetium(V) complexes with tetradentate triply deprotonated chelators.

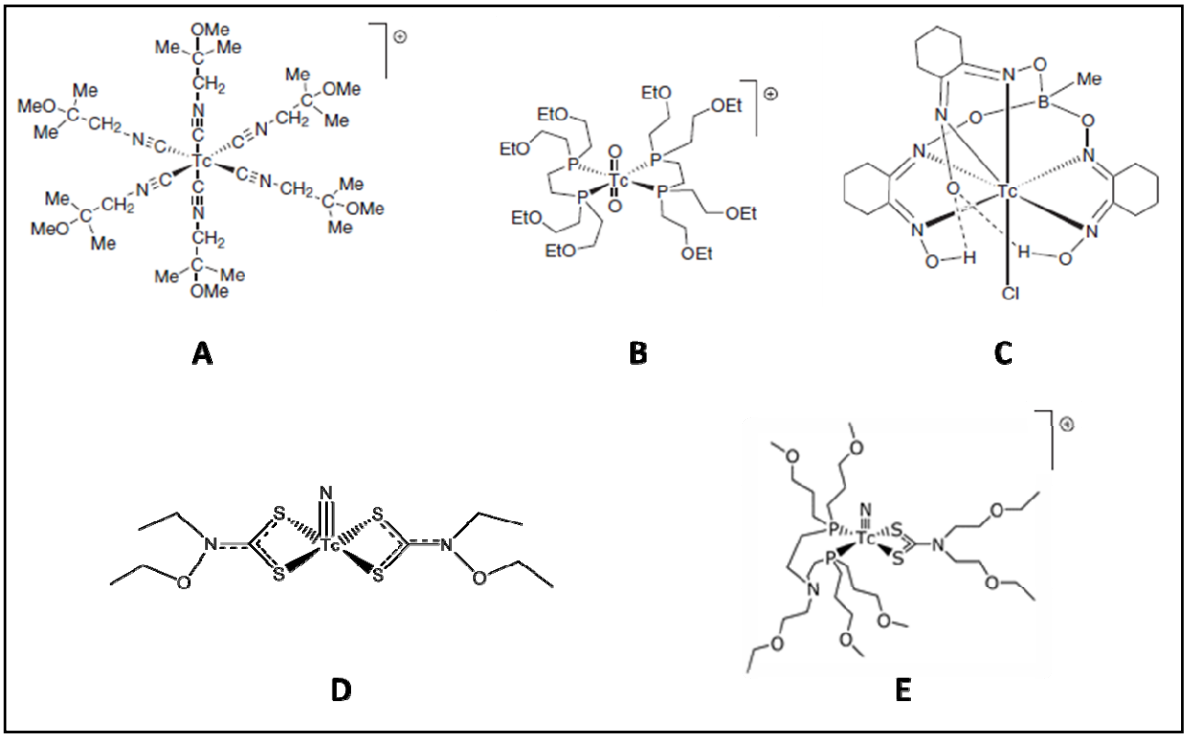

Figure 5: *technetium essential* radiotracer for cardiovascular imaging. A) ^{99m}Tc-sestamibi (Cardiolite®); B) [$^{99m}TcO_2$(tetrofosmin)$_2$]$^+$ (Tetrofosmin®, or Myoview®); ^{99m}Tc-teboroxime, Cardiotec® D) ^{99m}Tc-NOET; E) ^{99m}Tc-DBODC5

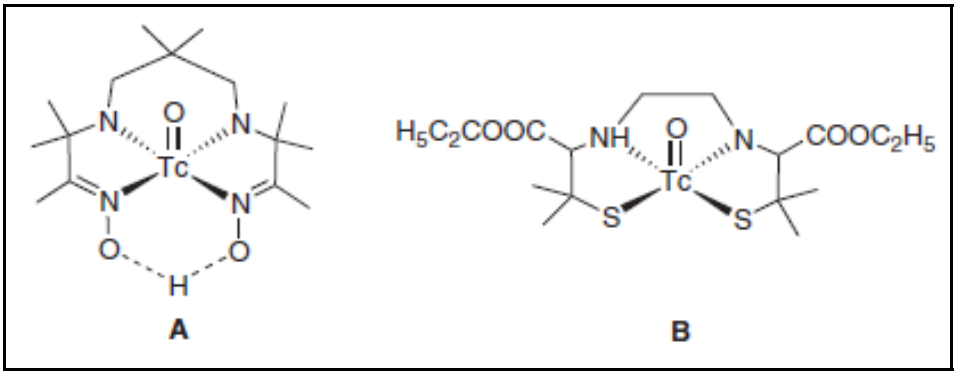

Figure 6: A) ^{99m}Tc-HMPAO (Ceretec®); B) ^{99m}Tc-ECD.

The complex with the dioxime ligand (RR,SS)-4,8-diaza-3,6,6,9-tetramethyl-undecane-2,10-dione dioxime (HMPAO, Figure 6A, commercially known as Ceretec®) is retained in the brain consequently to an enzymatic conversion into a more hydrophilic compound, which cannot re-penetrate the blood brain barrier. It is interesting to note that the HMPAO ligand has chiral centers and only its *d,l*-isomer leads to a technetium complex that is a suitable for clinical brain imaging. Complexes with the meso-form of the ligand are more resistant

against the enzymatic transformation, therefore, their re-distribution is much faster[30]. Another effective brain-imaging agent is the oxotechnetium(V) complex with the tetradentate diaminothiolate ligand ethylenecysteine ester dimer (ECD, Figure 6B)[31]. Only one of the two amino groups deprotonates during reactions with common $[TcO]^{3+}$ precursors giving the highly lipophilic technetium(V) complex, which is able to accumulate in the brain thanks to an *in vivo* hydrolysis of the ester side chains, which results in the formation of charged complexes which are trapped in the brain. The [^{99m}Tc(O)(ECD)] complex (Neurolite®) is particularly important for the evaluation of patients with ischemic strokes.

Finally, a first generation agent for the imaging of renal excretion is the ^{99m}Tc-MAG3 complex. It is an oxotechnetium(V) complex with the tetradentate peptide-like ligand mercaptoacetyltriglycine[32]. The carboxylic group of the complex is deprotonated at physiological pH making the compound monoanionic (Figure 7). After administration to the patient, the complex binds to a large extend to plasma proteins. These weak interactions allow excretion through tubular secretion and about 50% of the radioactivity is excreted after each blood pass through the kidneys[33]. For this excretion, the presence of a non-coordinated carboxylic group seems to be essential in order to be recognized by the corresponding receptors in the kidneys. The commercial introduction of the ^{99m}Tc-MAG3 kit has almost replaced the use of *o*-iodohippuran in diagnostic nuclear medicine.

The third generation technetium radiopharmaceuticals belong to the class of the *target-specific* compounds: they have, in their structure, a targeting moiety capable of deliver them by exploiting specific molecular interactions with certain molecular structures such as receptors or enzymes. The vector molecule could be a pharmacophore, a small peptide or even a monoclonal antibody or a fragment of it. ^{99m}Tc-TRODAT-1 is one of the first successful examples[34]. This technetium-labeled tropane is structurally derived from cocaine (Figure 8) which was conjugated with a chelating system suitable for the core $[^{99m}TcO]^{3+}$. TRODAT-1 is used for *in vivo* assessment of loss of dopamine neurons in Parkinson's disease due to its interaction with the post-synaptic dopamine transporter system in the brain[35].

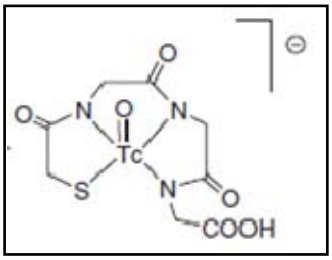

Figure 7: ^{99m}Tc-MAG3.

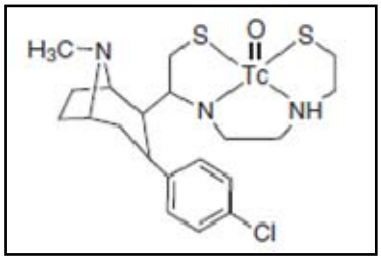

Figure 8: ^{99m}Tc-TRODAT-1.

Monoclonal antibodies and their fragments are also very adequate molecules for targeting pathologic processes such as tumors, infections, etc., both for diagnosis and therapy. ^{99m}Tc labeling was performed at the beginning by direct methods (*direct labeling*) by using either Sn(II) or mercaptoethanol to reduce the disulfide bonds to thiolate groups suitable for binding to technetium, probably as Tc(III) or Tc(V) complexes [29, 30]. This method is very simple and was successfully applied to different antibodies, some of which have reached clinical practice, for example Arcitumomab (CeaScan®) and Sulesumab (LeukoScan®), Fab' fragments of a murine monoclonal antibody directed against carcinoembryonic antigen, used for early diagnosis and monitoring of colorectal cancer[36, 37]. However, a disadvantage of this method is the lack of control over the labeling site with the risk of losing the inmunoreactivity of the resulting radiotracer. For this reason the development of new labeling strategies yielding pure and stable compounds of preserved bioactivity was required.

Indirect labeling using the so-called pendent approach[16] makes use of bifunctional chelating agents (BFCAs). A BFCA is a moiety that connects the biomolecule with a chelating unit for technetium through a linker (Figure 9); so, its structure comprises a donor atoms set able to chelating the metal or the metal core, and a functional group which allows to conjugate a biomolecule, through a linker if it is necessary. A linker is a moiety which effectively separates the metal complex and the biomolecule and serves to maintain the activity of the latter, minimizing the interaction with the metal complex. Actually, ^{99m}Tc-TRODAT-1 can be considered one of the results of this approach. Many other studies involving the $[^{99m}TcO]^{3+}$ core have been done. The BFCAs used with this core were always tetradentate with different, mixed hard/soft atom donor sets such as N_2S_2, (diamidedithiols, DADS; monoamidemonoaminedithiols, MAMA; diaminedithiols, DADT) and N_3S (triamidethiols, MAG3 like) (Figure 10)[20].

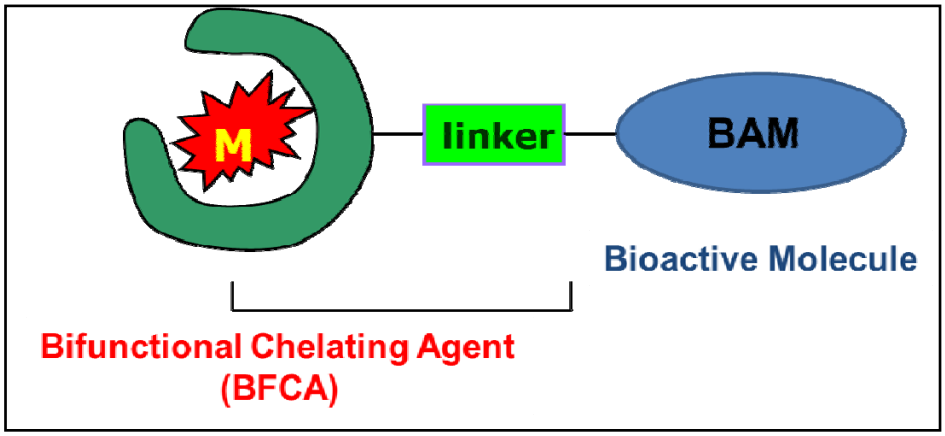

Figure 9: scheme of a target specific metal complex based on the BFCA approach.

The main limitation with the $[^{99m}TcO]^{3+}$/tetradentate BFCA-based systems is that the incorporation of a biomolecule into a tetradentate framework often requires complicated multi-step reactions and, once coordinated, such substituted chelates usually give rise to diastereoisomeric mixtures which might affect the biological properties of the resulting agent. In spite of this, the $N_xS_{(4-x)}$ system has been chosen in the development of a number of ^{99m}Tc-radiolabelled peptides and some of them, such as ^{99m}Tc-TRODAT-1, have been approved for clinical use. Other two examples are AcuTec® and NeoTect®, used for deep venous trombous detection and neuroendocrin $hSSTR_2$-positive tumor imaging respectively (Figure 11).

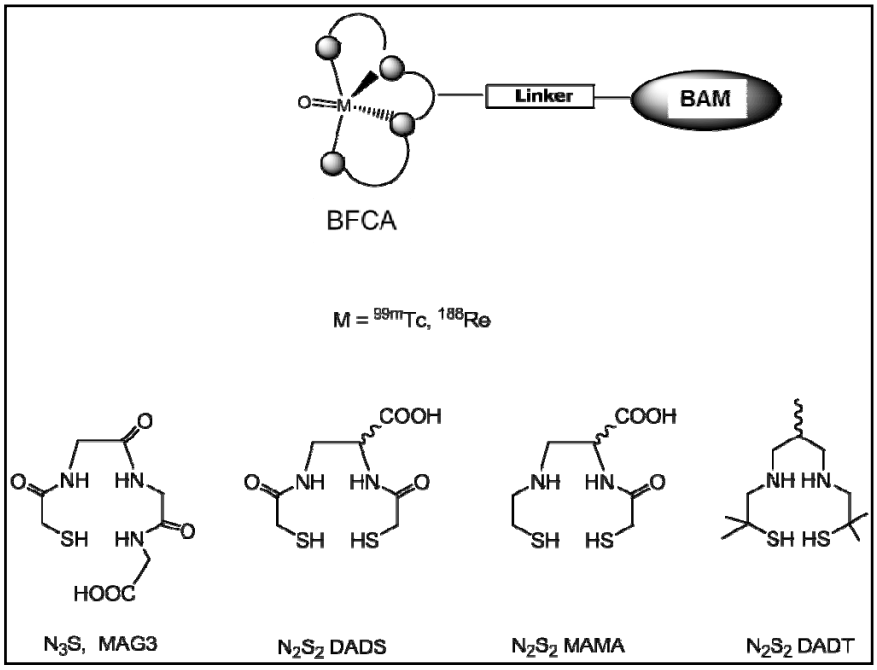

Figure 10: BFCA used in target specific technetium radiopharmaceuticals based on the core $[^{99m}TcO]^{3+}$.

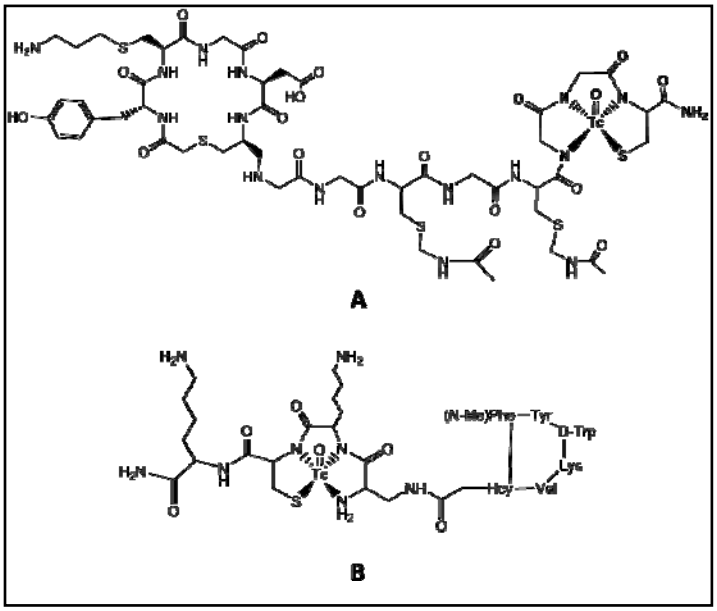

Figure 11: A) Structure of AcuTec®; B) Structure of NeoTect®.

In the modern indirect/BFCA approach, a crucial role is played by the *metal fragment* strategy, which is not only a way to accomplish a biomolecule labeling, but also and above all a fine chemistry concept. A *metal fragment* is a substitution-inert moiety comprising the metal (or a metal core) and a ligand. Together, they form a sort of "inorganic functional group" in which the metal core is strongly bound to the ligand, but the other coordination positions are usually spanned by weakly bound ligands (such as Cl or H_2O) that could be easily replaced by another incoming ligand carrying a specific set of donor atoms; in other words, those coordination positions are exchangeable and can be utilized to bind different suitable chelate ligands which, in this context, can be BFCAs conjugated with a chosen biomolecule (Figure 12). A complete paper describing the most used and interesting ^{99m}Tc-based metal fragments is (38), while (20) illustrates how this strategy has been used in the labeling of peptides (and biomolecules). Granted that none of the labeled biomolecules obtained so far has yet been approved for clinical use, and most of them are in preclinical phase, the principal currently employed metal fragments are three: ^{99m}Tc-tricarbonyl ($[^{99m}Tc^{I}(CO)_3]^+$)[1], ^{99m}Tc(N)-aminodiphosphine ($[^{99m}Tc^{V}(N)(PNP)]^{2+}$), and the so-called

[1] A commercial kit for the preparation of $[^{99m}Tc^{I}(CO)_3]^+$ (but also $[^{186/188}Re^{I}(CO)_3]^+$) in the form of $[^{99m}Tc^{I}(CO)_3(OH_2)_3]$, in which the three aquo ligands are easily exchangeable with other suitable ligands giving the final radiotracer, is available and known as IsoLink®.

"^{99m}Tc(III)-(4+1)" (Figure 13). Note that all of them are also used to develop technetium essential radiopharmaceuticals, such as ^{99m}Tc(N)-DBODC5.

In addition, [^{99m}Tc(HYNIC)]$^{+}$ (HYNIC = 6-Hydrazinopyridine-3-carboxylic acid, Figure 14) is also used; technically, it is different from the other metal fragments because the HYNIC moiety, to which the biomolecule is conjugated, strictly belongs to the metal core.

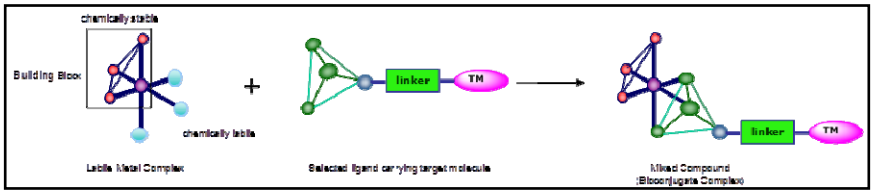

Figure 12: the metal fragment concept.

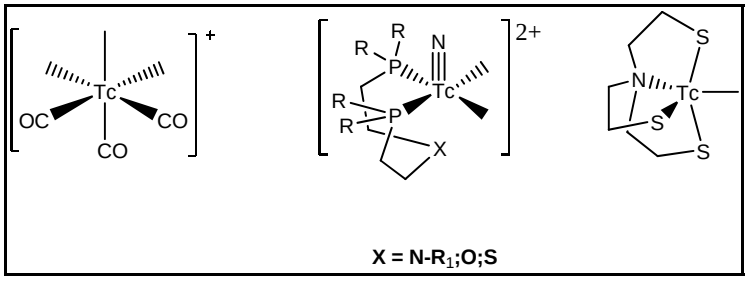

Figure 13: the three metal fragments [^{99m}Tc(CO)$_3$]$^{+}$, [^{99m}Tc(N)(PNP)]$^{2+}$ and ^{99m}Tc-(4 + 1).

1.3.3 One-pot synthesis, high radiochemical yields, high specific activities and kit formulation: basic requirements for application in Nuclear Medicine[(4)].

^{99m}Tc is obtained from the ^{99}Mo/^{99m}Tc generator as Na^{99m}TcO$_4$ in saline, so the synthesis of the tracer (whatever it is), has to be performed in aqueous solution. Little amounts of ethanol or DMSO could be allowed, but at low concentration. Due to its relatively short half-life (~6 h), the labeling should be completed within no more than 30-60 min. Furthermore, radiosynthesis has to be performed under sterile, pyrogen-free conditions, since almost all the ^{99m}Tc radiotracers are administered by intravenous injection. This specific need imposes any purification procedure to be avoided: the mixture should be injectable as it is at the completion of the reaction. Only a rapid quality control should be done to check the radiochemical purity of the final product, just before the administration. So, the final yield of the radiotracer (the so-called "*radiochemical yield*", or RCY) must be ≥ 90%, and the product

must be highly stable in the solution (preferably ≥ 6 h) because the injection of a mixture of ^{99m}Tc species will decrease organ specificity giving poor images. For all this reasons, a kit formulation is required.

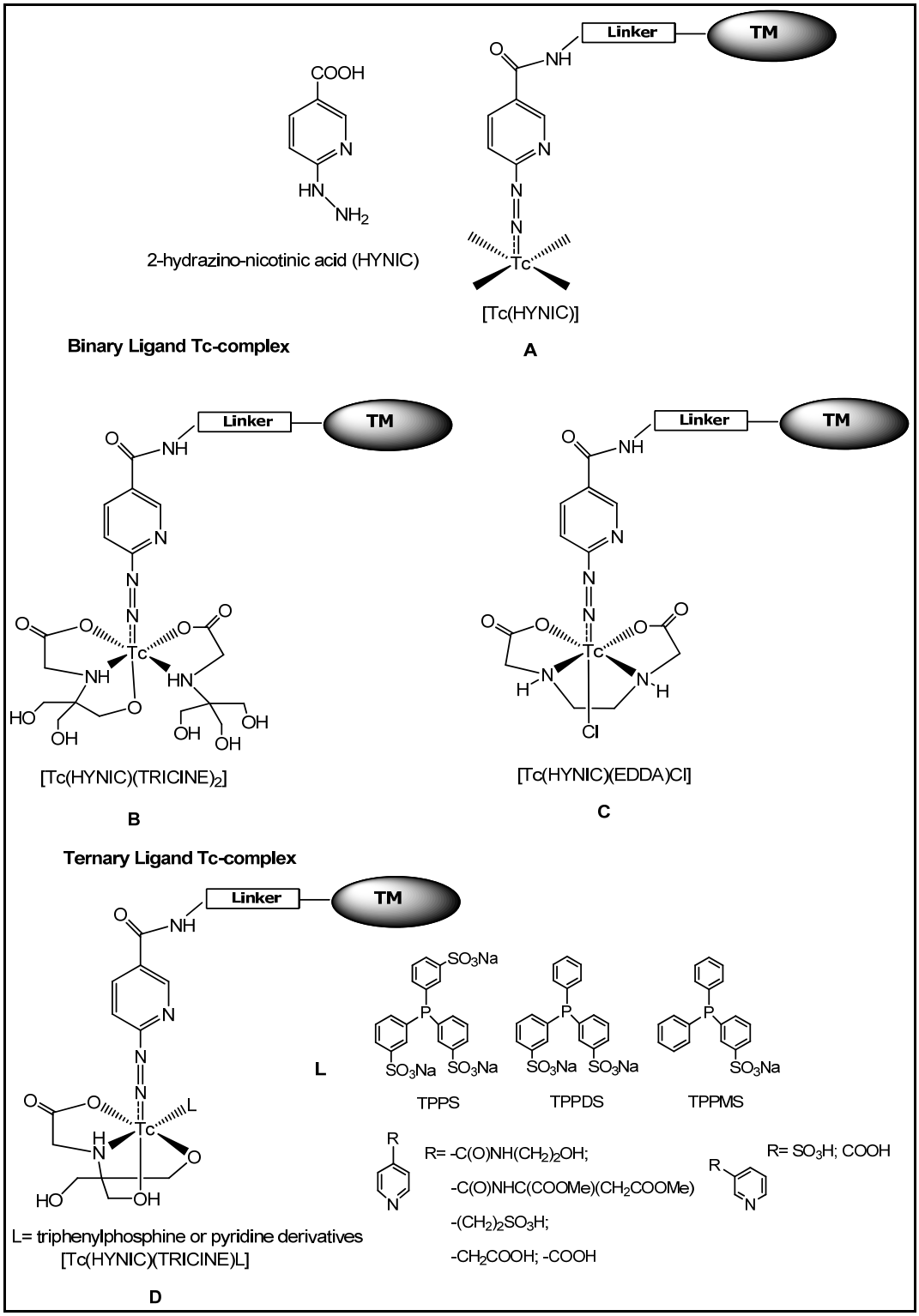

Figure 14: ^{99m}Tc-HYNIC core. HYNIC-containing chelating system.

The kits are sterile, pyrogen free, nonradioactive, lyophilized mixture stored under nitrogen in glass vials. For ^{99m}Tc radiotracers, a kit contains one or more ligands, a reducing agent and other constituents (buffering agents, antioxidant, solubilizing agent, weak transferring ligands, bulking agents, etc.) if needed. Obviously, all the components must be biocompatible and non-toxic.

A quick preparation of the tracer is attainable exploiting a one-pot synthesis. In the case of ^{99m}Tc, a one-pot synthesis is a single-step multi-component reaction involving $^{99m}TcO_4^-$, the reducing agent and ligands, performed at the tracer level (10^{-7}–10^{-6} M), in which pertechnetate is reduced by the reducing agent and, nearly simultaneously, the formation of multiple coordination bonds between the metal and the ligands occurs. The ^{99m}Tc-labeling should be accomplished by simply adding $^{99m}TcO_4^-$ into the formulation kit and heating the reaction mixture for a short period of time (preferably < 30 min), if needed. Of course the synthesis could also be accomplished in two or more steps, as long as the reaction is performed in a single vial and the reaction time is not too long, but a one-pot procedure is definitely the *optimum*. Of course, almost all of the above mentioned radiotracers are prepared according to these requirements, by means of suitable kits, and most of them are obtained through a one-pot synthesis.

In addition to all these requirements, the tracer should be produced in high specific activity. This means that a relatively low amount of ligands should be necessary to reach high radiochemical yields of the final compound. This requirement is very important in cases of target-specific radiopharmaceuticals, because the use of a large amount of the bioconjugated chelating agent causes the most of it to be non-radiolabeled at the end of the reaction: this may result in target site saturation as well as in unwanted pharmacological side effects, unless the final tracer undergoes a purification procedure, which is undesirable. For this reason, an ideal bioconjugated ligand should be used at very low concentration, between 10^{-4} – 10^{-6} M. A high specific activity could principally be achieved if: (i) the labeling reaction is performed under close to stoichiometric conditions; (ii) the unlabeled biomolecule is not active at all; or (iii) the cold unlabeled biomolecule remains bound to a solid resin and is automatically removed from the solution. Whereas the first approach is rather difficult to realize, some attempts for the second have been described in the literature. An example of the second approach is TRODAT for which the unlabeled CNS

receptor ligand does not cross the blood–brain barrier (BBB), hence, labeling can easily be performed at high concentrations. This is one of the very few exceptions of this strategy, and it is certainly not generally applicable. The third approach represents a wide and open field of challenging and promising research. A very limited number of papers appeared in the literature but none of them has been followed up further[39].

1.4 RHENIUM AND $^{186/188}$Re-BASED RADIOPHARMACEUTICALS

Together with technetium and manganese, rhenium belongs to the group 7 of the Periodic Table and is located in the third row of the transition metals. Naturally occurring rhenium is a mixture of ^{185}Re (37.4%), which is stable, and ^{187}Re (62.6%), which is unstable but has a very long half-life. There are 26 other recognized radioisotopes. ^{188}Re and ^{186}Re have become two of the most promising candidates for therapeutic applications in Nuclear Medicine due to their attractive nuclear properties (E_β max. = 2.12 and 1.1 MeV, $t_{1/2}$ = 17 h with a γ-emission of 155 keV (15 %) and $t_{1/2}$ = 90.64 h with a γ-emission of 137 keV (9.5 %) for ^{188}Re and ^{186}Re respectively), and the availability of ^{188}Re from a ^{188}W/^{188}Re radionuclide generator at carrier free levels[2]. Rhenium, as technetium's third row congener, exhibits many of the chemical properties of technetium. Furthermore, the lanthanide contraction, due to which the ionic radius of Tc and Re are almost equal, contributes to this chemical similarity. Consequently, Tc complexes and Re complexes with identical ligands have essentially identical coordination parameters, almost the same physicochemical properties and nearly the same biodistribution profiles. So, the studies of ^{99m}Tc complexes may be further expanded to the preparation of analogous rhenium compounds for therapy, leading to the paradigm of a *matched pair*, which means that the couple formed by a ^{99m}Tc-complex and the very same ^{186}Re- or ^{188}Re-complex can be used for diagnosis and therapy of the same disease (in other word, they can be used for *teragnostic* applications). Such a matched pair would be very attractive since it allows to perform dosimetry in advance and to follow how the diseased tissue respond to the cure, two very important points for the clinical decision process. Anyway, the ability to determine rhenium isotope dosimetry from technetium images is diminished in importance by the imageable γ-emissions of both ^{186}Re

and ^{188}Re. These emissions offer a further advantage of rhenium compared to other radionuclides such as ^{90}Y and ^{32}P, which have no imageable photons. In addition, although technetium and rhenium share many similarities in chemistry, they are not identical and careful validation of each pair is required; common chemical methods employed for the preparation of ^{99m}Tc radiopharmaceuticals starting from $[^{99m}TcO_4]^-$ can be easily transferred to the production of the corresponding $^{186/188}$Re radiopharmaceuticals starting from $[^{186/188}ReO4]^-$ in only a very limited number of cases. A major issue in transferring a chemical procedure from technetium to rhenium arises from the significant difference between the standard reduction potentials (E°) of these two metals. On the average, E° of redox reactions involving rhenium compounds is approximately 200 mV lower than that of the corresponding reactions carried out with technetium[40]. Therefore, rhenium is much more difficult to reduce an easier to oxidize (and re-oxidize). In addition, rhenium is more kinetically inert than technetium. These facts strongly limit the possibility to obtain $^{186/188}$Re radiopharmaceuticals in high yield using standard radiopharmaceutical procedures[41]. Despite this, an intensive research has been done and is still ongoing in order to obtain suitable and useful radiotherapeutic rhenium complexes and to achieve the matched pair. Recently, simple and efficient procedures for the preparation, in mild conditions, of ^{188}Re-complexes in intermediate/high oxidation states III/V from generator produced $Na[^{188}Re^{VII}O_4]$ have been proposed. These procedures differ from the commonly applied methods for the reduction of the $[^{188}Re^{VII}O_4]^-$ by the presence of additional reagents such as EDTA or oxalate anion[42-44]. The *EDTA-method* is based on the formation of $^{188}Re^{III}$-EDTA precursor, which easily undergo to an oxidative process allowing the preparation of various ^{188}Re-complexes in high oxidation states through a combined ligand exchange/re-oxidation reaction of $^{188}Re^{III}$-EDTA with suitable ligands[45-46]. The *oxalate-method*, inspired by a basic principle of inorganic chemistry called *expansion of the coordinating sphere*, is based on the addition of oxalate ions to a radiopharmaceutical preparation which, inducing a significant decrease in the standard reduction potential of the $[^{188}ReO_4]^-$ ion, changes the reaction mechanism[44]. This approach was also utilized to develop the first efficient procedure for producing the $[^{188}Re{\equiv}N]^{2+}$ core from $[^{188}ReO_4]^-$, under physiological conditions, and successfully applied in the preparation of stable symmetrical bis-substitute ^{188}Re(N)-complexes[47].

None of the rhenium complexes developed to date has yet been approved. Anyway, intensive studies has been done especially for the development of bone pain palliation agents, hepatocellular carcinoma and, more currently, of target-specific agents for anticancer radiotherapy (antibodies and peptides).

Patients with bone metastases suffer intense pain, which cannot be controlled by the use of either conventional analgesics or opioids. The administration of a radiopharmaceutical that selectively accumulate in bone metastases, providing a high local dose of low penetration β-radiation with minor irradiation of surrounding tissue, has found to be useful for pain palliation[48-51]. Among the evaluated rhenium radiocomplexes, surely the most important are $^{186/188}$Re-HEDP, (HEDP = hydroxyethylidene diphosphonate), which structure is not defined (and this is one of the reason why it was never been approved), and ^{186}Re/^{188}Re(V)-DMSA, or [$^{186/188}$Re(O)(DMSA)$_2$] (DMSA = meso-2,3-dimercaptosuccinic acid).

Hepatocellular carcinoma is a very frequent cancer with extremely high incidence in some countries of Asia and Africa. The radiopharmaceutical of election for this disease is ^{131}I-lipiodol[2], but it has the disadvantage of a very high emission which require the patient to be isolated for several days. ^{188}Rhenium-lipiodol can be synthesized[52], but the method is long and difficult. An alternative approach has been to prepare a ^{188}Re-sulphur colloid that is lipophilic enough to form a suspension in lipiodol; ^{188}Re-sulphur-lipiodol showed good retention in the liver cancer of animal models.

Another strategy is to prepare a well-defined lipophilic rhenium complex and dissolve it in lipiodol. Following this method, ^{188}Re(III)-SSS-lipiodol (^{188}Re(III)-SSS = [^{188}Re^{III}(S_3CPh)$_2$(S_2CPh)], see the Aim section for further discussion and figures) was prepared in high yields and showed very weak urinary elimination. Furthermore, the biodistribution in healhy pigs was close to that of 131I-lipiodol in humans, and in vivo studies with hepatoma bearing rats have also shown promising results[53]. A similar rationale was used in the development of ^{188}Re(V)-HDD-lipiodol (HDD = 4-hexadecyl-1,2,9,9- tetramethyl-4,7-diaza-1,10-decanethiol)[54]. The long alkyl chains were introduced in the metal–chelate moiety to create good hydrophobic interactions with lipiodol. ^{188}Rhenium(V)-HDD-lipiodol has been tested in patients, with promising preliminary results, but the labeling yields are low when compared with ^{188}Re(III)-

[2] Lipiodol is a iodinated poppy seed oil.

SSS-lipiodol, which may be a restricting factor for the synthesis of high therapeutic activities, and a significant urinary excretion has been observed[55]. A sharp improvement of this approach for labelling lipiodol was obtained through the introduction of the rhenium(V) nitrido bis(diethylthiocarbamate)complex ^{188}Re(V)-N-DEDC[47]. This compound can be prepared in very high yield using a lyophilized kit formulation, and exhibits a strong lipophilic character. It is, therefore, quantitatively extracted and tightly retained by lipiodol. The resulting ^{188}Re(V)-N-DEDC-lipiodol was investigated in a number of patients with hepatoma. The results showed that ^{188}Re(V)-N-DEDC-lipiodol is stable in vivo and is selectively accumulated in the tumour without any significant uptake in non-target tissues such as lungs, spleen and kidneys. This compound may, therefore, provide safe and effective therapy of unresectable hepatocellular carcinoma, either alone or in combination with transarterial chemoembolization[56].

Of course, even in the case of rhenium-based radiotherapeuticals, current studies are addressed to develop potential target specific agents. The above mentioned chemical similarities with technetium drive to explore basically the same strategies and metal fragments. In spite of different labeling technologies have been developed to prepare Tc-labeled biomolecules, and in principle all could be applied to the preparation of $^{186/188}$Re-analogues, only a limitate number of studies were reported and most of them are based on the bifunctional approach which employ tetradentate chelators (N_3S, N_2S_2, N_4) while the application of the other cores (HYNIC, $[^{188}Re(CO)_3]^+$, $[^{188}Re(N)(PNP)]^{2+}$, "^{188}Re-(4+1)") has not yet fully examined. Using $^{186/188}$Re, important criteria for any practical useful method in radiolabeling peptides are simplicity, label stability, and high specific radioactivity. Among the methods the use of MAG3 chelate seems to satisfy these criteria but only when the selected biomolecules (*i.e.* peptides) can resist to the high temperatures employed for labeling. For heat-sensitive biomolecules such as antibodies, complicate preconjugation labeling has to be used. The N_2S_2 chelators used for $[Re(V)=O]^{3+}$ core labeling and some tridentate chelators used for $[^{188}Re(CO)_3]^+$ building block labeling provided high radiochemical yields but the specific activities were low and heating still required. N_4 chelators and HYNIC seem to be not good ligands for ^{188}Re probably due to the loss of their chelating ability under strong acidic condition and/or the reoxidation of ^{188}Re-reduced to $[^{188}ReO_4]^-$ after chelation. With regard to $[M(N)(PNP)]^{2+}$ technology, it has been only recently

applied to the preparation, in high yield, of stable [^{188}Re(N)(PNP)]-based compounds [291, 292]. Nevertheless its application in synthesizing ^{188}Re(N)-labeled receptor-targeting radiopharmaceuticals has not yet been reported.

2. AIM

As discussed in the Introduction chapter, the stablest oxidation states of technetium and rhenium are I, III, V and VII and, to date, I and V are the most successfully employed in the development of radiopharmaceuticals, especially in the form of $[M^{I}(CO)_3]^+$ fragment and $[M^{V}=O]^{3+}$/$[O=M^{V}=O]^+$ and $[M^{V}\equiv N]^{2+}$ cores (M = ^{99m}Tc, $^{186/188}$Re). The commercial availability of a kit for the preparation of $[M^{I}(CO)_3]^+$ (IsoLink®), and the ease of preparation of the oxo and nitride cores have given a great contribution to the spread of their use. This statement is surely valid for ^{99m}Tc, whereas only a limited number of studies involving $^{186/188}$Re were reported.

^{99m}Tc(III) radiopharmaceuticals have been designed and clinically used (e.g. Teboroxime® and HIDA Scan®, see Introduction), and the relatively recent "M(III)-(4+1)" fragment is employed as a platform, but definitely less than $[M^{I}(CO)_3]^+$ or $[M^{V}=O]^{3+}$- and $[M^{V}\equiv N]^{2+}$-based systems. Nevertheless, a fair number of ^{99g}Tc(III) and "cold" $^{185/187}$Re(III) complexes are reported in literature, and represent models for potentially useful radiopharmaceuticals. These compounds show coordination number 5 with a trigonal-bipiramidal (tbp) geometry, or 6 with an octahedral environment or, in very few cases, distorted trigonal prismatic arrangement. The most common atom donor is sulphur, often supported by other atoms such as nitrogen, oxygen and/or phosphorus, and less frequently by other sulphur atoms[11-14].

Recently, rare examples of S_6 coordination sphere complexes ("sulfur rich") of the type $[M^{III}(R\text{-}PhCS_3)_2(R\text{-}PhCS_2)]$ and $[M^{III}(R\text{-}PhCS_3)_2(Et_2NCS_2)]$ have been presented[57] (Figure 15), and two of them are under evaluation as lymphocytes labeling agent for inflammation/infection imaging ($[^{99m}Tc(PhCS_3)_2(PhCS_2)]$)[58] and hepatocellular carcinoma radiotherapy ($[^{188}Re(PhCS_3)_2(PhCS_2)]$-lipiodol)[53].

Mevellec et al. and, later, Lepareur at al., highlighted that these compounds possess effective similarities, from the structural and electronic point of view, with other M(III)

complexes such as $[^{99g}Tc^{III}\{Ph_2P(C_6H_4S\text{-}o\}_3]$[59] and $[^{99g}Tc^{III}\{Ph_2P(C_6H_4NH\text{-}o\}_2\{Ph_2P(C_6H_4NH_2\text{-}o\}]$[60], although they exhibit different coordination spheres (S_6 vs P_3S_3 vs P_3N_3).

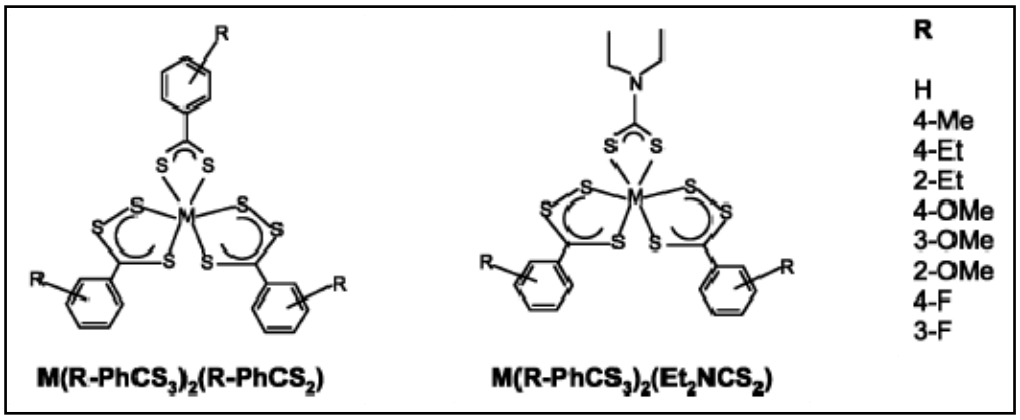

Figure 15: $[M^{III}(R\text{-}PhCS_3)_2(R\text{-}PhCS_2)]$ and $[M^{III}(R\text{-}PhCS_3)_2(Et_2NCS_2)]$ complexes.

By utilizing the octahedral description sketched in Figure 16, all the structures display two identical ligands providing two apical trans-positioned π-acceptor donors ($S_{thiourea}$ or P), connected with two strong cis-positioned σ-donors ($S_{thiolate}$ or N); this configuration seems to strongly affect the bonding of the third bidentate ligand, which could be chemically different from the others (dithiobenzoate or dithiocarbamate, another phosphinotiolate or a protonated phosphinoamine): in fact, the bond lengths are significantly longer than those reported for the other bonds in the coordination sphere (see the table in Figure 16).

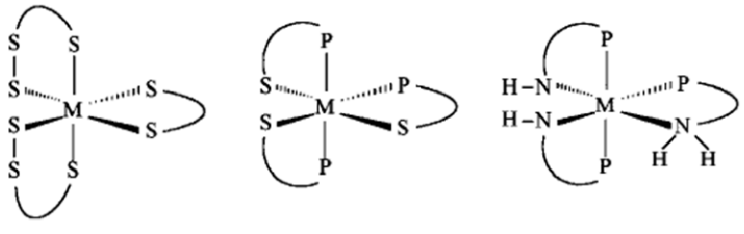

1		2		3		4		5	
Tc-S(1)	2.349(4)	Tc-S(1)	2.344(1)	Re-S(1)	2.385(5)	Tc-P(1),	2.477(1)	Tc-P(1),	2.483(2)
Tc-S(2)	2.231(4)	Tc-S(2)	2.221(2)	Re-S(2)	2.237(5)	Tc-S(1)	2.489(2)	Tc-N(1)	2.048(5)
Tc-S(4)	2.354(4)	Tc-S(4)	2.346(1)	Re-S(4)	2.365(5)	Tc-P(2),	2.406(1)	Tc-P(2),	2.430(2)
Tc-S(5)	2.227(4)	Tc-S(5)	2.233(1)	Re-S(5)	2.240(5)	Tc-S(2)	2.258(1)	Tc-N(2)	1.948(5)
Tc-S(7)	2.510(4)	Tc-S(7)	2.508(2)	Re-S(7)	2.527(5)	Tc-P(3),	2.424(1)	Tc-P(3),	2.436(2)
Tc-S(8)	2.478(5)	Tc-S(8)	2.497(2)	Re-S(8)	2.513(5)	Tc-S(3)	2.297(1)	Tc-N(3)	1.979(5)

Figure 16

It appears that the particular combination of σ-donor and π-acceptor atoms around the coordinating metal center constitutes very stable moieties ($[M(S_4)]^+$, $[M(P_2S_2)]^+$ and $[M(P_2N_2]^+$) whose arrangement tends to drive the system toward the tbp geometry. The latter occurrence is what actually happens in the case of another related complex, $[Re^{III}(\kappa P,\kappa S\text{-}Ph_2PC_2H_4S)_2(\kappa S\text{-}Ph_2PC_2H_4S)]$[62] (figure 17). In this compound the three ligands are phosphinothiolates analogous to those of the complex $[^{99g}Tc^{III}\{Ph_2P(C_6H_4S\text{-}o\}_3]$, but having the S and the P atoms connected by an alkyl chain (ethylene) instead of being *o*-positioned in an aromatic ring; this difference makes the complex show a pentacoordinated tbp geometry, displaying a $[M(P_2S_2)]^+$ moiety and the third phosphinothiolate bound to the metal as a monodentate thiolate. The analogue Tc(III) complex $[^{99g}Tc^{III}(\kappa P,\kappa S\text{-}Ph_2PC_2H_4S)_2(\kappa S\text{-}Ph_2P(O)C_2H_4S)]$[63] exhibits the same structure.

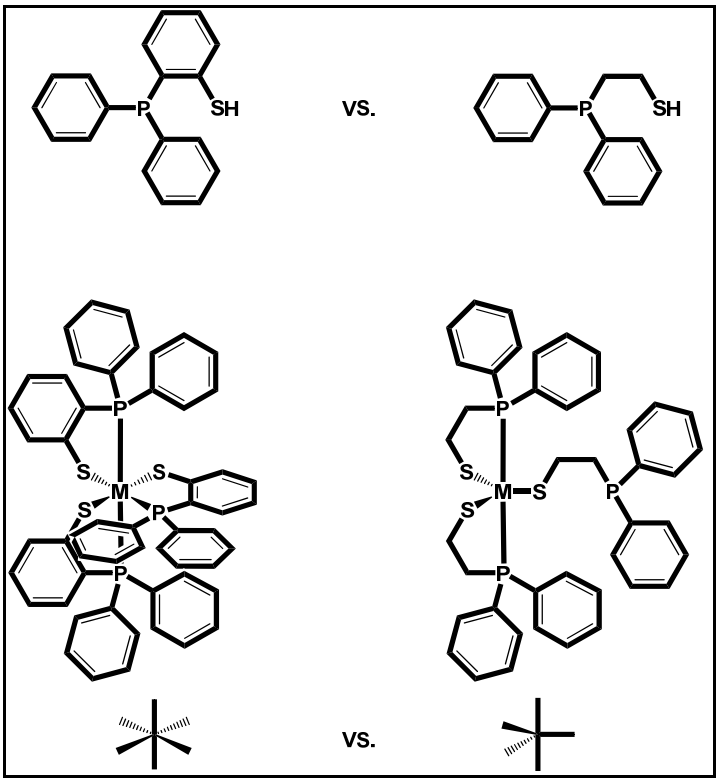

Figure 17: octahedral versus trigonal bipyramidal geometry in two related phosphinothiolate Re/Tc-complexes.

This behavior could be ascribed to the lack of π-electronic conjugation within the alkyl-phosphinothiolate, whereas only if the third ligand is able to delocalize electron density *via* π-orbitals the system can evolve to the distorted octahedral geometry. In this case, the

expansion of the coordination number is balanced by the lengthening of the bonds of the third bidentate ligand[57b-c].

Accordingly, it should be possible to obtain hexacoordinated octahedral complexes based on the highly stable $[M^{III}(\kappa P,\kappa S\text{-}Ph_2PC_2H_4S)_2]^+$ moiety using a third π-conjugated bidentate ligand, such as a dithiocarbamate. These type of mixed complexes have not yet been reported, even though Dilworth et al. obtained and described the analogue $[Re^{III}\{PPh_2(C_6H_4S\text{-}o)\}_2(S_2CNEt_2)]\cdot Me_2CO$[63] (Figure 18); anyway, in the latter complex the phosphinothiolate ligands $Ph_2P(C_6H_4S\text{-}o)^-$ instead of $Ph_2PC_2H_4S^-$, and still today it remains an isolated example of a potentially wider class of M(III) complexes.

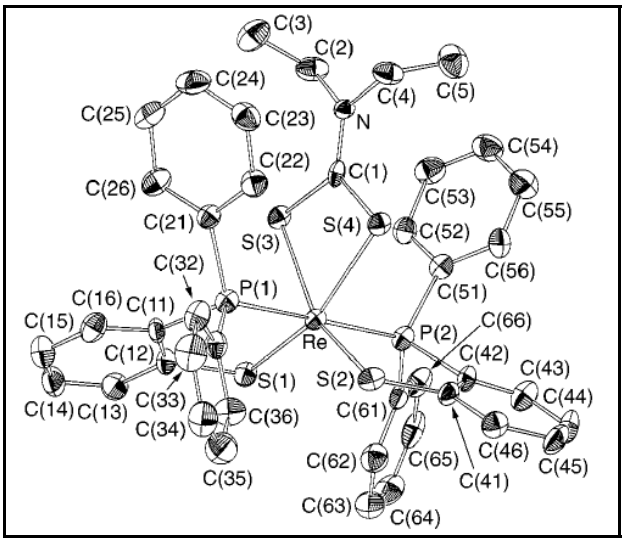

Figure 18: structure of the complex $[Re^{III}\{PPh_2(C_6H_4S\text{-}o)\}_2(S_2CNEt_2)]\cdot Me_2CO$

Our interest in this type of complexes is based on some considerations. The asymmetric structure of these complexes could allow a good modulation of their own physicochemical properties through appropriate modifications of the ligands and, in addition, derivatizations of L can be used to introduce a biologically active molecule, giving the possibility to obtain target specific radiolabeled compounds. From this point of view, dithiocarbamates were initially chosen because they have demonstrated their ability to bind similar moieties such as $[M(PhCS_3)_2]^+$ (M = ^{99g}Tc, ^{99m}Tc, $^{185/187}$Re) and $[Re^{III}\{PPh_2(C_6H_4S\text{-}o)\}_2]^+$ (see above) and they are easily obtainable. Finally, it is definitely worth exploring and evaluating new technetium- and rhenium-based building blocks, because they might be useful for the development of novel

radiopharmaceuticals, increasing the opportunities in labeling procedures and offering solutions which are not immediately obvious right now. In this wider perspective, this work moves the first steps toward the use of the here proposed $[M^{III}(PS)_2]$- moiety as an alternative metal fragment.

Thus, new mixed hexacoordinated M(III) complexes of the type $[M^{III}(PS)_2(L)]$, where M = Re, ^{99g}Tc, PS = 2-(diphenylphosphino)ethanethiolate ($Ph_2PC_2H_4S^-$, from now on indicated as PS2), 2-(dicyclohexylphosphino)ethanethiolate ($Cy_2PC_2H_4S^-$, PScy) or 2-(diisopropylphosphino)ethanethiolate (i-$Pr_2PC_2H_4S^-$, PSiso) and L = dithiocarbamate, have been prepared and fully characterized. The use of diverse phosphinothiolates (with phenyl- and aryl- substituents at the phosphorus) and dithiocarbamates is reported. Then, four selected ^{99m}Tc-analogues have been prepared and evaluated in order to verify if radiocomplexes of the type $[^{99m}Tc^{III}(PS)_2(L)]$ could be obtained through a one-pot labeling procedure, and to assess their stability in physiological conditions and *in vivo* biodistribution in healthy Sprague Dawley rats.

3. EXPERIMENTAL

3.1 MATERIALS AND METHODS

3.1.1 REAGENTS AND SOLVENTS

All the common reagents and solvents for reactions were purchased from Aldrich Chemicals (Milan, Italy) as reagent grade products, and were used as such without further purification, as well as deuterated solvents for NMR analysis, carbon disulfide, ammonium pyrrolidinedithiocarbamate (NH_4L1), $[Re^{V}(O)Cl3(PPh3)_2$ and tetrabutylammonium perrhenate ($[NBu_4][ReO_4]$). Sodium 4-(2-methoxyphenyl)piperazine-1-dithiocarbamate (NaL4), sodium 2-(4-(2-methoxyphenyl)piperazin-1-yl)ethyldithiocarbamate (NaL5) and 4-(4-(2-methoxyphenyl)piperazin-1-yl)butyldithiocarbamate (NaL6) were prepared using published procedures[64]. 2-(Diphenylphosphino)ethanethiol (PS2H), 2-(dicycloesylphosphino)ethanethiol (PScyH) and 2-(diisopropylphosphino)ethanethiol (PSisoH) were purchased from Argus Chemicals (Prato, Italy) and stored under nitrogen because of their air-sensitivity. $[Re^{III}Cl_3(MeCN)(PPh_3)_2]$ and $[^{99g}TcCl_3(MeCN)(PPh_3)_2]$ were prepared following the reported methods[65]. Ammonium pertechnetate ($[NH_4][^{99g}TcO_4]$) was obtained from Oak Ridge National Laboratory and purified from the black contaminant ($^{99g}TcO_2 \cdot nH_2O$) by addition of H_2O_2 (30%, w/w in water) and aqueous ammonia at 80 °C, followed by recrystallization from hot water. Solid samples of purified ammonium pertechnetate were obtained by slow evaporation of the solvent with heating at 40 °C.

Dinuclear μ-oxo rhenium(V) complexes, $[Re_2O_3(L)_4]$ (L = L1-4), were prepared as previously described by Rowbottom et al.[66]. Characterization data for these compounds are not reported in this section, but briefly listed in Table 2 (Page 53).

HPLC-grade acetonitrile was purchased from VWR International and used without further purification; HPLC-aqueous solvent was prepared using milli-Q® water (18.2 MΩ·cm ionic purity). Saline solution was obtained from NovaSelect (Tito Scalo, PZ, Italy). Technetium-

99m, as $Na^{99m}TcO_4$, was eluted from a $^{99}Mo/^{99m}Tc$ generator (Elumatic III, IBA CIS bio, France) using 0.9% saline.

3.1.2 PHYSICAL MESUREMENTS

Carbon, hydrogen, and nitrogen analyses were performed using a Perkin–Elmer elemental analyzer model 240B.

^1H, ^{13}C, and ^{31}P NMR spectra were acquired at 298 K with a Brucker AMX 300 or Brucker AMX 400 spectrometer, using $SiMe_4$ as the internal reference (^1H and ^{13}C) and 85% aqueous H_3PO_4 as the external reference (^{31}P).

Electrospray ionization (ESI) mass spectrometry measurements were performed with an ESI time-of-flight Mariner biospectrometry workstation (PerSeptive Biosystems, Stafford, TX, USA).

Cyclic voltammetry measurements were performed on a BAS (Bioanalytical System Inc.) CV-1B cyclic voltammograph at 293 K under an atmosphere of dinitrogen, in anhydrous deoxygenated dichloromethane solutions (3.5×10^{-3} mol/dm^3) with [n-Bu_4N][ClO_4] (0.1 mol/dm^3) as the supporting electrolyte, by using a conventional three electrode cell, recording at 0.2 V/sec. A platinum-disk electrode (area ca. 1.28 mm^2) was used as the working electrode, a platinum wire as the counter electrode, and a silver wire as a quasi-reference electrode. Controlled potential coulometries were performed using an Amel model 721 integrator, in an H-shaped cell containing, in arm 1, a platinium gauze working electrode and an Ag/Ag^+ reference isolated inside a salt bridge by a medium-glass frit and, in arm 2, an auxiliary platinium-foil electrode.

3.1.3 CHROMATOGRAPHY

Thin layer chromatography was performed on silica gel F254S plates (Merck, Milan, Italy). Dry column flash chromatography purifications were carried out in 4 cm x 2 cm columns, using high purity silica gel (grade 9385 pore size 60 Å, 230-400 mesh particles), and reagent grade solvents, and applying vacuum by means of a mechanical pump.

HPLC analyses were used to evaluate the radiochemical yield (RCY) and the stability as radiochemical purity (RCP) of the ^{99m}Tc-complexes. HPLC was performed on a Beckman System Gold instrument equipped with a programmable solvent Model 126, a scanning detector Module 166 (λ = 216 μm) and a radioisotope detector Model 3200 Bioscan, using a RP Symmetry C8 (5.0 μm, 100 Å, 4.6 × 250 mm) column with a RP C8 Guard precolumn. Mobile phase: solvent A = aqueous ammonium acetate 0.01 M (pH = 7), solvent B = acetonitrile; 0 – 30 min B = 90% (isocratic); flow rate = 1 ml/min.

3.2 SYNTHESES

3.2.1 SYNTHESIS OF DITHIOCARBAMATE LIGANDS L2 AND L3

4-(ethoxycarbonyl)piperidinedithiocarbamate, 4-(ethoxycarbonyl)piperidinium salt (EtOOCPipL2). To a solution of 4-(ethoxycarbonyl)piperidine (1.57 g, 10 mmol) in diethyl ether (50 ml), cooled at 4 °C in a water/ice bath, an ethanol solution of carbon disulfide (1.20 ml, 20 mmol in 5 ml of ethanol) was added dropwise and the reaction mixture was stirred until the room temperature was reached. The white precipitate was filtered off, washed three times with diethyl ether and dried under vacuum. Yield: 90%. Every attempt to obtain other salts of the dithiocarbamate such as sodium, potassium, ammonium or triethylamino, using common procedures, was not successful, since the 4-(ethoxycarbonyl)piperidinium salt was always collected.

Anal. Calcd. for $C_{17}H_{30}N_2O_4S_2$ (MW = 390.52): C, 52.28%; H, 7.74%; N, 7.17%; found: C, 52.46%; H, 7.81%; N, 7.08%.

ESI(-)-MS: *m/z* 232.03 ([M – EtOOCPip]$^-$, 100%); ESI(+)-MS: *m/z* 158.12 ([EtOOCPip]$^+$, 100%).

^{1}H NMR (300 MHz, DMSO-d_6): δ (ppm) = 1.18 (m, 3H, C(O)OCH2C*H3*); 1.35-2.10 (3 m, 4H, C*H*2CHC(O)OEt); 2.60 (m, 2H, CH2C*H*C(O)OEt); 2.85-3.35 (3 m, 8H, S2CNC*H*2); 4.07 (m, 4H, C(O)OC*H2*CH3) S2CNC*H*2); 5.53 (m, 2H >NH_2^+).

^{13}C NMR (300 MHz, DMSO-d_6): δ (ppm) = 13.98 (s, C(O)OCH2*C*H3); 24.70 (s, *C*H2CHC(O)OEt carbossipipe); 37.80 (s, *C*HC(O)OEt); 42.26 (s, S2CN*C*H2); 60.16 (C(O)O*C*H2CH3); 173.27 (s, *C*=O); 192.98 (*C*S2).

Sodium N-adamatyldithiocarbamate (L3). To a mixture of 1-amino-adamantane (1.51 g, 10 mmol) and NaOH (0.6 g, 15 mmol) in ethanol (60 ml), cooled at 4 °C in a water/ice bath, an ethanol solution of carbon disulfide (1.20 ml, 20 mmol in 5 ml of ethanol) was added dropwise under stirring, and the reaction mixture was stirred until the room temperature was reached. The solvent was partially evaporated under vacuum (rotavapor), then diethyl ether was added and the white precipitate was filtered off, washed three times with diethyl ether and dried under vacuum. Yield: 90%.

Anal. Calcd. for $C_{11}H_{16}NS_2Na$ (MW = 249.37): C, 52.98%; H, 6.47%; N, 5.62%; found: C, 53.11%; H, 6.78%; N, 5.50%.

ESI(-)-MS: *m/z* 226,07 ($[M - Na]^-$, 100%).

^{1}H NMR (300 MHz, DMSO-d_6): δ (ppm) = 1.58, 1.97, 2.05 (3 m, 13 H, adamantane ring); 7.27 (s, 1 H, S_2CNH).

^{13}C NMR (300 MHz, DMSO-d_6): δ (ppm) = 29.90, 40.76, 41.98 (3 s, adamantine ring); 54.14 (s, C*quat*. adamantane); 214.56 (s, CS_2).

3.2.2 SYNTHESIS OF $[Re^{III}(PS)_2(L)]$ COMPLEXES (1-8)

All reactions were performed under a dinitrogen or argon atmosphere using standard Schlenk techniques, and solvents were purged with nitrogen or argon before use. Work up and purification procedures were accomplished at normal atmospheric conditions, except for complexes **7** and **8**.

General procedures. Five different methods were followed to synthesize rhenium(III) complexes, as described below. The eluents for the chromatographic purifications are specified case by case hereinafter.

METHOD A. To an orange suspension of $[Re^{III}Cl_3(MeCN)(PPh_3)_2]$ (13.9 mg, 0.016 mmoli) in toluene (1.5 ml), PS ligand (0.048 mmol, 3 eq.), dissolved in 1 ml of ethanol, and L ligand (0.080 mmol, 5 eq. if PS = PS2H; 0.040 mmol, 2.5 eq. if PS = PScyH or PSisoH), dissolved in 3 ml of ethanol, were added using a syringe through a rubber septum. The resulting mixture was refluxed while stirring for 1 h, becoming progressively clear and bright green. The solvent was then removed by a gentle dinitrogen stream.

Alternatively, a two-step procedure was used. To the initial orange suspension, PS ligand was first added and the resulting mixture was refluxed and stirred for 30 minutes, during which time it became a dark brown solution. The L ligand was then added and the reaction mixture turned to clear and bright green in few minutes. The solvent was then removed by a gentle dinitrogen stream.

The residual solid was dissolved in dichloromethane (3 ml), filtered and extract with water (3 x 3 ml) to remove excess L ligand. The organic phase was dried with anhydrous sodium sulfate and the solvent was evaporated giving an impure bright green solid which was purified by dry column flash chromatography.

METHOD B. This method was used only for selected Re(III) complexes (**1-4)**. The complex $[Re_2O_3(L)_4]$ (0.008 mmol, 1 eq.) was suspended in acetone (5 ml) or toluene/ethanol (1.5/3.5 ml) giving a yellow to dark brown suspension. PS ligand (0.048 mmol, 6 eq.), dissolved in 1 ml of acetone or ethanol was then added using a syringe through a rubber septum. The resulting mixture was refluxed and stirred for 12 h. The solvent was then removed by a gentle dinitrogen stream. The residual solid was dissolved in dichloromethane (3 ml), filtered and extract with water (3 x 3 ml) to remove excess L ligand. The organic phase was dried with anhydrous sodium sulfate and the solvent was evaporated giving an impure bright green solid which was purified by dry column flash chromatography.

METHOD C. To an olive green suspension of $[Re^{V}(O)Cl3(PPh_3)_2]$ (11.6 mg, 0.014 mmol) in toluene (1.5 ml), PS ligand (0.048 mmol, 3.5 eq.), dissolved in 1 ml of ethanol, and L ligand (0.080 mmol, 5 eq. if PS = PS2H; 0.040 mmol, 2.5 eq. if PS = PScyH or PSisoH), dissolved in 3 ml of ethanol, were added using a syringe through a rubber septum. The resulting mixture was refluxed while stirring for 1 h, becoming progressively clear and bright green. The solvent was then removed by a gentle dinitrogen stream. The residual solid was dissolved in dichloromethane (3 ml), filtered and extract with water (3 x 3 ml) to remove excess L ligand. The organic phase was dried with anhydrous sodium sulfate and the solvent was evaporated giving an impure bright green solid which was purified by dry column flash chromatography.

METHOD D. To a mixture of $[NBu_4][ReO_4]$ (6.9 mg, 0.014 mmol) and triphenylphosphine (14.6 mg, 0.056 mmol) in methanol (0.5 mL), concentrated aqueous HCl (0.03 mL) was added and the mixture was refluxed 1 h. The resulting olive green mixture was allowed to cool to room temperature and triethylamine (0.05 ml) was added to neutralized the acid. PS ligand

(0.048 mmol, 3.5 eq.), dissolved in 1 ml of ethanol, and L ligand (0.080 mmol, 5 eq. if PS = PS2H; 0.040 mmol, 2.5 eq. if PS = PScyH or PSisoH), dissolved in 3 ml of ethanol, were added using a syringe through a rubber septum. The resulting mixture was refluxed while stirring for 1 h, becoming progressively clear and bright green. The solvent was then removed by a gentle dinitrogen stream. The residual solid was dissolved in dichloromethane (3 ml), filtered and extract with water (3 x 3 ml) to remove excess L ligand. The organic phase was dried with anhydrous sodium sulfate and the solvent was evaporated giving an impure bright green solid which was purified by dry column flash chromatography.

[Re(PS2)$_2$(L1)] (1). The crude product was dissolved in 1 ml n-hexane/dichloromethane 1:1 mixture. Then it was transferred into a silica gel column set for dry column flash chromatography and eluted with n-hexane/dichloromethane 1:1 (5 ml x 2) and dichloromethane (5 ml x 3). The pure dichloromethane fractions were collected and the solvent was removed by a gentle dinitrogen stream. Yield: 70% (method A and C); 62% (method B); 68% (method D).

Elemental Analysis: Calc. for $C_{33}H_{36}NP_2ReS_4$ (MW: 823.06): C, 48.16%; H, 4.41%; N, 1.70%; Found: C, 47.33%; H, 4.25%; N, 1.93%.

ESI(+)-MS *m/z*: 823.06 (M^+, 100%).

^{31}P NMR (400 MHz, CD_2Cl_2): δ (ppm) = 25.97 (s)

^{1}H NMR (400 MHz, CD_2Cl_2): δ (ppm) = 1.64 (m, 4H, $S_2CNCH_2CH_2$ pirrolidine); 2.38 (m, 2H, PCH_2CH_2S); 2.90 (m, 2H, PCH_2CH_2S); 3.06 (m, 2H, PCH_2CH_2S); 3.30 (m, 4H, $S_2CNCH_2CH_2$ pirrolidine); 3.52 (m, 2H, PCH_2CH_2S); 7.28 (m, 2H, *H*arom p); 7.36 (m, 4H, *H*arom m); 7.40 (m, 2H, *H*arom p'); 7.41 (m, 4H, *H*arom m'); 7.65 (m, 4H, *H*arom o'); 7.67 (m, 4H, *H*arom o).

^{13}C NMR (CD_2Cl_2): δ (ppm) = 25.14 (s, $N(CH_2)_2(CH_2)_2$ pirrolidine); 36.57 (s br, PCH_2); 47.64 (s, $N(CH_2)_2(CH_2)_2$ pirrolidine); 56.09 (s br, SCH_2); 127.32 (s, *C*arom m'); 128.26 (s, *C*arom m); 128.81 (s, *C*arom p'); 129.69 (s, *C*arom p); 132.87 (s, *C*arom o'); 133.65 (s, *C*arom o); ~137.69 (s, $C_{quat-\ arom}P$); ~139.55 (s, $C_{quat-arom}P$) ; ~197.30 (CS_2). Note: signals marked ~ are derived from HMBC only.

[Re(PS2)$_2$(L2)] (2). The crude product was purified as described for compound **1**. Yield: 77% (method A and C); 60% (method B); 68% (method D).

The complex was soluble in chlorinated solvents and DMSO, slightly soluble in methanol, insoluble in n-hexane, diethyl ether and water.

Elemental Analysis: Calc. for $C_{37}H_{42}NO_2P_2ReS_4$ (MW: 909.15): C, 48.88%; H, 4.66%; N, 1.54%; found: C, 48.86%; H, 4.72%; N, 1.52%.

ESI(+)-MS: *m/z* 909.10 (M^+, 100%).

^{31}P NMR (400 MHz, CD_2Cl_2): δ (ppm) = 27.10 (s).

^{1}H NMR (400 MHz, CD_2Cl_2): δ (ppm) = 1.13 (m, 2H, C*H*$_2$CHC(O)OEt); 1.28 (m, 3H, C(O)OCH$_2$C*H*$_3$); 1.61 (m, 2H, C*H*$_2$CHC(O)); 2.31 (m, 1H, CH$_2$C*H*C(O)OEt); 2.38 (m, 2H, C*H*$_2$P,); 2.67 (m, 2H, S$_2$CNC*H*$_2$); 2.88 (m, 2H, C*H*$_2$P,); 3.02 (m, 2H SC*H*$_2$); 3.57 (m, 2H SC*H*$_2$); 3.94 (m, 2H, S$_2$CNC*H*$_2$); 4.15 (m, 2H, C(O)OC*H*$_2$CH$_3$); 7.28 (m, 2H, Harom p); 7.35 (m, 4H, Harom m); 7.40 (m, 2H, Harom p'); 7.41 (m, 4H, Harom m'); 7.62 (m, 4H, Harom o'); 7.64 (m, 4H, Harom o).

^{13}C NMR (400 MHz, CD_2Cl_2): δ (ppm) = 13.98 (s, C(O)OCH$_2$*C*H$_3$); 27.11, 27.24 (2s, *C*H$_2$CHC(O)OEt carbossipipe); 36.18 (s br, *C*H$_2$P); 40.16 (s, *C*HC(O)OEt); 43.19 (s, S$_2$CN*C*H$_2$); 55.04 (s br, S*C*H$_2$); 60.47 (C(O)O*C*H$_2$CH$_3$); 127.07 (s br, Carom m'); 127.84 (s br, Carom m); 128.46 (s br, Carom p'); 129.29 (s br, Carom p); 132.30 (s br, Carom o'); 133.24 (s br, Carom o), ~ 137.13, ~ 138.79, ~ 139.05 ($C_{quat.arom}$P); 173.52 (s, *C*=O); ~ 198.80 (*C*S$_2$). Note: signals marked ~ are derived from HMBC only.

[Re(PS2)$_2$(L3)] (3). The crude product was dissolved in 1 ml n-hexane/dichloromethane 1:1 mixture. Then it was transferred into a silica gel column set for dry column flash chromatography and eluted with dichloromethane 1:1 (5 ml x 3) and dichloromethane/methanol 97:3 (5 ml x 3). The pure dichloromethane/methanol fractions were collected and the solvent was removed by a gentle dinitrogen stream. Average yield: 65% (all methods gave almost the same yield).

The complex was soluble in chlorinated solvents and DMSO, slightly soluble in methanol, n-hexane, diethyl ether and insoluble water.

Elemental Analysis: Calc. for $C_{39}H_{44}NP_2ReS_4$ (MW 903.14): C, 51.86 %; H, 4.91 %; N, 1.55 %; found: C, 52.02 % ; H, 4.96 %; N, 1.52 %.

ESI(+)-MS *m/z*: 709.03 ([M – 194]$^+$ 100%, assignable to the [Re(PS2)$_2$(SH)]$^+$ species; 903.14 (M^+, 50%).

^{31}P NMR (400 MHz, CD_2Cl_2): δ (ppm) = 27.04 (s)

^{1}H NMR (400 MHz, CD_2Cl_2): δ (ppm) = 1.54, 1.57, 1.64, 1.96 (m, 13H, *H*adamantane); 2.46 (m, 2H, PC*H*$_2$); 2.85 (m, 2H, PC*H*$_2$); 2.97 (m, 2H, SC*H*$_2$); 3.38 (m, 2H, SC*H*$_2$); 5.50 (1H, S_2CN*H*); 7.38 (m, 2H, Harom p'); 7.38 (m, 4H, Harom m'); 7.39 (m, 2H, Harom p); 7.42 (m, 4H, Harom m); 7.52 (m, 4H, Harom o'); 7.71 (m, 4H, Harom o).

^{13}C NMR (400 MHz, CD_2Cl_2): δ (ppm) = 29.59, 39.95, 41.17 (3s, *C*adamantane); 36.40 (s br, P*C*H$_2$), 54.64 (s br, S*C*H$_2$); 54.77 (s, $C_{quat.}$ adamantane); 127.74 (s, *C*arom m'); 127.80 (s, *C*arom m); 128.62 (s, *C*arom p'); 129.17(s, *C*arom p); 132.25 (s, *C*arom o'); 133.12 (s, *C*arom o); ~ 137.76 ($C_{quat.arom}$P); ~ 139.43 ($C_{quat.arom}$P); ~ 187.90 (s, *C*S$_2$). Note: signals marked ~ are derived from HMBC only.

[Re(PS2)$_2$(L4)] (4). The crude product was purified as described for compound **1** and **2**. Yield: 68% (methods B and C); 58% (method A); 67% (method D). The complex was soluble in chlorinated solvents and DMSO, slightly soluble in methanol, n-hexane, diethyl ether and insoluble water.

Elemental Analysis: Calc. for $C_{40}H_{43}N_2OP_2ReS_4$ (MW: 944.20): C, 50.88%; H, 4.59%; N, 2.97%; found: C, 51,02 % ; H, 4,66 %; N, 2,90 %.

ESI(+)-MS *m/z*: 944.13 (M^+, 100%).

^{31}P NMR (400 MHz, CD_2Cl_2): δ (ppm) = 27.04 (s).

^{1}H NMR (400 MHz, CD_2Cl_2): δ (ppm) = 2.40 (m, 2H, PC*H*$_2$CH$_2$S); 2.62 (m, 4H, NCH$_2$C*H*$_2$N piperazine); 2.90 (m, 2H, PC*H*$_2$CH$_2$S); 3.03 (m, 2H, SC*H*$_2$CH$_2$P); 3.47 (m, 4H, NC*H*$_2$CH$_2$N piperazine); 3.59 (m, 2H, SC*H*$_2$CH$_2$P); 3.82 (s, 3H, OC*H*$_3$); 6.81 (m, 1H, Harom o L4); 6.88 (m, 1H, Harom m L4); 6.95 (m, 1H, Harom m L4); 7.04 (m, 1H, Harom p piperazina); 7.28 (m, 2H, Harom p' PS2); 7.35 (m, 4H, Harom m' PS2); 7.40 (m, 2H, Harom p PS2); 7.41 (m, 4H, Harom m PS2); 7.62 (m, 4H, Harom o PS2); 7.64 (m, 4H, Harom o' PS2).

^{13}C NMR (400 MHz, CD_2Cl_2): δ (ppm) = 36.21(s br, P*C*H$_2$); 43.99 (S_2CN*C*H$_2$CH$_2$N piperazine); 49.97 (S_2CNCH$_2$*C*H$_2$N piperazine); 55.20 (s br, S*C*H$_2$); 55.21 (s, O*C*H$_3$); 111.44 (s, Carom m L4); 118.29 (s, Carom o L4); 120.85 (s, Carom m' L4); 123.21 (s, Carom p L4); 127.12 (s, *C*arom m' PS2); 127.87 (s, *C*arom m PS2); 128.52 (s, *C*arom p' PS2); 129.31 (s, *C*arom p PS2); 132.30 (s, *C*arom o' PS2); 133.24 (s, *C*arom o PS2); ~ 137.35 ($C_{quat.arom}$P PS2); ~ 139.15 ($C_{quat.arom}$P PS2);

~ 140.70 ($C_{quat.arom}$-N L4); ~ 152.20 ($C_{quat.arom}$-OCH_3 L4); ~ 199.22 (s, CS_2). Note: signals marked ~ are derived from HMBC only.

[Re(PS2)$_2$(L5)] (5). The crude product was purified as described for compound **3**. Average yield obtained following methods A, C and D: 66% (all the methods gave almost the same yield). The complex was soluble in chlorinated solvents and DMSO, slightly soluble in methanol, n-hexane, diethyl ether and insoluble water.

Elemental Analysis: Calc. for $C_{42}H_{48}N_3OP_2ReS_4$ (MW: 987.26): C, 51.10 %; H, 4.90 %; N, 4.26 %; found: C, 51,22 %; H, 4,99 %; N, 4,18 %.

ESI(+)-MS *m/z*: 493,58 ($[M + H]^{2+}$, 100%); 987,16 (M^+, 10%).

^{31}P NMR (400 MHz, CD_2Cl_2): δ (ppm) = 26.77 (s); 26.99 (s)

^{1}H NMR (400 MHz, CD_2Cl_2): δ (ppm) = 2.21 (m, 2H, NHCH$_2$CH_2N); 2.42 (m, 2H, PCH_2CH$_2$S); 2.43 (m, 4H, NCH_2CH$_2$N piperazine); 2.86 (m, 2H, PCH_2CH$_2$S); 2.99 (m, 4H, NCH$_2$CH_2N piperazine); 3.03 (m, 2H, SCH_2CH$_2$P); 3.08 (m, 2H, NHCH_2CH$_2$N) ; 3.11 (m, 2H, SCH_2CH$_2$P); 3.86 (s, 3H, OCH_3); 6.22 (m, 1H, NHCH$_2$CH$_2$N); 6.89 (m, 1H, Harom m L5); 6.93 (m, 1H, Harom o L5); 6.94 (m, 1H, Harom m L5); 7.00 (m, 1H, Harom p L5); 7.32 (m, 2H, Harom p PS2); 7.38 (m, 4H, Harom m PS2); 7.39 (m, 2H, Harom p' PS2); 7.39 (m, 4H, Harom m' PS2); 7.57 (m, 4H, Harom o' PS2); 7.68 (m, 4H, Harom o PS2).

^{13}C NMR (400 MHz, CD_2Cl_2): δ (ppm) = 36.32(s br, PCH$_2$); 38.38(s br, SCH$_2$); 50.24 (s, NCH$_2$CH$_2$N piperazine); 50.33 (S$_2$CNCH$_2$CH$_2$N piperazine); 52.77 (s, NCH$_2$CH$_2$N piperazine); 55.15 (s, OCH$_3$); 55.17 (S$_2$CNCH$_2$$CH_2$N piperazine); 111.46 (s, Carom m L5); 118.12 (s, Carom o L5); 120.99 (s, Carom m' L5); 122.66 (s, Carom p L5); 127.27 (s, *C*arom m PS2); 127.84 (s, *C*arom m' PS2); 128.55 (s, *C*arom p PS2); 129.28 (s, *C*arom p' PS2); 132.28 (s, *C*arom o PS2); 133.11 (s, *C*arom o' PS2); ~ 137.47 ($C_{quat.arom}$P); ~ 139.10 ($C_{quat.arom}$P); ~ 141.50 ($C_{quat.arom}$-N); ~ 152.40 ($C_{quat.arom}$-OCH_3); ~203.42 (s, CS_2). Note: signals marked ~ are derived from HMBC only.

[Re(PS2)$_2$(L6)] (6). The crude product was purified as described for compound **3** and **5**.

The complex was soluble in chlorinated solvents and DMSO, slightly soluble in methanol, n-hexane, diethyl ether and insoluble water.

Elemental Analysis: Calc. for $C_{44}H_{52}N_3OP_2ReS_4$ (MW 1014.32): C, 52.05%; H, 5.16%; N, 4.14%; found: C, 52.12%; H, 5.20%; N, 4.10%.

ESI(+)-MS *m/z*: 507.59 ($[M + H]^{2+}$, 100%); 709.03 ($[Re(PS2)_2(SH)]^+$, 10%).

^{31}P NMR (400 MHz, CD_2Cl_2): δ (ppm) = 25.70 (s); 25.76 (s)

^1H NMR (400 MHz, CD_2Cl_2): δ (ppm) = 1.31 (m, 2H, $NHCH_2C\mathit{H_2}CH_2CH_2N$); 1.42 (m, 2H, $NHCH_2CH_2C\mathit{H_2}CH_2N$); 2.17 (m, 2H, $NHCH_2CH_2CH_2C\mathit{H_2}N$); 2.41 (m, 2H, $PC\mathit{H_2}CH_2S$); 2.49 (m, 4H, $NC\mathit{H_2}CH_2N$ piperazine); 2.86 (m, 2H, $PC\mathit{H_2}CH_2S$); 3.00 (m, 2H, $NHC\mathit{H_2}CH_2CH_2CH_2N$); 3.03 (m, 2H, $SC\mathit{H_2}CH_2P$); 3.04 (m, 4H, $NCH_2\mathit{CH_2}N$ piperazine); 3.53 (m, 2H, $SC\mathit{H_2}CH_2P$); 3.86 (s, 3H, $OC\mathit{H_3}$); 6.89 (m, 1H, Harom o L6); 6.91 (m, 1H, Harom m L6); 6.94 (m, 1H, Harom m L6); 7.01 (m, 1H, Harom p L6); 7.32 (m, 6H, Harom p + m PS2); 7.37 (m, 6H, Harom p' + m' PS2); 7.57 (m, 4H, Harom o' PS2); 7.68 (m, 4H, Harom o PS2); 8.44 (m, 1H, $N\mathit{H}CH_2CH_2CH_2CH_2N$).

^{13}C NMR (400 MHz, CD_2Cl_2): δ (ppm) = 24.44 (s, $NHCH_2CH_2\mathit{C}H_2CH_2N$); 26.34 (s, $NHCH_2\mathit{C}H_2CH_2CH_2N$); 36.30 (s br, $P\mathit{C}H_2$); 42.08 (s, $NH\mathit{C}H_2CH_2CH_2CH_2N$); 49.92 ($N\mathit{C}H_2CH_2N$ piperazine); 52.97 (s, $N\mathit{C}H_2CH_2N$ piperazine); 55.22 (s, $O\mathit{C}H_3$); 55.38 (s br, $S\mathit{C}H_2$); 55.18 ($NH\mathit{C}H_2CH_2CH_2\mathit{C}H_2N$); 111.36 (s, Carom o L6); 118.38 (s, Carom m L6); 122.66 (s, Carom m' L6); 122.86 (s, Carom p L6); 127.25 (s, *C*arom m PS2); 127.81 (s, *C*arom m' PS2); 128.46 (s, *C*arom p PS2); 129.18 (s, *C*arom p' PS2); 132.38 (s, *C*arom o PS2); 133.14 (s, *C*arom o' PS2); ~ 137.69 ($C_{quat.arom}$-P); ~ 139.49 ($C_{quat.arom}$-P); ~ 141.40 ($C_{quat.arom}$-N); ~ 152.60 ($C_{quat.arom}$-OCH_3); 202.28 (s, $C\mathit{S}_2$). Note: signals marked ~ are derived from HMBC only.

[Re(PScy)$_2$(L1)] (7). The crude product was purified as described for compound **1**, but working under dinitrogen or argon atmosphere. Average yield obtained following methods A, C and D: 74% (all the methods gave almost the same yield).

The complex was soluble in chlorinated solvents and DMSO, slightly soluble in methanol, n-hexane, diethyl ether and insoluble water.

ESI(+)-MS *m/z*: 847.25 (M^+, 100%).

Elemental Analysis: Calc. for $C_{33}H_{60}NP_2ReS_4$ (MW 847,25): C, 46.78%; H, 7.14%; N, 1.65%; found: C, 46.52%; H, 7.03%; N, 1.74%.

[Re(PSiso)$_2$(L1)] (8). The crude product was purified as described for compound **1**, but working under dinitrogen or argon atmosphere. Average yield obtained following methods A, C and D: 74% (all the methods gave almost the same yield).

The complex was soluble in chlorinated solvents and DMSO, slightly soluble in methanol, n-hexane, diethyl ether and insoluble water.

ESI(+)-MS *m/z*: 687.14 (M^+, 100%).

Elemental Analysis: Calc. for $C_{21}H_{44}NP_2ReS_4$ (MW 687,00): C, 36.71%; H, 6.46%; N, 2.04%; found: C, 36.68%; H, 6.51%; N, 3.99%.

^{31}P NMR (400 MHz, CD_2Cl_2) δ (ppm) = 23.77 (s, br $\Delta\nu_{1/2} \cong 65$ Hz).

^{1}H NMR (400 MHz, CD_2Cl_2): δ (ppm) = 1.10 (m, 6H, PCHC*H$_3$'*); 1.23 (m, 6H, PCHC*H$_3$*); 1.36 (m, 6H, PCHC*H$_3$*); 1.48 (m, 6H, PCHC*H$_3$'*); 1.78 (m, 2H, PC*H$_2$*CH$_2$S); 1.96 (m, 2H, NCH$_2$C*H$_2$* piperidine); 1.97 (m, 2H, PC*H$_2$*CH$_2$S); 2.69 (m, 2H, PC*H'*); 2.74 (m, 2H, PC*H*); 3.05 (m, 2H, SC*H$_2$*CH$_2$P); 3.26 (m, 2H, SC*H$_2$*CH$_2$P); 3.90 (m, 4H, NC*H$_2$C*H$_2$ piperidine).

^{13}C NMR (400 MHz, CD_2Cl_2): δ (ppm) = 18.74 (s, PCH*C*H$_3$); 18.85 (s br, PCH*C*H$_3$); 19.28 (s PCH*C*H$_3$'); 20.16 (s, PCH*C*H$_3$'); 25.05 (s, NCH$_2$*C*H$_2$ piperidine); 28.58 (s br, PC*H'*); 30.48 (s br, P*C*H$_2$), 30.49 (s, P*C*H); 47.1 (s, N*C*H$_2$CH$_2$ piperidine); 59.33 (s br, S*C*H$_2$); 197.25 (*C*S$_2$).

3.2.3 SYNTHESIS OF [^{99g}Tc^{III}(PS)$_2$(L)] COMPLEXES (9-10)

Caution! ^{99g}Tc is a weak *β*-emitter ($E_β$ = 0.292 MeV, $t_{1/2}$ = 2.12 x 10^5 years). All manipulations were carried out in a laboratory approved for low-level radioactivity using monitored hoods and gloveboxes. When handled in milligram amounts, ^{99g}Tc does not present a serious health hazard, since common laboratory glassware provides adequate shielding. Bremsstrahlung is not a significant problem, due to the low energy of the *β*-particles. However, normal radiation safety procedures must be used at all times, especially with solid samples, to prevent contamination and inhalation. All reactions and manipulations were performed under a nitrogen or argon atmosphere using standard Schlenk techniques, and solvents were purged with nitrogen or argon before use. Work up and purification procedures were accomplished at normal atmospheric conditions.

General procedures. Technetium complexes were prepared following the one pot procedure described above in METHOD A, starting from [^{99g}TcCl$_3$(MeCN)(PPh$_3$)$_2$]. The amounts of the ligands and solvents were the same as reported above. Then, the complexes were purified as described for compound **1**.

[^{99g}Tc(PS2)$_2$(L1)] (9). Yield: 77%

Elemental Analysis: Calc. for $C_{33}H_{36}NP_2S_4Tc$ (MW 735.76): C, 53.87 %; H, 4.93 %; N, 1.90 %; trovato: C, 53.97 % ; H, 5.03 %; N, 1.57 %.

ESI(+)-MS *m/z*: 735.36 (M^+, 100%).

^{31}P NMR (400 MHz, CD_2Cl_2): δ (ppm) = 64.29 (s br, $\Delta\nu_{1/2} \cong 270$ Hz)

^{1}H NMR (400 MHz, CD_2Cl_2): δ (ppm) = 1.63 (m, 4H, $S_2CNCH_2CH_2$ pirrolidine); 2.52 (m, 2H, PCH_2CH_2S); 2.96 (m, 2H, $S_2CNCH_2CH_2$ pirrolidine); 3.05 (m, 2H, $S_2CNCH_2CH_2$ pirrolidine); 3.10 (m, 2H, PCH_2CH_2S); 3.14 (m, 2H, PCH_2CH_2S); 3.94 (m, 2H, PCH_2CH_2S); 7.28 (m, 6H, *H*arom p' + m'); 7.36 (m, 6H, *H*arom p + m); 7.53 (m, 4H, *H*arom o); 7.54 (m, 4H, *H*arom o').

^{13}C NMR (CD_2Cl_2): δ (ppm) = 24.82 (s, $N(CH_2)_2(CH_2)_2$ pirrolidine); 32.75 (s br, PCH_2); 45.34 (s br, SCH_2); 48.23 (s, $N(CH_2)_2(CH_2)_2$ pirrolidine); 126.83 (s, *C*arom m'); 127.75 (s, *C*arom m); 128.33 (s, *C*arom p'); 129.12 (s, *C*arom p); 132.21 (s, *C*arom o'); 133.06 (s, *C*arom o); ~133.97 (s, $C_{quat-\ arom}P$); ~136.21 (s, $C_{quat-arom}P$) ; 199.35 (CS_2). Note: signals marked ~ are derived from HMBC only.

[^{99g}Tc(PSiso)$_2$(L1)] (10). Yield: 67%

Elemental Analysis: Calc. for $C_{21}H_{44}NP_2S_4Tc$ (MW 599.69): C, 42.06 %; H, 7.40 %; N, 2.34 %; trovato: C, 42.44 % ; H, 7.51 %; N, 2.23 %.

ESI(+)-MS *m/z*: 599.80 {100%, [^{99g}Tc(PSiso)$_2$(DTC-L1)]$^+$}

^{31}P NMR (400 MHz, CD_2Cl_2): δ (ppm) = 69.8 (s vbr, $\Delta\nu_{1/2} \cong 700$ Hz)

^{1}H NMR (400 MHz, CD_2Cl_2): δ (ppm) = 1.00 (m, 6H, $PCHCH_3'$); 1.10 (m, 6H, $PCHCH_3$); 1.22 (m, 6H, $PCHCH_3$); 1.34 (m, 6H, $PCHCH_3'$); 1.91 (m, 2H, NCH_2CH_2 piperidine); 2.0 (m, 2H, PCH_2CH_2S); 2.1 (m br, 2H, PC*H*), 2.11 (m, 2H, PCH_2CH_2S); 2.52 (m, 2H, PC*H'*); 3.08 (m, 2H, SCH_2CH_2P); 3.65 (m, 2H, SCH_2CH_2P); 3.83 (m br, 4H, NCH_2CH_2 piperidine).

^{13}C NMR (400 MHz, CD_2Cl_2): δ (ppm) = 18.4 (s, PCHC*H*$_3$); 18.61 (s, PCHC*H*$_3$); 19.3 (s, PCH*C*H$_3$'); 19.95 (s, PCH*C*H$_3$'); 25.13 (s, NCH$_2$*C*H$_2$ piperidine); 25.29 (s br, P*C*H'); 26.00 (s br, P*C*H); 26.10 (s br, P*C*H$_2$); 47.9(s br, S*C*H$_2$); 48.0 (s, N*C*H$_2$CH$_2$ piperidine); 193.54 (*C*S$_2$).

3.3 X-RAY CRYSTALLOGRAPHY

Single crystals of **1**, **2**, **7** and **9** of X–ray quality were grown by slow diffusion of hexane into a dichloromethane solution.

***Complexes 1, 2 and 9*.** The selected specimens were mounted on a glass fiber and centered on the goniometer head of an Oxford Diffraction Gemini E diffractometer, equipped with a 2K × 2K EOS CCD area detector and sealed–tube Enhance (Mo) and (Cu) X–ray sources. The diffraction data collections (ω–2ϑ scans) were carried out at room temperature, by using graphite–monochromated Mo K*a* radiation (*l* = 0.71073 Å), in a 1024 × 1024 pixel mode, using 2 × 2 pixel binning. The diffraction intensities were corrected for Lorentz and polarization effects and also for absorption. Empirical multi–scan absorption corrections using equivalent reflections were performed with the scaling algorithm *SCALE3 ABSPACK*. The collection, reduction and finalization of the raw diffraction data were done by means of the CrysAlis Pro software[(1)]. Accurate unit–cell parameters were determined during the whole data collection by least–squares refinement of all unique reflection positions. Two reference frames were collected after every 50 frames in order to investigate crystal deterioration; no sign of systematic changes was noticed neither in peak positions nor in intensities. The structures were solved by means of the heavy–atom methods using SHELXTL–NT[(2)] and refined by full–matrix least–squares methods based on F_o^2 with SHELXL–97[(3)].

***Complex 7*.** A suitable specimen was fastened on the top of a glass capillary and centered on the goniometer head of a Philips PW1100 diffractometer generously made available by colleagues of the C.N.R.–I.C.I.S. Institute of Padua, Italy. Data were collected with *ω*–2ϑ scans, at room temperature, by using graphite–monochromated Mo Ka radiation (*l* = 0.71073 Å) and corrected for Lorentz/polarization effects. An absorption correction was also performed by means of *y*–scans[(1)]. The unit cell parameters were determined by least–squares refinement of 30 well centered high–angle reflections, and three standard

reflections were checked every 100 measurements to ensure for crystal and equipment stability. No sign of deterioration was detected. The structure was solved by direct methods, with SHELXTL NT and refined by standard full–matrix least–squares based on F_o^2 with the SHELXL–97 program.

3.3 SYNTHESIS AND EVALUATION STUDIES OF THE ^{99m}Tc-RADIOLABELED COMPLEXES

3.3.1 PREPARATION OF THE ^{99m}Tc-RADIOLABELED COMPLEXES OF THE GENERAL FORMULA [^{99m}Tc(PSiso)$_2$(L)].

METHOD A. In a capped and nitrogen-saturated Pyrex® vial were added 1 ml of degassed EtOH, 0.1 mg of $SnCl_2$ dissolved in 0.1 ml of degassed saline, 0.5 mg of PSiso dissolved in 0.1 ml of degassed EtOH and the appropriate amount of L ligand (L1 = 0.46 mg; L2 = 1.65 mg; L3 = 0.7 mg; L4 = 1.62 mg) dissolved in 0.2 ml of degassed EtOH. Then, $Na^{99m}TcO_4$ saline solution (0.250 ml, 50.0 – 800 MBq) was added to the vial, and the reaction mixture was vortexed and heated at 75 °C for 30 min. RCYs were in the range of 91%-97% (determined by HPLC).

METHOD B. In a capped and nitrogen-saturated Pyrex® vial were added 0.6 ml of degassed γ-cyclodextrin saline solution (10 mg/ml), 0.1 mg of $SnCl_2$ dissolved in 0.1 ml of degassed saline, 0.5 mg of PSiso dissolved in 0.5 ml of degassed γ-cyclodextrin saline solution (10 mg/ml) and the appropriate amount of L ligand (see method A) dissolved in 0.2 ml of degassed saline. Then, $Na^{99m}TcO_4$ saline solution (0.250 ml, 50.0 – 800 MBq) was added to the vial, and the reaction mixture was vortexed and heated at 75 °C for 30 min.

3.3.2 RADIOLABELING EFFICIENCY OF THE LIGANDS

The radiolabeling efficiency of the ligands was determined following the method A (previously described) as labeling procedure. The concentrations of ligands were progressively decreased, adding to the vial the appropriate ligands solutions. The amounts of

ligands, expressed both as molar concentration and milligrams, are reported in Figure 4. The RCY at 30 min was determined by HPLC.

3.3.3 IN VITRO STABILITY STUDIES: PBS SOLUTION AND CYSTEINE (Cys), GLUTATHIONE (GSH) AND EDTA CHALLENGE

Method A was followed to prepare the complexes. Then, HPLC purification of the obtained compounds was performed in order to eliminate the free ligands, and to isolate the desired compound in the case of $[^{99m}Tc(PSiso)_2(L3)]$. A fraction of the reaction mixture (containing 37 – 185 MBq) was withdrawn, concentrated to a maximum volume of 0.1 ml by nitrogen stream (if necessary), and injected in the HPLC instrument; the HPLC fraction containing the product was collected in a glass vial and evaporated by nitrogen stream, then the residue was dissolved in an adequate amount of EtOH.

Stability of the purified complexes at physiological buffered pH was evaluated. 50 µl of the $[^{99m}Tc^{III}(PSiso)_2(L)]$ ethanolic solution was added to a propylene test tube containing PBS (450 µl; pH 7.4). The mixture was vortexed and incubated at 37 °C for 24h. Aliquots of the mixture were withdrawn and analyzed by HPLC at 0.5, 1, 2, 3 and 24 h.

Challenge experiments were carried out on the purified complexes using an excess of cysteine (Cys), or glutathione (GSH) or ethylenediaminotetraacetic acid (EDTA). 50 µl of an aqueous 10 mM solution of cysteine hydrochloride was added to a propylene test tube containing PBS (400 µl; pH 7.4) and the $[^{99m}Tc^{III}(PSiso)_2(L)]$ complex (50 µl of the ethanolic solution). Aliquots of the mixture were withdrawn and analyzed by HPLC at 0.5, 1, 2, 3 and 24 h. A similar procedure was applied using GSH (50 µL, 10 mM) or EDTA (50 µL, 10 mM) as the challenge ligand. The experiments were performed in duplicate.

3.3.4 DETERMINATION OF LOGP VALUES

n-Octanol/water partition coefficients were determined by vortex mixing (20 min) 3 mL of n-octanol, 3 mL of PBS (pH = 7.4), and 100 µl of the radiolabeled compound purified as previously described. After centrifugation (3,000 g for 10 min), aliquots (100 µl) of both the organic and the aqueous phases were collected and counted with a γ-counter. Partition

coefficients were expressed as (activity concentration in n-octanol)/(activity concentration in water).

3.3.5 BIODISTRIBUTION STUDIES

Animal experiments were carried out in compliance with the relevant national laws relating to the conduct of animal experimentation.

Biodistributions were carried out in rats. ^{99m}Tc complexes were purified by HPLC before injection, as previously described. After purification, the activity recovered was further diluted with saline to obtain a final solution that was 10% in EtOH content. Male Sprague–Dawley rats weighing 180–200 g were anesthetized with an intraperitoneal injection of Zoletil 100 (40 mg/kg). A jugular vein was surgically exposed and 0.1 ml (300–370 kBq) of the solution containing the radioactive complex was injected. The rats (n = 2) were killed by cervical dislocation at different time points (2, 10, 20, 60, 120 min) after injection. The blood was withdrawn from the heart with a syringe immediately after death and quantified. Organs were excised, rinsed in saline, weighed, and the activity was counted in a NaI well counter. The results were expressed as the percentage of injected dose per gram (%ID/g) and are summarized in Table 6, 7, 8 and 9.

4. RESULTS AND DISCUSSION

4.1 RESULTS

4.1.1 SYNTHESIS OF THE L LIGANDS

Most of the ligands used in this work were purchased or prepared following the procedures previously reported in literature, as indicated in the Experimental section. Anyway, dithiocarbamates L2 and L3 were synthesized as 4-(ethoxycarbonyl)piperidinium and sodium salt respectively according to the scheme in Figure 19.

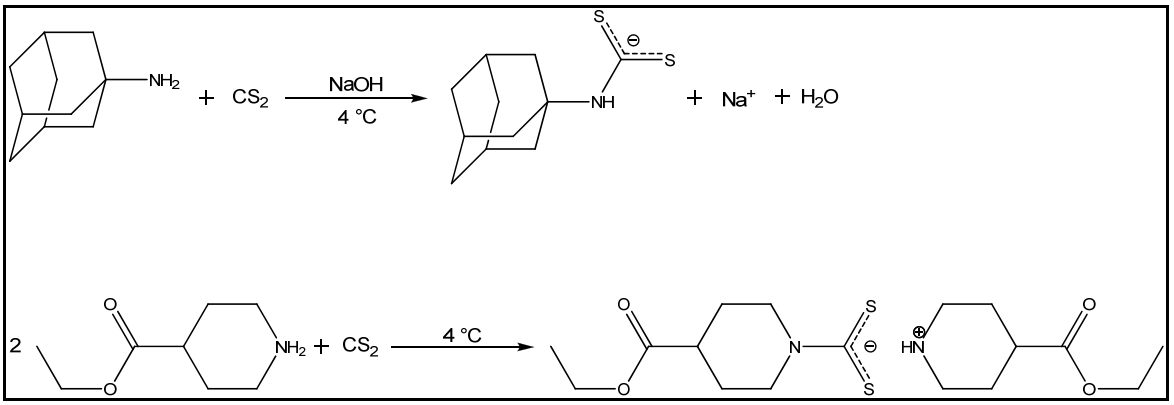

Figure 19: synthesis of dithiocarbamate ligands L3 (above) and L2 (bottom).

Attempts to obtain sodium, potassium, ammonium or triethylammonium salts of L2 in high yields failed. In fact, NaOH or KOH as bases of course caused the hydrolysis of the ester group; on the other hand, the use of alternative bases such as aqueous ammonia or triethylamine, in suitable solvents (ethanol or acetone), always gave the 4-(ethoxycarbonyl)piperidinium salt as main product. Thus, the use of diethyl ether as solvent, without base, which cause the direct precipitation of the 4-(ethoxycarbonyl)piperidinium salt as unique and clean product, was the best choice for our purposes.

4.1.2 SYNTHESIS OF THE RHENIUM AND TECHNETIUM-99g COMPLEXES

Mixed, asymmetrical, hexacoordinated rhenium(III) and technetium(III)-99g complexes of the general formula $[M^{III}(PS)_2(L)]$ were prepared, fully characterized and compared each other. The used ligands are depicted in Figures 20, a detailed scheme of the evaluated synthesis ways is sketched in Figures 21 and 22, and the obtained complexes are shown in Figure 23.

The complexes were synthesized in moderate to good yield (within the range 60-80%) starting from precursors where the metal was in different oxidation states (III, V, VII), involving ligand exchange and/or reduction-ligand exchange reactions according to the scheme in Figure 21 and 22. In all the cases, the reaction progress could be followed by TLC on silica gel (the complexes appeared as clear bright green spots generally at $0.6 < R_f < 0.8$[1]). For compounds **7** and **8**, TLC should be performed under inert atmosphere otherwise the products quickly oxidize turning from green to red and changing their chromatographic properties (see below). In addition, the reaction mixtures could be eventually checked by ESI(+) mass spectrometry (*vide infra*), after the dilution of the sample with acetonitrile or methanol

Using $[Re^{III}Cl_3(MeCN)(PPh_3)_2]$, complexes $[Re^{III}(PS)_2(L)]$ were obtained via a simple one-pot ligand-exchange reaction with PS and L, simultaneously added as ethanol solutions to an orange toluene suspension of the starting complex (*i*). The reaction mixture was refluxed for 1 hour. In order to understand the reactivity of the involved species, and in particular what was the best $[Re^{III}Cl_3(MeCN)(PPh_3)_2]$/PS2/L1 molar ratio required to reach the quantitative conversion of the starting complex to the final desired product, the synthesis of **1** was taken as reference and subjected to a qualitative study in which different quantities of PS and L ligands were used keeping constant the concentration of the starting complex and the reaction conditions, and checking the reaction mixture by TLC on silica gel (pure dichloromethane as eluent) and ESI(+) mass spectrometry. In this way, it was found that:

1) the best $[Re^{III}Cl_3(MeCN)(PPh_3)_2]$/PS/L1 molar ratio was 1/3/5;
2) using stoichiometric quantities ($[Re^{III}Cl_3(MeCN)(PPh_3)_2]$ = 1 eq., PS2 = 2 eq. and L1 = 1 eq.), the starting complex was not totally converted in the final compound and

[1] Values obtained with the suitable eluents indicated for the chromatographic purification in the Experimental section.

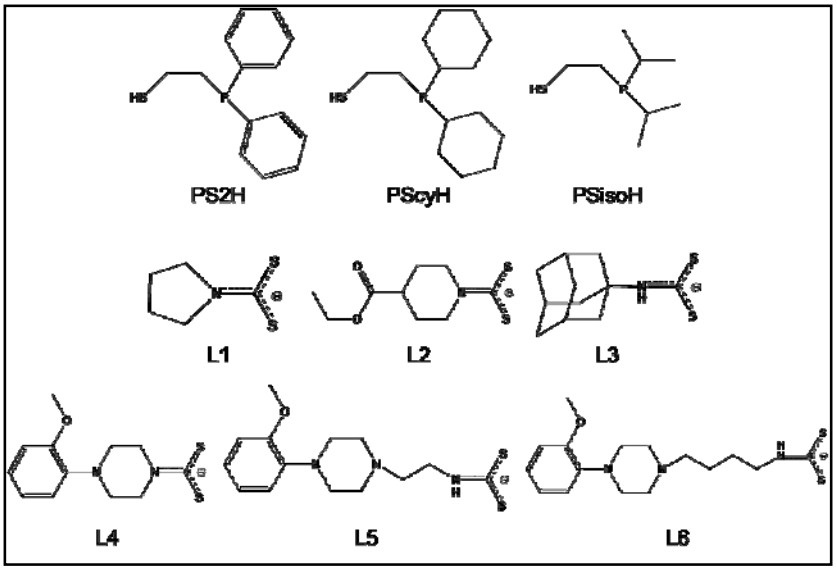

Figure 20: ligands used in this work.

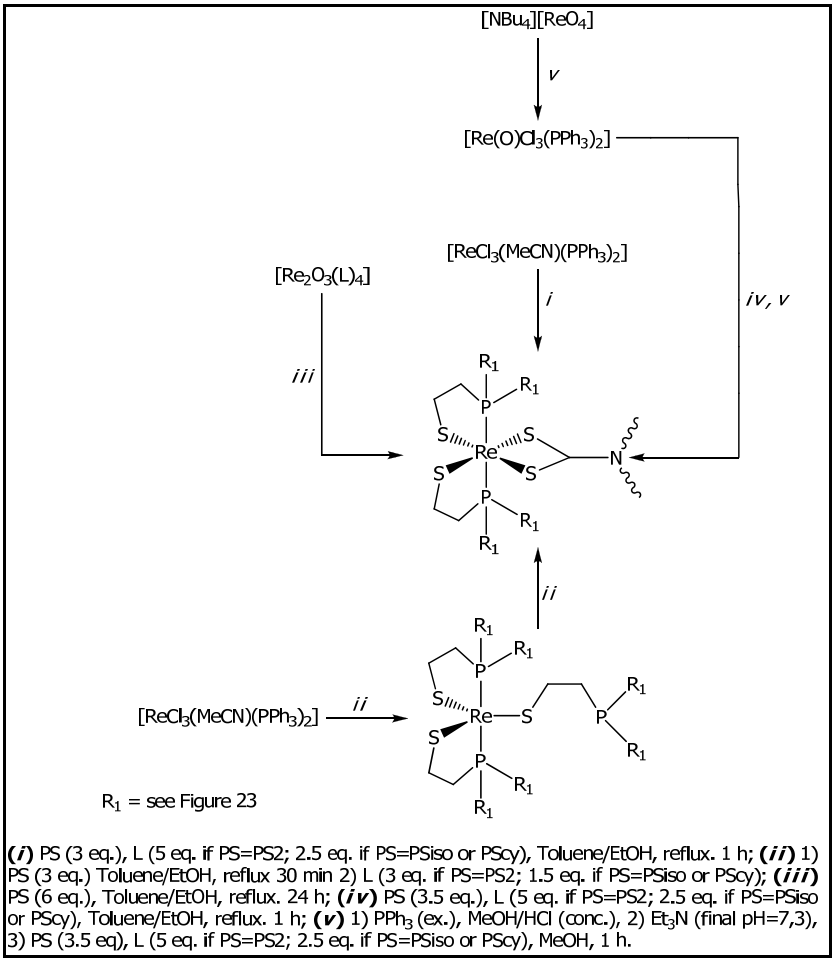

Figure 21: synthesis of Rhenium complexes.

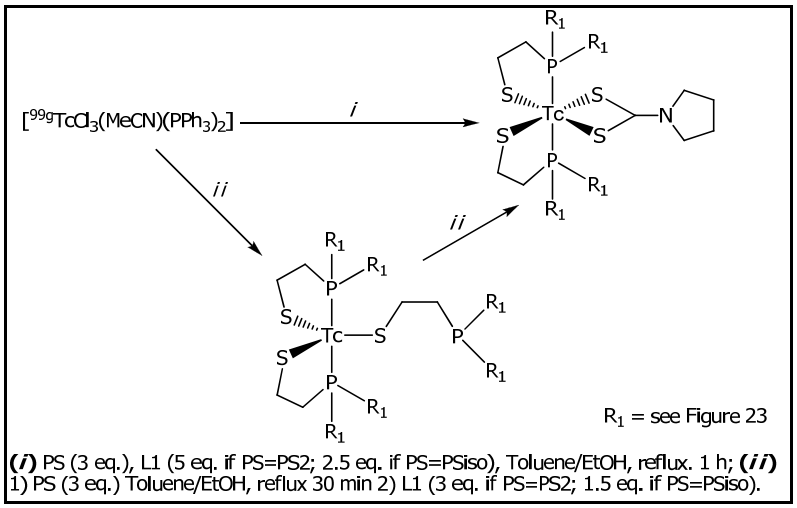

Figure 22: synthesis of Technetium complexes.

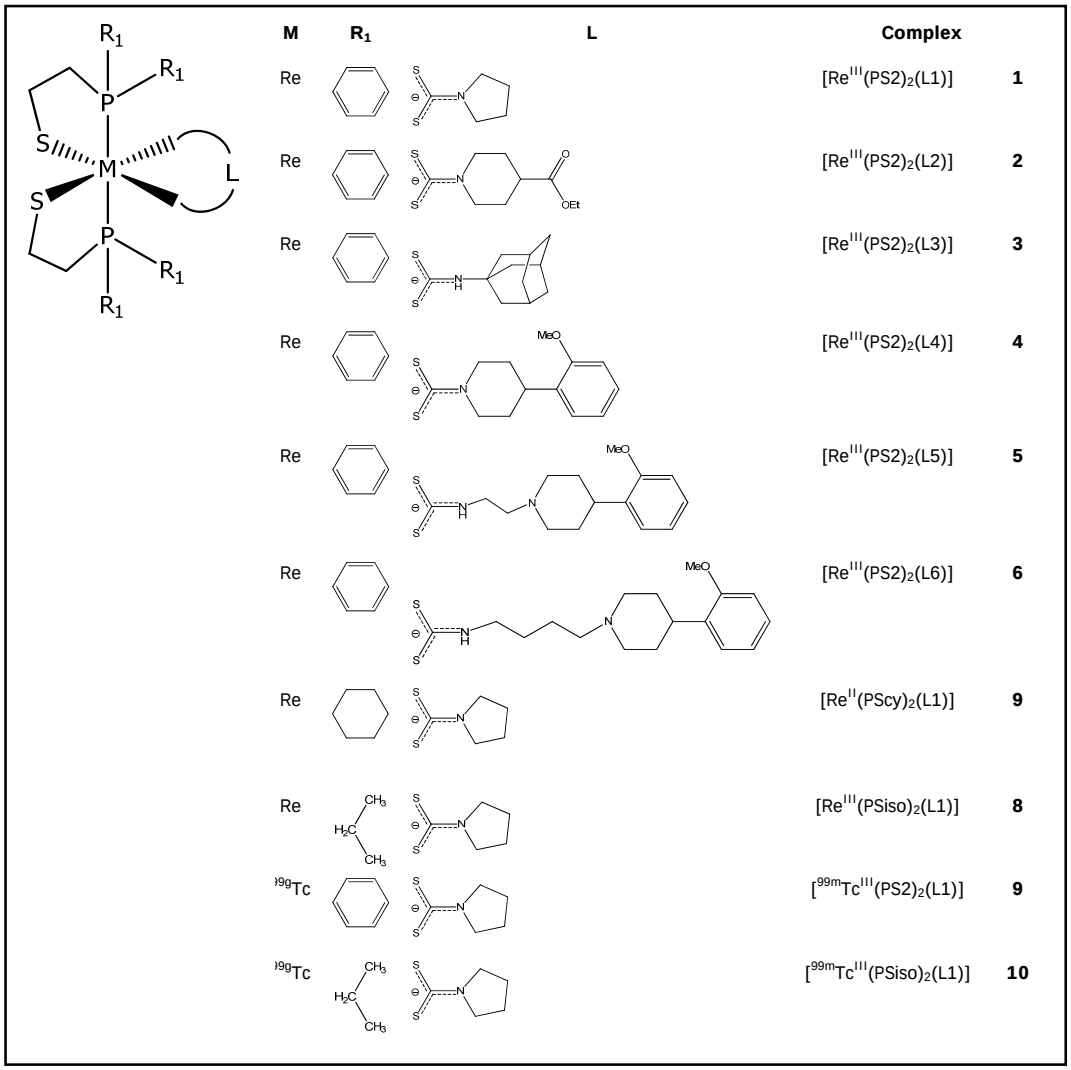

Figure 23: complexes obtained in this work.

many other species were co-formed (TLC profile of the reaction mixture was very complicated showing red, violet and green spots);

3) using lower amounts of PS2 (ratio 1/PS2/5, with PS2 < 3 eq.) the formation of other not well defined red compounds was observed (various red spots on TLC profile and $^{185/187}$Re-patterned signals in mass spectra);
4) the use of lower amounts of L1 (ratio 1/3/L1, with L1 < 5 eq.) led to the co-formation of a dark brown by-product identified as the $[Re^{III}(\kappa S,\kappa P\text{-}PS2)_2(\kappa S\text{-}PS2)]$[61] complex.

Point 4 suggested that pure $[Re^{III}(\kappa S,\kappa P\text{-}PS2)_2(\kappa S\text{-}PS2)]$ should be able to exchange the monodentate phosphinothiol with the dithiocarbamate: in fact, the reaction of this complex with L1 gave the final $[Re^{III}(PS2)_2(L1)]$ (*ii*); moreover, lower amount of dithiocarbamate was required (3 eq.), even though less than 3 equivalents of L1 cause the conversion to be not quantitative. Furthermore, at reflux conditions the reaction was very fast (few minutes). Finally, a two steps reaction was carried out starting from $[Re^{III}Cl_3(MeCN)(PPh_3)_2]$ and passing through the formation of the penta-coordinated intermediate, without isolating it but simply adding to the mixture an ethanol solution of L1 (3 eq.), obtaining the same results.

Similar studies have been performed afterward on the synthesis of **7** and **8**, finding that the best molar ratios were 1/3/2.5 in the case of the one pot method and 1/3/1.5 for the two step reaction. The hypothetical $[Re^{III}(\kappa S,\kappa P\text{-}PSiso)_2(\kappa S\text{-}PSiso)]$ and $[Re^{III}(\kappa S,\kappa P\text{-}PScy)_2(\kappa S\text{-}PScy)]$ species were never been isolated and characterized, but only detected at ESI(+) mass spectrometry.

As specified in Figure 22 and in the experimental section, the technetium(III) analogues **9** and **10** were prepared accordingly only to method *i* and *ii*, starting from $[^{99g}Tc^{III}Cl_3(MeCN)(PPh_3)_2]$ without isolating the intermediate tris-phosphinotiolate complexes.

The synthesis according to Dilworth et al.[63] was also explored for selected complexes (**1**-**4**), starting from the dinuclear, μ-oxo rhenium(V) intermediates $[Re_2O_3(L)_4]$ (method indicated as *iii* in the scheme). $[Re_2O_3(L)_4]$ (L = L1-4) complexes were prepared as previously described by Rowbottom et al.[66], and some characterization data are reported in Table 2. The μ-oxo rhenium(V) complexes were set to react with the phosphinothiol in refluxing acetone or toluene/ethanol. Since the phosphinothiol is the reducing agent as well as ligand, 6 equivalents are required for the reaction to be completed. In both solvent mixtures the reactions were

slower and the yields were lower (60%-65%) than those observed by Dilworth in the synthesis of $[Re^{III}\{PPh_2(C_6H_4S\text{-}2)\}_2(S_2CNEt_2)]\cdot Me_2CO$. No positive effects were observed by increasing the amount of phosphinotiol or the reaction time. This behavior is probably imputable to the extremely low solubility of the μ-oxo starting complexes in the used solvents, even at refluxing temperatures. On the other hand, the $[Re_2O_3(L)_4]$ complexes were found to be near to completely insoluble in the most common solvents.

Table 2: Rhenium(V) μ-oxo $[Re_2O_3(L)_4]$ complexes

Complex (MW, color)	**ESI(+)-MS (m/z)**	**IR (KBr) υ(cm^{-1})**
$[Re_2O_3(L1)_4]$ (1005,43 Da brown-yellow)	494,97	667,88s (*υ*Re−O−Re) 950w (*υ*Re=O) 1498,92s (*υ*CN) 950 (*υ*CS)
$[Re_2O_3(L2)_4]$ (1349,78 Da, dark brown)	666.91	668,87s (*υ*Re−O−Re) 914,41m (*υ*Re=O) 1507,22s (*υ*CN) 1037,90m (*υ*CS) 1725,16s; 1265,31s (*υ*C=O estere)
$[Re_2O_3(L3)_4]$ (1326.95 Da, brown-yellow)	655.47	666,32s (*υ*Re−O−Re) 930w (*υ*Re=O) 1500,92s (*υ*CN) 950 (*υ*CS)
$[Re_2O_3(L4)_4]$ (1489,97 Da, off brown)	737,06	673,65s (*υ*Re−O−Re) 749,6m (*υ*C−Harom) 922m (*υ*Re=O e *υ*CS) 1499,10s (*υ*CN)

The use of the $[Re^{V}OCl_3(PPh_3)_2]$ as starting complex was assessed as well (method *iv*), in the same conditions of method *i* but using a further excess of phosphinethiol (3.5 eq.), since even in this case it acted also as the reducing agent toward rehenium(V). The course and the yield of the reactions were the same as seen for the method *i*. Even in this case, using a lower amount of phosphinothiol cause the formation of other unidentified species (plausibly, the question is

further complicated because in those conditions the reduction of the starting compound could be not complete), and using less dithiocarbamate the formation of the tris-phosphinotiolate pentacoordinated complex was observed.

Eventually, the use of the perrhenate anion was also considered. The procedure used in this work involved the preliminary reduction of the rhenium(VII) with triphenilphosphine in a strong acidic ethanol solution (concentrated chloridric acid in ethanol), followed by neutralization with triethylamine and the addition of the ligand (*v*); the molar ratios ReO_4^-/PS/L were 1/3.5/5 in the case of the use of PS2 and 1/3.5/2.5 in the case of the use of PSiso and PScy. This suggested that the preliminary reduction generate a rhenium(V) species (ideally the complex $[Re^{V}OCl_3(PPh_3)_2]$), so the following reaction with the ligands could be the same as *iv*.

All the complexes were purified by dry column flash chromatography. Extreme care was taken in the chromatographic purification of complexes **7** and **8**, performing the procedure under inert nitrogen (or argon) atmosphere, because the contact with silica gel on open air lead to a degradation process (not investigated in this work) in which the compounds quickly and quantitatively turns from green to red. Since TLC and ESI(+) mass spectrometry data indicated quantitative conversion of the starting compound in most cases, the decrease in final yields was essentially due to the purification procedure.

4.1.3 CHARACTERIZATION OF THE RHENIUM AND TECHNETIUM-99g COMPLEXES

All the complexes were fully characterized by elemental analysis, ESI(+) mass spectrometry, multinuclear NMR and cyclic voltammetry. X-ray diffraction analysis was performed on suitable single crystals of compounds **1**, **2**, **7** and **9**. Elemental analysis of chromatographic purified or crystallized products confirm the given formulae, indicating the absence of crystallization solvents.

Electrospray Ionization Mass Spectrometry. All the mass spectra showed the monocationic $[M(PS)_2(L)]^+$ (M^+) species as common feature (Figure 24A), indicating the extraction of an electron rather than a protonation; plausibly, the positive capillary voltage, set to 4.3 kV, oxidized the M(III) metal center to the M(IV) without any changes in the coordination sphere. In

the cases of **5** and **6**, the spectra showed the bicationic, monoprotonated $[M + H]^{2+}$ species (due to the presence of a tertiary alkyl-amino group in the dithiocarbamate moiety), which is predominant with respect to the M^+ ion (Figure 24B and C). **3** is the only compound that underwent a fragmentation, and its spectrum displayed two ions (Figure 24D): one is the M^+ generated from the oxidation process (m/z = 903, 52% relative abundance), and the other is the $[M - 194]^+$ fragment (m/z = 709, 100% relative abundance). The latter could be reasonably assigned to the $[Re(PS2)_2(SH)]^+$ species, resulting from the electron extraction along with the loss of the neutral adamantil-isothiocyanate, that is not detectable in the ESI(+) spectrum. This type of fragmentation is in accordance with one of the possible dithiocarbamate decomposition processes, which involve the reaction sketched in Figure 25[67]. Anyway, the further elucidation of this proposed fragmentation is out of the scope of this work.

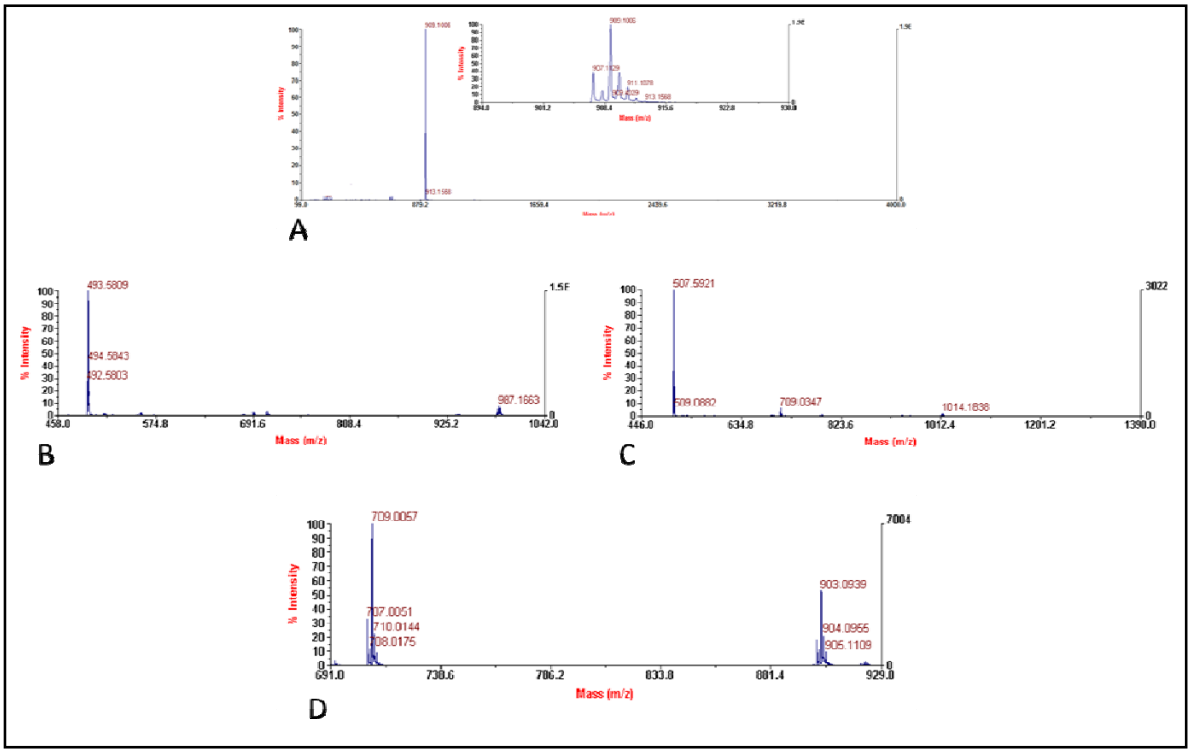

Figure 24: mass spectra of compounds **2** (A), **5** (B), **6** (C) and **3** (D).

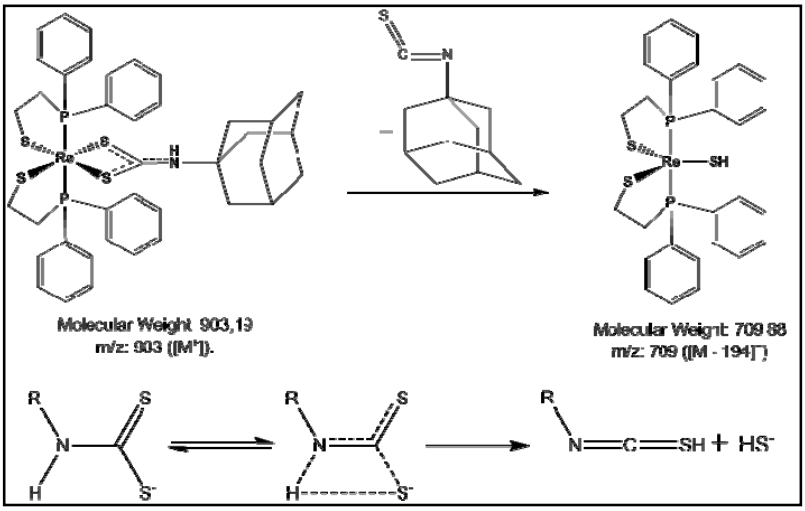

Figure 25: proposed fragmentation for complex **3** (top), in accordance with a previously reported degradation mechanism of monoalkyl dithiocarbamates.

NMR. ^{31}P, ^{1}H and ^{13}C NMR spectra at 298 K in dichloromethane-d_4 have been collected, and 2D experiments (COSY, TOCSY, HMQC, HMBC and NOESY) were performed for the complete assignment of the proton and carbon signals. The spectra of all the complexes gave sharp peaks in a narrow window typical of diamagnetic species.

Most of the ^{31}P spectra show a singlet at δ 23.77-27.04 ppm (Re-complexes) and 64.28-69.75 ppm (Tc-complexes). In certain cases the signal being broad or very broad (complex **8**: δ 23.77 ppm, $\Delta\nu_{1/2}$ ca. 65 Hz; complexes **9**: δ 64.28 ppm, $\Delta\nu_{1/2}$ ca. 270 Hz; complex **10**: 69.75 ppm, $\Delta\nu_{1/2}$ ca. 700), or even splitted in two different signals very close each other (complex **5**: δ 26.77 and 26.99 ppm; complex **6**: δ 25.70 and 25.76 ppm). Broadening of the signals for technetium complexes (**9** and **10**) cannot be discussed only in terms of scalar coupling with the quadrupole nucleus ^{99g}Tc, because the proton spectra do not show so much broad lines. Broadening or splitting of the signals could instead indicate a slowdown of certain molecular motions responsible of the switching between different conformations, in which the two phosphorous nuclei within the complex are magnetically unequivalent. At 298 K, for those complex could be $k < \text{or} << \Delta\omega$ (where k is the kinetic constant of the motion and $\Delta\omega$ is the difference between the Larmor frequencies of the nuclei in the different conformations). The elucidation of the nature of these molecular motions is out of the scope of this work.

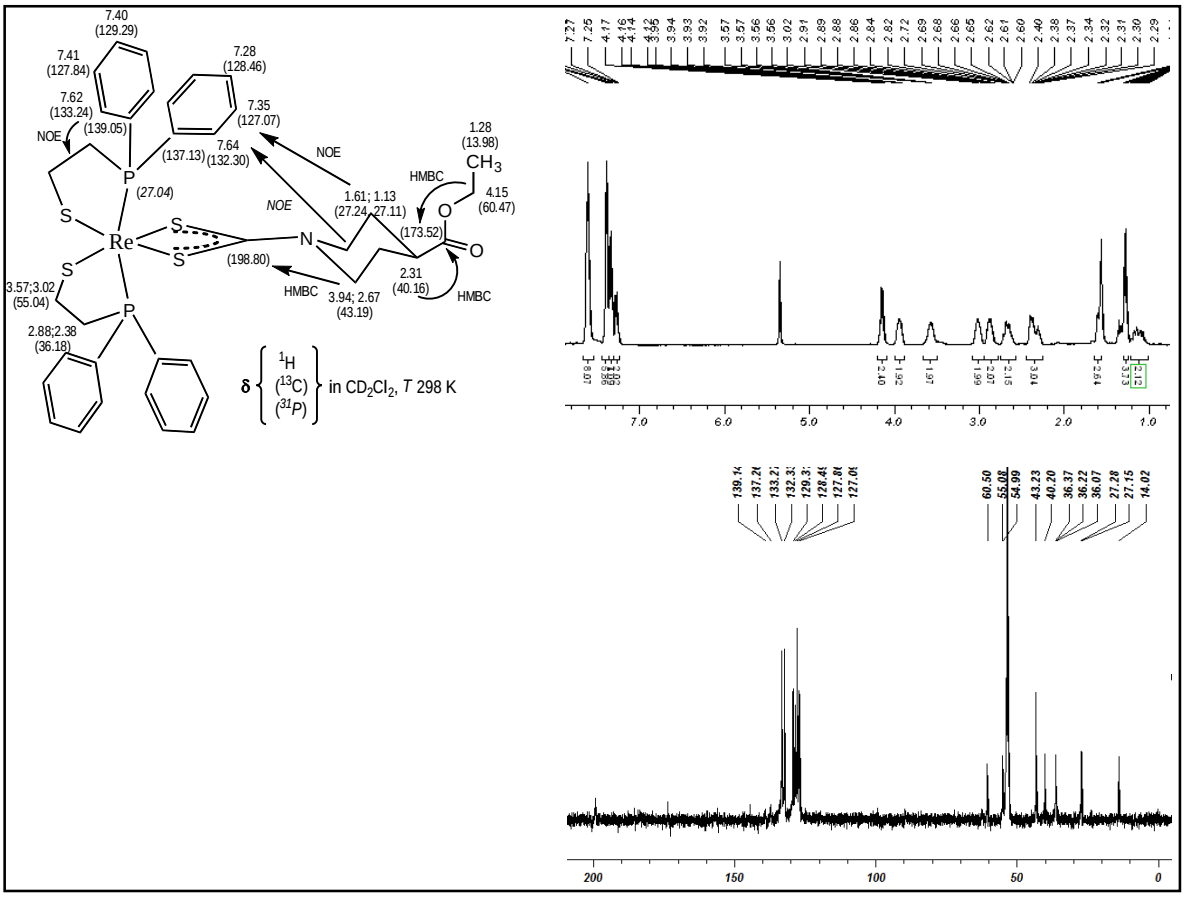

Figure 26: as an example, schematic representation of the complex **2** with most of the NMR data from mono- and bidimensional spectra, along with an overview of ^{1}H and ^{13}C spectra, are here given. Note: dithiocarbamate and quaternary aromatic carbons are derivable from HMBC spectrum only.

^{1}H NMR spectra clearly display different sets of signals corresponding to phosphinothiolate and dithiocarbamate ligands. As an example, in Figure 26 proton and carbon spectra of complex **2** are presented, along with a schematic representation of the molecule including most of the NMR data from mono- and bidimensional spectra. The ^{1}H NMR spectrum is very informative. It shows four set of aromatic protons centered at δ 1.27, 1.34, 1.39 and 1. ppm (*p'*, *m'*, *p* + *m* and *o* + o' relative integration 2:4:6:8, 20 H in total). The two aromatic rings at each phosphorous atoms are magnetically unequivalent. The aliphatic region displays the signals generated by the methylene protons of the phosphinothiolates and the dithiocarbamate protons. The former give rise to a *pattern* of four multiplets at δ 2.38, 2.88, 3.02 and 3.57 ppm, due to the fact that the protons within each methylene group are not magnetically equivalent. This feature is distinctive

and basically conserved among all the complexes. The dithiocarbamate moiety in compound **2** originates a quite complex set of multiplets, in which it is possible to distinguish the axial protons (δ 1.13, 2.31 and 2.67 ppm), the equatorial protons (δ 1.61 and 3.94 ppm), and those of the ethoxycarbonyl moiety (δ 2.31 and 4.15 ppm). NOESY spectrum shows a dipolar interaction between the axial protons at δ 1.13 and 1.61 and the PS2 phenyl protons in *meta* position.

Similar features are observable in the spectra of the other complexes, in accordance with the relative structures. For complexes **7**, **8** and **10** the aliphatic region is more crowded, due to the presence of the signals of the cyclohexyl- and isopropyl- substituents at the P atom of PScy and PSiso.

Cyclic Voltammetry. All the obtained complexes were found to be indefinitely stable in open air and in dichloromethane solution. Cyclic voltammetry was used to thoroughly probe the electronic properties of all the complexes, assessing their redox stability. Data are reported in Figure 27 and cyclic voltammograms of **1** and **9** are shown as examples. For all the complexes two reversible one-electron oxidations were observed, and only **9** displayed a reversible one-electron reduction. The oxidations were assigned by coulombmetric experiments to the formation of M(IV) and M(V), while the reduction was assigned to the Tc(III)/Tc(II) couple.

X-ray Crystallography. X-ray quality single crystals of complexes **1**, **2**, **7**, and **9** were obtained by slow diffusion of n-hexane into saturated dichlorometane solutions. The crystal structures are shown in Figure 28, whereas the main crystallographic data and selected bond distances and angles are listed in Table 3 and 4 respectively. At a glance, it can be seen that the triclinic crystals of **1** and **9** are isomorphic and isostructural.

In all cases, the metal center lies in a distorted trigonal prism environment realized by the four sulfur and the two phosphorus atoms. The geometry of the complexes were confirmed by comparison with the structure of $[Re(S_2CPh)(S_3CPh)_2]$[57a], taken as trigonal prism template, using the molecule overlay feature of *Mercury*[68]. It shows that the "inner cores" are essentially identical and superimposable. The RMS deviations for the overlays of all the coordination sphere atoms (including the metal) are within 0.1-0.2 Å.

The structures exhibit an overall "*butterfly*" shape mainly determined by the phosphinothiolate ligands occupying four of the six coordination position around the metal

atom. The phosphorus P(1) and P(2) donors are placed in *trans* to each other with P(1)–M–P(2) equal to 172.5°, 178.2°, 170.89° and 172.5° in **1**, **2**, **7** and **9** respectively.

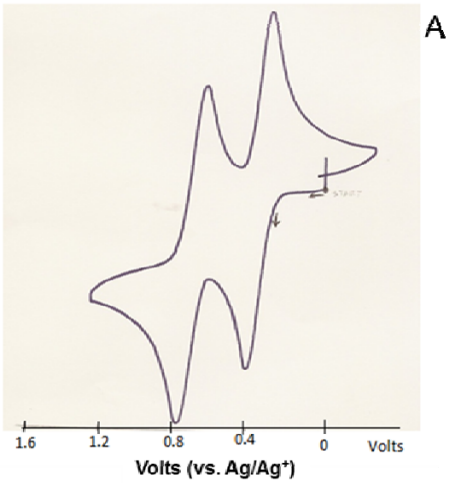

		$E_{M(III)/M(II)}$	$E_{M(III)/M(IV)}$	$E_{M(IV)/M(V)}$
$[Re(PS2)_2(L1)]$	1		-0,31	0,05
$[Re(PS2)_2(L2)]$	2		-0,29	0.09[a]
$[Re(PS2)_2(L3)]$	3		-0,32	0,03
$[Re(PS2)_2(L4)]$	4		-0,24	0,12
$[Re(PS2)_2(L5)]$	5		-0,38	b
$[Re(PS2)_2(L6)]$	6		-0,39	c
$[Re(PScy)_2(L1)]$	7		-0,49	0,1
$[Re(PSiso)_2(L1)]$	8		-0,51	0,08
$[^{99g}Tc(PS2)_2(L1)]$	9	-1.88	-0,33	0,11
$[^{99g}Tc(PSiso)_2(L1)]$	10		-0,41	0,2

[a]Irreversible process (by changing the potential scan speed from 200 to 500 mV/s the corresponding anodic wave was never observed)
[b, c] Reversible processes but the complex undergoes a chemical transformation.

Figure 27: cyclic voltammogram of complex **1** (A) and (**9**) and voltammetric data for all the complexes referenced to the Fc/Fc^+ couple. Data recorded at 200 mV/sec, in dry and degassed dichlorometane with 0.1 M TBAP supporting electrolyte, Pt disk working electrode, Ag wire quasi-reference electrode.

The two phosphinothiolate and the dithiocarbamate ligands define, respectively, two five- and a four-membered rings around the metal center. The two five-membered rings are here designated as P(1) ring (which comprises the P(1) atom) and P(2) ring (which comprises the P(2) atom). Almost all of them assume an *envelope* conformation. In **1**, this arrangement is nearly ideal, with C(1) and C(3) at the flap, while in the corresponding technetium complex **9**, P(2) is almost in the *half chair* shape; in complex **7**, P(2) is definitely in a *half chair* conformation, with P(2) and C(3) at the opposite side of the ideal plane, whereas P(1) has an *envelope* shape with P(1) at the flap; in **2**, both rings are in the *envelope* arrangement (C(1) and C(3) at the flap), but

showing a little twisting. The four-membered rings defined by the M, S(1), S(2) and C(5) atoms is planar in all the complexes.

Table 3: Crystallographic Data for the two complexes $[Re(PS2)_2(L1)]$ (1), $[Re(PS2)_2(L2)]$ (2), $[Re(PScy)_2(L1)]$ (7) and $[^{99g}Tc(PS2)_2(L1)]$ (9).

	1	**2**	**7**	**9**
Empirical formula	$C_{33}H_{36}NP_2S_4Re$	$C_{37}H_{42}NO_2P_2S_4Re$	$C_{33}H_{60}NP_2S_4Re$	$C_{33}H_{36}NP_2S_4Tc$
Formula weight	823.01	909.10	847.20	734.77
Wavelength (Å) / Temperature (K)	0.71073 / 296.0	0.71073 / 296.0	0.71073 / 293	0.71073 / 294.1
Crystal system	triclinic	monoclinic	triclinic	triclinic
Crystal size	0.25 × 0.18 × 0.15	0.30 × 0.08 × 0.08	0.20 × 0.15 × 0.10	0.40 × 0.32 × 0.22
Space group	*P* – 1 (No. 2)	*P* $2_1/c$ (No. 14)	*P* – 1 (No. 2)	*P* – 1 (No. 2)
a (Å)	9.9336(1)	10.6162(1)	9.993(2)	9.9059(4)
b (Å)	11.2215(3)	18.9895(2)	10.779(3)	11.2652(5)
c (Å)	15.3854(5)	19.7505(2)	17.715(3)	15.4555(5)
□ (deg)	74.413(3)		97.09(3)	74.017(3)
□ (deg)	85.808(3)	105.180(1)	98.05(2)	85.992(3)
□ (deg)	86.609(3)		97.68(2)	86.651(3)
Volume ($Å^3$)	1646.12(9)	3842.7(1)	1852.7(7)	1652.6(1)
Z (molecules/unit cell)	2	4	2	2
Calculated density (Mg m^{-3})	1.660	1.571	1.519	2.215
Absorption coefficient, μ (cm^{-1})	4.07	3.496	36.15	1.214
F(000)	820	1824	868	1134
Independent (unique) reflections / R_{int}	7538 / 0.028	9479 / 0.029	6816 / 0.016	13481 /0.061
Observed reflections [$I > 2□(I)$]	6062	7456	6724	8622
Data / parameters / restraints	7538 / 370 / 0	9479 / 382 / 13	6816/ 370 / 0	13481/ 367 / 0
Goodness–of–fit [a] on F^2	0.881	1.071	1.254	0.972
Final *R* indices [$I > 2□(I)$]	R_1 [b] = 0.0261;	R_1 [b] = 0.0275;	R_1 [b] = 0.0299;	R_1 [b] = 0.0464;
	wR_2 [c] = 0.0464	wR_2 [c] = 0.0668	wR_2 [c] = 0.0777	wR_2 [c] = 0.0998
Largest difference peak and hole (e$Å^{-3}$)	0.848 and –1.430	1.216 and –0.770	1.035 and –0.572	0.929 and –0.685

The coordination sphere comprises three different types of bonds: M–P, M–$S_{thiolate}$, and M–$S_{dithicarbamate}$. While the distances are virtually identical *within* a type of bond, the main variations are observed *between* the different types: the bond distances ranges are 2.349(1)–2.387(1), 2.2431(6)–2.266(1) and 2.507(1)–2.5481(6) for M–P, M–$S_{thiolate}$, and M–$S_{dithicarbamate}$ respectively. These differences seems to be basically in accordance with those observed in the complexes $[M^{III}(R\text{-}PhCS_3)_2(R\text{-}PhCS_2)]$, $[M^{III}(R\text{-}PhCS_3)_2(Et_2NCS_2)]$, $[^{99g}Tc^{III}\{Ph_2P(C_6H_4S\text{-}o\}_3]$ and $[^{99g}Tc^{III}\{Ph_2P(C_6H_4NH\text{-}o\}_2\{Ph_2P(C_6H_4NH_2\text{-}o\}]$ discussed in the Aim section. Even in the cases here reported, the two identical ligands (phosphinothiolates) appears to be strongly bound to the metal center while the bond distances between the metal and the third ligand (dithiocarbamate) are considerably longer.

With respect to the dithiocarbamate ligand, it is interesting to note that in all the complexes the two C–S bond lengths are nearly identical and close to the C–S single bond, and the short C–N bond indicates a high degree of double bond character. This suggests a greater contribution of the structure (IV) of the four possible resonance structures shown in Figure 29.

Table 4: Selected Bond Lengths (Å)

	1	**2**	**7**	**9**
M–S(1)	2.546(1)	2.518(1)	2.520(1)	2.5481(6)
M–S(2)	2.524(1)	2.507(1)	2.520(1)	2.5242(6)
M–S(3)	2.251(1)	2.259(1)	2.259(1)	2.2431(6)
M–S(4)	2.266(1)	2.262(1)	2.256(1)	2.2656(6)
M–P(1)	2.363(1)	2.350(1)	2.380(1)	2.3708(6)
M–P(2)	2.368(1)	2.349(1)	2.387(1)	2.3732(6)
S(3)–C(4)	1.835(3)	1.857(4)	1.848(5)	1.835(3)
S(4)–C(2)	1.848(3)	1.851(3)	1.858(5)	1.846(3)
P(1)–C(1)	1.829(3)	1.842(4)	1.846(5)	1.839(3)
P(2)–C(3)	1.841(3)	1.846(3)	1.850(5)	1.845(3)
S(1)–C(5)	1.703(3)	1.696(4)	1.695(5)	1.711(3)
S(2)–C(5)	1.700(3)	1.703(4)	1.705(5)	1.701(3)
N–C(5)	1.330(4)	1.334(4)	1.336(6)	1.322(3)

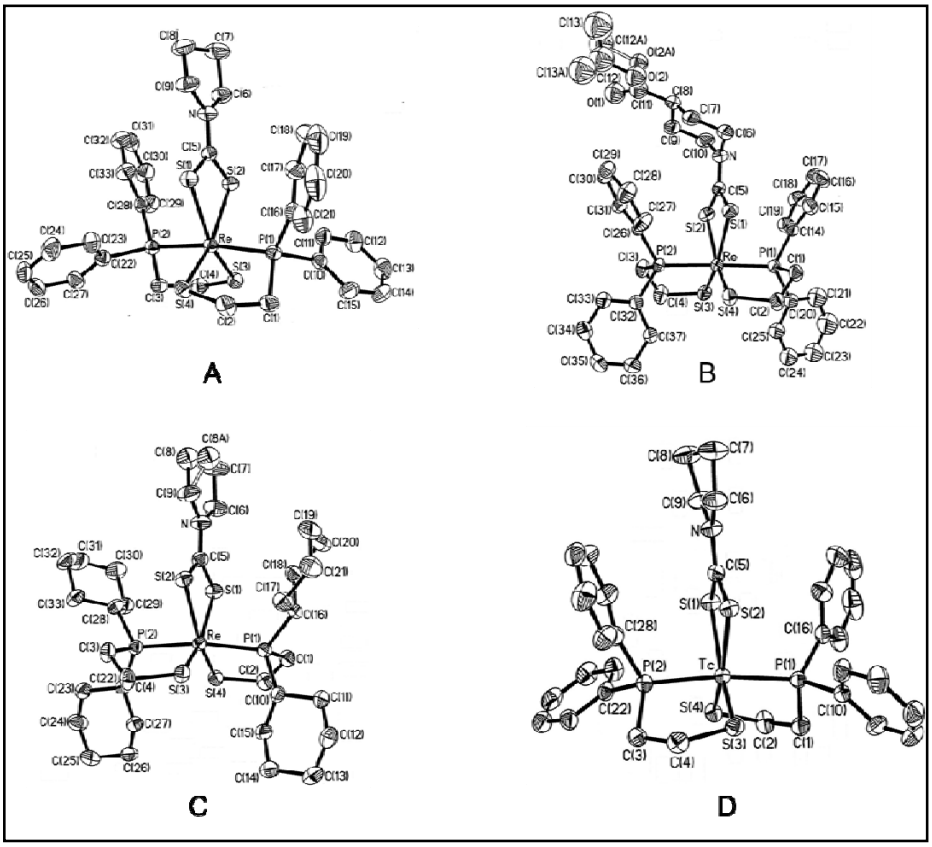

Figure 28: ORTEP diagrams of complexes **1** (A), **2** (B), **7** (C) and **9** (D).

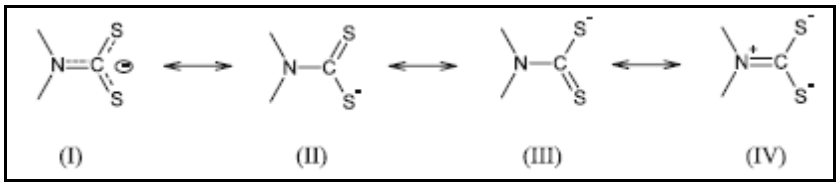

Figure 29

4.1.4 SYNTHESIS AND EVALUATION OF THE ^{99m}Tc-RADIOLABELED COMPLEXES OF THE GENERAL FORMULA [$^{99m}Tc^{III}(PSiso)_2(L)$]

Radiosynthesis. Four radiolabeled compounds of the type [^{99m}Tc(PSiso)$_2$(L)] have been prepared and evaluated *in vitro* and *in vivo* on healthy Sprague Dawley rats. PSiso-complexes have been chosen because previous studies showed that the presence of aromatic rings in the structure (which are in PS2 ligand) leads to poor pharmacodynamic properties, especially an unacceptably high liver uptake. The complex [^{99m}Tc(PSiso)$_2$(L1)] (**11**) was selected as prototype

compound for the pilot study. The synthesis was carried out as outlined in Figure 30A, according to a one-pot procedure: a $Na^{99m}TcO_4$ saline solution (freshly eluted from the generator) was added to a Pyrex® vial containing an hydroalcoholic solution of all the other reagents ($SnCl_2$, used as reducing agent, and the ligands). The solvent was an EtOH/saline mixture (79/21) and the total volume was 1.650 ml. HPLC was used to follow the reaction, as well as to determine the chemical identity of the formed ^{99m}Tc-complex by comparison with the corresponding ^{99g}Tc-analogue **9**; RCY (radiochemical yield, expressed as percentage), was estimated by integration of chromatographic peaks (Figure 30B).

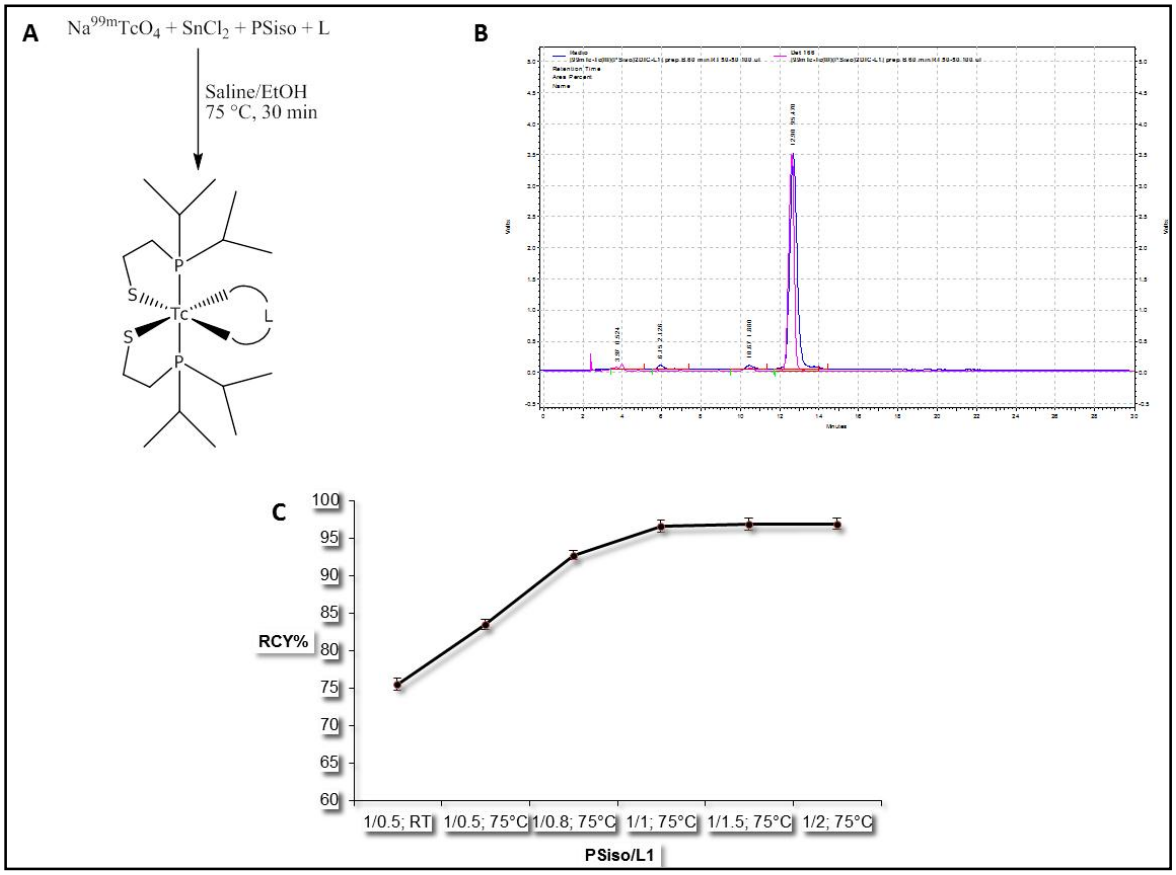

Figure 30: A) synthesis of [$^{99m}Tc^{III}(PSiso)_2(Ln)$] complexes (scheme). B) RP-HPLC chromatogram of [$^{99m}Tc^{III}(PSiso)_2(L1)$]: comparison of [$^{99m}Tc^{III}(PSiso)_2(L1)$] (blue trace) and the [$^{99g}Tc^{III}(PSiso)_2(L1)$] analogue (pink trace); chromatographic conditions: see the Experimental section. C) RCY% variation for the synthesis of [$^{99m}Tc^{III}(PSiso)_2(L1)$] as a function of the ligand concentration ratio (PSiso/L1), with: [PSiso] = 3.4 x 10^{-3} M; 30 min reaction time; temperature as indicated in the graph (RT = room temperature); ethanol/saline mixture (about 79/21) as solvent (1.650 ml total volume).

Fixing the reaction time at 30 min and PSiso concentration at 3.4 x 10^{-3} M, (equal to 1 mg in the total volume), the RCY has been optimized considering the temperature and the amount of L1 ligand (in terms of PSiso/L1 concentration ratio, [PSiso]/[L1]) as variables (Figure 30C). In these conditions, a high yield (96.07% ± 1,62) was achieved heating the mixture at 75 °C and using at least a 1/1 ratio of ligands ([PSiso] = [L1] = 3.4 x 10^{-3} M; L1 amount was equal to 0.92 mg of L1 in the same total volume). Formation of a small amount of radioactive by-products was detected in HPLC profiles. Those compounds were not characterized, but there are some indications about their possible nature. Following the same reaction procedure but using only PSiso as ligand (without L), a mixture of radiolabeled compounds was obtained, which HPLC profile (evaluated under the same chromatographic conditions) showed peaks exactly coincident with those observed as impurities in the chromatogram of the desired complex (Figure 31). Adding at this point the L ligand (carrying out a two-step labeling) the formation of the final mixed complex was observed, but some impurities still remained; quantitative formation was never achieved by increasing the amount of L ligand, neither with the one pot procedure nor with the two-step protocol.

Radiolabeling efficiency. The radiolabeling efficiency of the ligands has been evaluated (Figure 32). In detail, ligands concentrations were gradually decreased following the standardized one pot procedure and keeping the same reaction conditions previously described, and RCYs at 30 min were determined by HPLC. The ligands showed a relatively low efficiency, since the RCY was higher than 90% only with concentration in the order of 10^{-3} M (3.4 x 10^{-3} M and 1.7 x 10^{-3} M).

Synthesis in water medium. Use of water as solvent for labeling is required for *in vivo* use (see Introduction). Thus, another aspect that has been considered in this preliminary study is the possibility to perform the labeling in a totally aqueous medium (saline solution). Since neither PSiso nor the final complex are water soluble, a co-solubilizing agent, such as a cyclodextrin, is required; a 10 mg/ml saline solution of γ-cyclodextrin was used. The RCYs were in the range 96% – 91%, see Table 5.

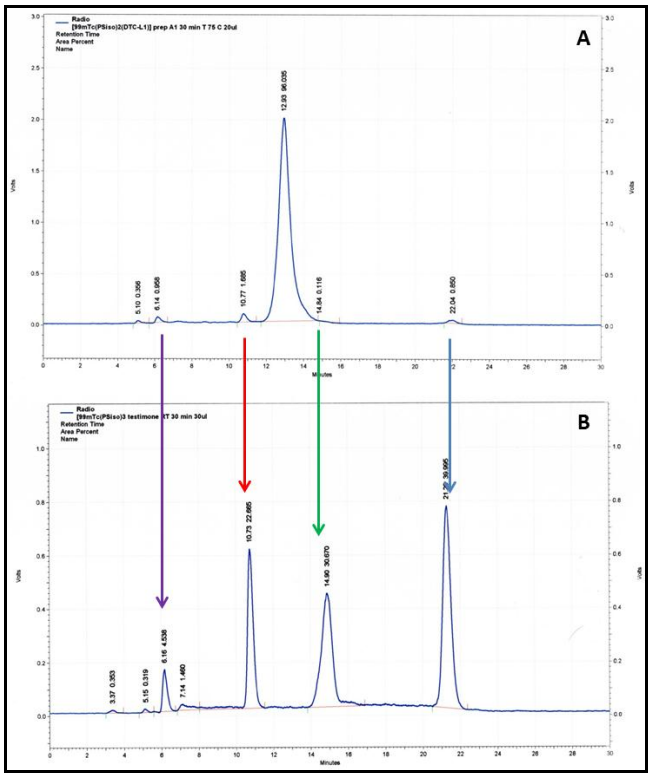

Figure 31: A) RP-HPLC chromatogram of [$^{99m}Tc^{III}(PSiso)_2(L1)$]. B) RP-HPLC chromatogram (same conditions of A) of the crude product obtained performing the labeling with PSiso ligand only. Note that the impurities visible in A are perfectly coincident with most of the B chromatogram peaks.

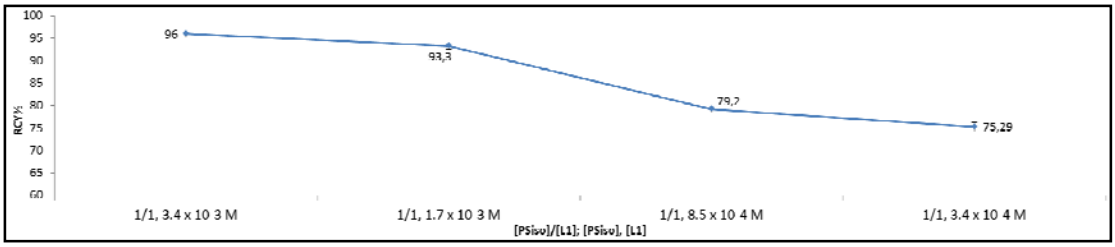

Figure 32: RCY% variation (for the synthesis of [$^{99m}Tc^{III}(PSiso)_2(L1)$]) as a function of the ligands concentrations. The concentrations were gradually scaled down keeping the ratio [PSiso]/[L1] = 1. The reaction conditions were: ethanol/saline mixture (about 79/21) as solvent (1.650 ml total volume), temperature 75 °C and 30 min reaction time.

Basing on all these results, [$^{99m}Tc(PSiso)_2(L2)$] (**12**), [$^{99m}Tc(PSiso)_2(L3)$] (**13**) and [$^{99m}Tc(PSiso)_2(L4)$] (**14**) has been prepared. Data are reported in Table 5. The RCYs are referred to reactions conducted under the conditions described in the Experimental section. The RCY for

13 was not acceptable, and no variation of the RCY was observed changing the reaction conditions (ligand concentration and ligand molar ratio, pH and reaction time). All the compounds were found to be lipophilic, as expected, with logP values in the range of 1.52 – 3.18.

Table 5: HPLC data for the obtained ^{99m}Tc(III)- complexes.

Complexes	**HPLC, R_t**		**RCY%**		**LogP**
	^{99g}Tc-complexes	^{99m}Tc-complexes	Method A	Method B	
$[Tc^{III}(PSiso)_2(L1)]$	12.65 ± 0.05	13.04 ± 0.29	96.07 ± 1,62	96.09 ± 0.29	3.18
$[Tc^{III}(PSiso)_2(L2)]$	—	11.26 ± 0.30	94.14 ± 2.69	91.23 ± 0.13	2.27
$[Tc^{III}(PSiso)_2(L3)]$	—	11.23 ± 0.21	80.45 ± 0.89	—	2.20
$[Tc^{III}(PSiso)_2(L4)]$	—	12.89 ± 0.53	94.51 ± 0.79	93.24 ± 0.54	1.52

HPLC: RP Symmetry C8 (5.0 µm, 100 Å, 4.6 × 250 mm) column with RP C8 Guard precolumn. Mobile phase: A = aqueous ammonium acetate 0.01 M (pH = 7), solvent B = acetonitrile; 0 – 30 min B = 90% (isocratic), 1 ml/min.

In vitro stability studies. Stability studies were performed on the HPLC-purified compounds, using HPLC to evaluate the radiochemical purity (RP, expressed as percentage RP%) of the compounds over time. The radiocomplexes remained stable in their reaction mixture for at least 24 h after labeling. Same occurrence was observed for HPLC-purified compounds dissolved in EtOH or in PBS with 10% EtOH. In both cases the incubation temperature was set at 37 °C (Figure 33). Challenge experiments with Cysteine (Cys), glutathione (GSH) and ethylenediaminotetraacetic acid (EDTA) have also been performed. HPLC-purified complexes were incubated with the transchelating agent at 37 °C for 24 h. All the complexes were stable toward transchelation with Cysteine and GSH within 3 hours; the formation of a more hydrophilic compound was observed in the HPLC profile of the complexes after 24 h, reasonably as consequence of a reaction with the challenge agent. Anyway, RPs% were never reduced to less than 60%. The inertness toward EDTA is uncertain, since the retention times did not change but the peaks have become considerably broad. As an example, the stability of **11** was also evaluated at different pH: 1.5 (aqueous HCl), 7.4 (phosphate buffer 0.2 M) and 12 (aqueous NaOH). The complex was unstable in the acidic medium (Figure 34).

In vivo biodistribution studies. Tissue distribution in male Sprague Dawley rats of the obtained complexes was investigated. Results, expressed as percentage of dose per gram (% ID/g), are reported in Tables 6-9. Figure 35 shows liver, spleen, intestine, kidney and brain uptakes over time. The complexes were rapidly cleared from the blood (less than 2% ID/g at already 2 min post-injection), and mostly uptaken by the liver and the spleen. Intestine uptake gradually increased within 2 hours, and the final retained activity was relatively high for **11** and**13** (about 13% ID/g), and quite low for **12** and **14** (about 3% ID/g). Kidney uptakes were very low, as well as the renal clearances. A very small amount of the injected activity was excreted in the urine; in the case of **11**, **13** and **14**, the urine collected at 2 h post-injection had a HPLC-detectable radioactivity, so they were analyzed and the chromatograms revealed a peak coincident with the native compound. This means that a very little amount of the injected activity is excreted without being metabolized, but in the majority is eliminated by the hepatobiliary system: this could explain the increasing of the activity in the intestine. Finally, no brain uptake was observed, indicating that these compounds do not cross the ematoencephalic barrier.

4.2 DISCUSSION

In general, asymmetric hexacoordinated complexes of the general formula $[M^{III}(PS)_2(L)]$ have been easily obtained through different synthesis methods in moderate to high yield. The one pot reactions indicate that the stability of the final product is the driving force towards selective formation of the mixed hexacoordinated $M^{III}P_2S_4$ arrangement, when a mixture of ligands co-exist in the reaction mixture. The presence of the tris-phosphinotiolate pentacoordinated complex $[M^{III}(\kappa S,\kappa P\text{-}PS)_2(\kappa S\text{-}PS)]$[2] in the final product when not enough excess of dithiocarbamate is used (see above) indicates that its formation competes with the quantitative formation of the $[M^{III}(PS)_2(L)]$ complex. Reasonably, this means that the formation of the stable

[2] Only $[Re^{III}(\kappa S,\kappa P\text{-}PS2)_2(\kappa S\text{-}PS2)]$ was isolated and characterized (data compared with those published by Maina et al.). Other $[M^{III}(\kappa S,\kappa P\text{-}PS)_2(\kappa S\text{-}PS)]$ were only detected by mass spectrometry; however we are quite sure that the observed species were those types of pentacoordinated complexes.

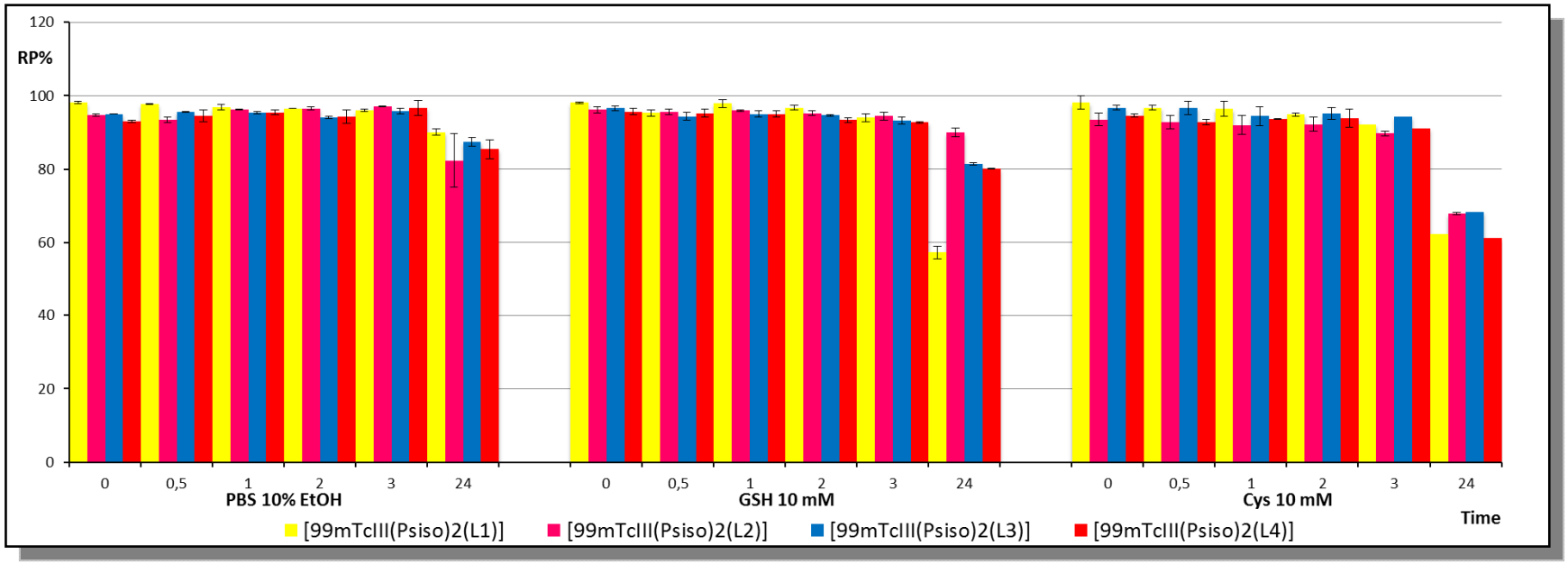

Figure 34: *In vitro* stability of ^{99m}Tc(III) complexes evaluated at 37°C for 24 h in PBS 10% EtOH and toward transchelation with GSH 10 M and Cys 10 M.

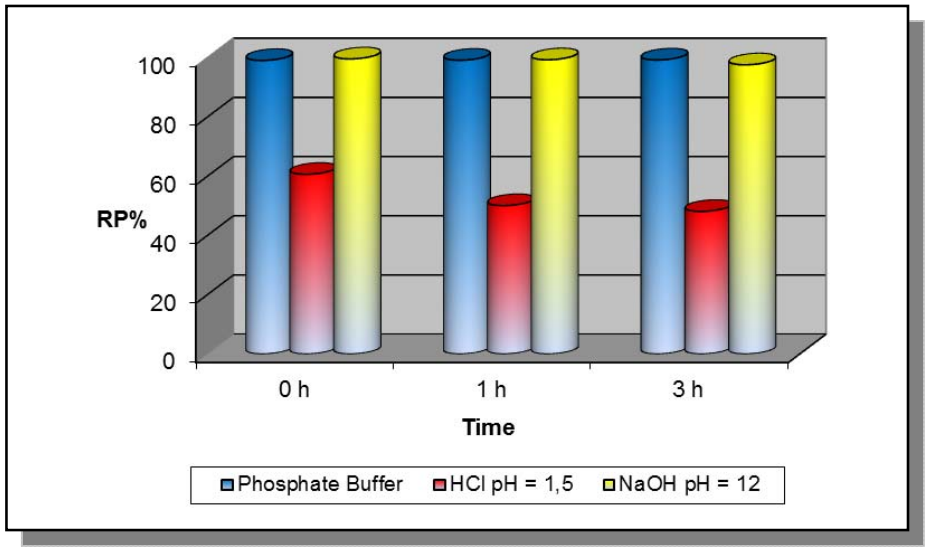

Figure 35: *In vitro* stability of [^{99m}Tc^{III}(PSiso)$_2$(L1)] complexes evaluated at 37°C within 3 h at different pH (phosphate buffer 0.1 M, pH = 7.4; HCl 0.1 M pH = 1.5 and NaOH 0.1 M pH = 12)

Table 6: Biodistribution data of [$^{99m}Tc^{III}(PSiso)_2(L1)$] in male Sprague–Dawley rats.

Organ	2 min	20 min	60 min	120 min
Blood	1,74 ± 0,40	0,73 ± 0,17	0,81 ± 0,17	0,48 ± 0,11
Brain	0,10 ± 0,03	0,05 ± 0,01	0,04 ± 0,01	0,03 ± 0,00
Heart	0,88 ± 0,21	0,74 ± 0,02	1,14 ± 0,02	1,15 ± 0,18
Lungs	4,19 ± 1,12	2,25 ± 0,56	2,64 ± 0,18	2,05 ± 0,42
Liver	9,43 ± 2,56	9,41 ± 0,37	9,54 ± 0,07	8,83 ± 0,42
Spleen	12,22 ± 3,16	10,34 ± 3,72	10,28 ± 2,12	6,30 ± 0,41
Kidney	1,28 ± 0,25	0,96 ± 0,00	1,55 ± 0,07	1,47 ± 0,00
Stomach	0,20 ± 0,02	0,34 ± 0,09	0,39 ± 0,09	0,82 ± 0,53
Intestine	0,45 ± 0,14	3,62 ± 0,31	8,92 ± 1,64	13,05 ± 1,03
Pancreas	0,27 ± 0,06	0,30 ± 0,01	0,34 ± 0,09	0,45 ± 0,03
Muscle	0,08 ± 0,00	0,12 ± 0,00	0,19 ± 0,01	0,21 ± 0,06
Bone	0,21 ± 0,00	0,22 ± 0,00	0,37 ± 0,03	0,34 ± 0,02
Urine	0,00 ± 0,00	0,00 ± 0,00	0,18 ± 0,23	0,24 ± 0,27

Table 7: biodistribution data of [$^{99m}Tc^{III}(PSiso)_2(L2)$] in male Sprague–Dawley rats.

Organ	2 min	10 min	20 min	60 min	120 min
Blood	1,88 ± 0,36	0,69 ± 0,03	0,55 ± 0,02	0,49 ± 0,16	0,40 ± 0,22
Brain	0,08 ± 0,01	0,04 ± 0,00	0,05 ± 0,00	0,04 ± 0,01	0,05 ± 0,00
Heart	0,73 ± 0,15	0,57 ± 0,07	0,51 ± 0,08	0,65 ± 0,09	0,50 ± 0,00
Lungs	2,31 ± 0,06	1,47 ± 0,12	1,43 ± 0,09	1,33 ± 0,01	1,09 ± 0,10
Liver	8,91 ± 0,13	9,83 ± 0,61	8,12 ± 0,06	8,12 ± 0,01	7,70 ± 0,35
Spleen	9,36 ± 9,28	11,96 ± 0,80	7,27 ± 2,41	5,47 ± 2,77	3,77 ± 0,81
Kidney	0,56 ± 0,12	0,51 ± 0,05	0,54 ± 0,09	0,65 ± 0,11	0,93 ± 0,01
Stomach	0,14 ± 0,01	0,32 ± 0,09	0,30 ± 0,17	0,28 ± 0,01	0,27 ± 0,09
Intestine	0,15 ± 0,06	1,36 ± 0,48	0,98 ± 0,03	3,11 ± 0,13	2,52 ± 1,11
Pancreas	0,21 ± 0,09	0,25 ± 0,02	0,23 ± 0,04	0,31 ± 0,01	0,28 ± 0,03
Muscle	0,05 ± 0,01	0,06 ± 0,01	0,08 ± 0,01	0,11 ± 0,00	0,13 ± 0,02
Bone	0,21 ± 0,04	0,22 ± 0,04	0,22 ± 0,02	0,23 ± 0,01	0,20 ± 0,02
Urine	0,00 ± 0,00	0,01 ± 0,01	0,02 ± 0,02	0,04 ± 0,01	0,05 ± 0,02

Table 8: Biodistribution data of [$^{99m}Tc^{III}(PSiso)_2(L3)$] in male Sprague–Dawley rats.

Organs	2 min	20 min	60 min	120 min
Blood	1,50 ± 0,03	0,76 ± 0,01	0,71 ± 0,02	2,02 ± 2,27
Brain	0,08 ± 0,00	0,07 ± 0,00	0,05 ± 0,00	0,04 ± 0,01
Heart	1,13 ± 0,10	1,02 ± 0,08	1,25 ± 0,09	0,88 ± 0,00
Lungs	1,88 ± 0,37	1,52 ± 0,16	1,61 ± 0,19	1,01 ± 0,03
Liver	7,02 ± 1,02	6,57 ± 0,09	6,18 ± 0,70	4,01 ± 0,03
Spleen	7,43 ± 3,05	7,72 ± 1,23	3,68 ± 0,07	2,68 ± 0,93
Kidney	2,90 ± 0,14	2,56 ± 0,20	2,75 ± 0,01	2,20 ± 0,04
Stomach	0,37 ± 0,01	0,56 ± 0,06	0,92 ± 0,36	0,76 ± 0,28
Intestine	0,62 ± 0,10	1,40 ± 0,73	6,65 ± 3,41	8,25 ± 3,57
Pancreas	0,47 ± 0,05	0,49 ± 0,11	0,44 ± 0,02	0,42 ± 0,01
Muscle	0,15 ± 0,03	0,16 ± 0,02	0,16 ± 0,01	0,15 ± 0,01
Bone	0,36 ± 0,03	0,38 ± 0,03	0,41 ± 0,08	0,31 ± 0,01
Urine	0,00 ± 0,00	0,01 ± 0,01	0,71 ± 0,22	0,15 ± 0,05

Table 9: Biodistribution data of [$^{99m}Tc^{III}(PSiso)_2(L4)$] in male Sprague–Dawley rats.

Organ	2 min	10 min	20 min	60 min	120 min
Blood	0,96 ± 0,17	0,67 ± 0,11	0,88 ± 0,20	0,98 ± 0,11	1,02 ± 0,44
Brain	0,05 ± 0,01	0,04 ± 0,00	0,07 ± 0,00	0,06 ± 0,00	0,06 ± 0,01
Heart	0,25 ± 0,02	0,30 ± 0,00	0,29 ± 0,03	0,41 ± 0,03	0,46 ± 0,09
Lungs	1,03 ± 0,20	0,77 ± 0,06	1,01 ± 0,23	1,07 ± 0,11	1,18 ± 0,27
Liver	10,01 ± 0,36	6,98 ± 2,25	10,10 ± 0,74	8,59 ± 0,11	8,75 ± 3,24
Spleen	11,21 ± 3,18	9,18 ± 1,77	10,33 ± 2,64	5,56 ± 0,42	6,34 ± 1,06
Kidney	0,50 ± 0,01	0,54 ± 0,02	0,55 ± 0,02	0,65 ± 0,06	0,96 ± 0,38
Stomach	0,16 ± 0,05	0,28 ± 0,10	0,19 ± 0,01	0,40 ± 0,01	0,37 ± 0,03
Intestine	0,10 ± 0,00	0,20 ± 0,02	0,66 ± 0,02	1,60 ± 1,20	2,86 ± 0,92
Pancreas	0,13 ± 0,01	0,15 ± 0,02	0,13 ± 0,00	0,17 ± 0,01	0,29 ± 0,19
Muscle	0,05 ± 0,00	0,05 ± 0,00	0,05 ± 0,00	0,07 ± 0,01	0,08 ± 0,02
Bone	0,26 ± 0,01	0,21 ± 0,00	0,23 ± 0,03	0,26 ± 0,01	0,36 ± 0,10
Urine	0,00 ± 0,00	0,08 ± 0,05	0,06 ± 0,08	0,14 ± 0,00	0,16 ± 0,16

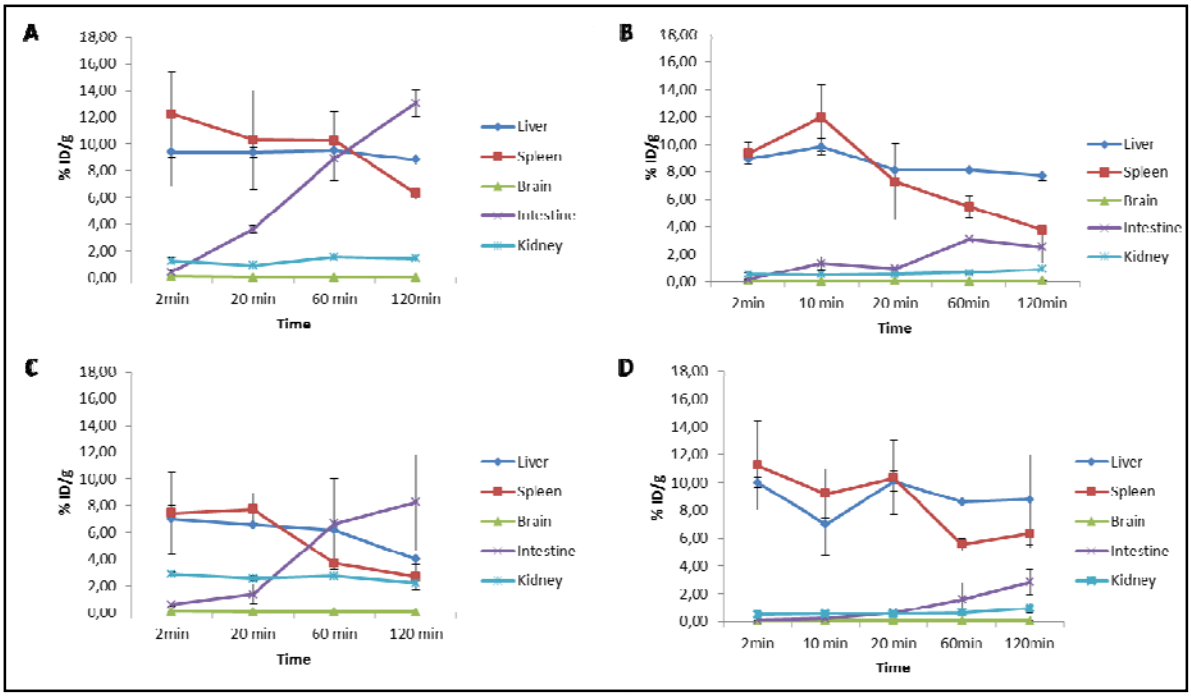

Figure 37: liver, spleen, intestine, kidneye and brain distribution of the complexes over time. A: $[^{99m}Tc^{III}(PSiso)_2(L1)]$; B: $[^{99m}Tc^{III}(PSiso)_2(L2)]$; C: $[^{99m}Tc^{III}(PSiso)_2(L3)]$; D: $[^{99m}Tc^{III}(PSiso)_2(L4)]$.

moiety $[M^{III}(\kappa S,\kappa P\text{-}PS)_2]^+$ is straightforward, but the third coordinating position is subject to an exchange equilibrium in which PS and L are in competition. This result shows as the dithiocarbamate is able to replace the monodentate phosphinothiol ligand in the pentacoordinated complex $[M^{III}(\kappa S,\kappa P\text{-}PS)_2(\kappa S\text{-}PS)]$, as distinctly observed in the case of the reaction between L1 and $[M^{III}(\kappa S,\kappa P\text{-}PS2)_2(\kappa S\text{-}PS2)]$ as an example. This occurrence is notable since Maina et al. reported that the preparation of $[Re^{III}(PS2)_2(SR)]$ complexes by transchelation of $[Re^{III}(\kappa S,\kappa P\text{-}PS2)_2(\kappa S\text{-}PS2)]$ with a generic aliphatic or aromatic thiol is not possible, due to the inability of the thiol to exchange with the phospinothiolate[(61)]. This result clearly suggests as an appropriate selection of the chelating system allows to obtain new series of asymmetrical complexes containing on $[Re^{III}(\kappa S,\kappa P\text{-}PS)_2]^+$ moiety.

As expected on the basis of previous investigations on isostructural technetium and rhenium systems, rhenium complexes are generally easier to oxidize. However, in this case this behavior is heavily affected by the phosphinothiolate. In fact, complex **1** and **9** are equally stable, showing almost superimposable cyclic voltammograms, whilst **8** is easier to oxidize by 100 mV

than the corresponding Tc-complex **10**. Furthermore, the latter complex is easier to oxidize by 100 mV than the analogue complex **9** (in which the phosphinothiolate is arylic), whereas **7** and **8**, in both which the phosphinothiolate is completely alkylic, has approximately the same potential. Finally, **1** is more stable than **7** and **8** by 180 and 200 mV respectively. These data indicate that alkyl-phosphinothilates decrease the redox stability of the M(III) complexes determining a greater oxidizability. Even though no quantitative estimation of the σ/π-properties of the used phosphinothiols has been done neither here nor before, PScy and PSiso should reasonably be more electron-rich ligands and stronger σ-donors with respect to PS2, and for this reason should efficiently stabilize the electron-poor M(IV). On the other hand, the phenyl-substituted phosphinothiol PS2 should be a better π-acid and therefore better stabilize the electron-rich M(III) state. This behavior is more evident in the case of complex **9**, which is the only one that shows a reduction process to the Tc(II) state: the higher stabilizing effect of the phosphinothiol, combined to the greater stability of technetium at low oxidation states compared to rhenium, allows the reduction of the complex.

Crystal structures of **1**, **2**, **7** and **9** confirm the mononuclear nature, the hexacoordination and the distorted octahedral geometry, all of which were expected. Stoichiometry of the ligands and bond distances within the coordination sphere are basically in accordance with those observed in the complexes $[M^{III}(R\text{-}PhCS_3)_2(R\text{-}PhCS_2)]$, $[M^{III}(R\text{-}PhCS_3)_2(Et_2NCS_2)]$, $[^{99g}Tc^{III}\{Ph_2P(C_6H_4S\text{-}o\}_3]$ and $[^{99g}Tc^{III}\{Ph_2P(C_6H_4NH\text{-}o\}_2\{Ph_2P(C_6H_4NH_2\text{-}o\}]$ discussed in the Aim section. In fact, the two identical ligands (phosphinothiolates in this work) appears to be strongly bound to the metal center, while the bond distances between the metal and the third ligand (here dithiocarbamate) are considerably longer. These structural features strongly support the model previously proposed (see Aim section), in which two identical ligands provide two apical trans-positioned π-acceptor donors, connected with two strong cis-positioned σ-donors, whereas the third different ligand, characterized by an electronic conjugation within the two donor atoms, binds the metal with quite long bond distances.

At tracer level, $[^{99m}Tc(PSiso)_2(L)]$ complexes (**11**-**14**) are obtainable in high radiochemical yield following a simple one-pot procedure. Results indicated that it is also possible to perform the labeling in a totally aqueous media by using γ-ciclodextrin. The complexes were stable in

physiological pH (PBS solution with 10% EtOH) and toward transchelation with glutathione and cysteine. Hence, the $[^{99m}Tc^{III}(PS)_2]$– building block is very stable and potentially suitable for a $^{99m}Tc^{III}$-based radiopharmaceutical. Despite these significant outcomes, the biodistribution in rats of all tracers was found to be not remarkable, since liver and spleen uptakes were too high and no other interesting tissue distribution features were displayed (especially no BBB penetration occurred). The high liver uptake could be owing to the strong lipophilicity of the complexes. Thus, the $[^{99m}Tc(PSiso)_2(L)]$ complexes here reported are still not eligible for imaging purposes. All of them are basically *metal essential*, and it is evident that their physicochemical characteristics do not impart to themselves useful biodistribution features. On one hand, a number of structural modification should be done to achieve better pharmacokinetical properties. In particular, the ligands should include hydrophilic groups in order to decrease the lipophilicity and, confidently, lead to a reduction of the liver uptake. On the other hand, an interesting approach could be focusing on the evaluation of a $[M^{III}(PS)_2]$-based target-specific, through the conjugation of the L ligand with a biomolecule. In this context, ligands L4-6 contain the 2-methoxyphenylpiperazine moiety, which displays a potent and specific affinity for 5-HT_{1A} receptors and has already been considered as a targeting biomolecule for ^{99m}Tc-complexes in an our previous work[(64)]; however, even though we have no information about the binding properties of $[^{99m}Tc(PSiso)_2(L4)]$, biodistribution profile clearly indicates that it is not adequate for the 5-HT_{1A} receptor imaging. For this reason, tracers comprising L5 and L6 should be considered and tested. However, labeling experiments showed that dithiocarbamates provide a quite low specific activity (a relatively large amount of ligand must be used to obtain the final compound). This might limit but not excludes the possibility of applying $[^{99m}Tc^{III}(PS)_2]$– building block to the preparation of target-specific radiotherapeutical agents. In this context, the selection of other types of L ligands, which of course should afford higher specific activity, must be considered for further progress of this work.

5. CONCLUSION

A new series of hexacoordinate asymmetrical $[M^{III}(PS)_2(L)]$ (M = Re, ^{99g}Tc; PS = PS2 or PSiso; L = DTCn or MPy) complexes have been prepared and fully characterized. They were stable in all the investigated conditions. These compounds represent a good model for the development of novel $^{99m}Tc/^{186/188}Re$-agents useful in theragnostic applications. Their asymmetry allows a good modulation of the biological and pharmacokinetical behavior of the final compounds through appropriate modifications of the coligand L and using chemically different phosphinotiolates (such as PS2 and Psiso); derivatizations of L can also be used to introduce a biologically active molecule in order to obtain target specific radiolabeled compounds. Studies are currently in progress in order to transfer this technology at tracer level.

On these basis, stable $[^{99m}Tc^{III}(PSiso)_2(L)]$ radiotracers have been prepared in high radiochemical yield following a one-pot procedure in both hydroalcoholic and totally aqueous (with γ-ciclodextrin) solvent. Despite the significant outcomes, biodistribution in healthy rats showed very high liver and spleen uptakes, and no other interesting tissue distribution features were displayed. So, the complexes here presented are still not eligible for imaging purposes. The $[^{99m}Tc^{III}(PS)_2]$– building block is very stable and potentially suitable for a $^{99m}Tc^{III}$-based radiopharmaceutical, but a number of structural modification should be done to achieve better pharmacokinetical properties. An interesting option could be also focusing on the evaluation of $[M^{III}(PS)_2]$-based target-specific agents through the conjugation of the L ligand with a suitable biomolecule. In this context, the relatively low specific activity of the dithiocarbamate shuld be taken in account, because it might limit (but not excludes) this approach. The selection of other types of more efficient L ligands must be considered for further progress of this work.

6. REFERENCES

1. Liu S., The role of coordination chemistry in the development of target specific radiopharmaceuticals, 2003, *Chem. Soc. Rev.*, 33, 445–461.
2. Rey A. M., Radiometal Complexes in Molecular Imaging and Therapy, 2010, *Curr. Med. Chem.,* 17, 3673-3683.
3. Bhattacharyya S., Dixit M., Metallic radionuclides in the development of diagnostic and therapeutic radiopharmaceuticals, 2011, *Dalton Trans.*, 40, 6112-6128.
4. Liu S., Chakraborty S., ^{99m}Tc-centered one-pot synthesis for preparation of ^{99m}Tc radiotracers, 2011, *Dalton Trans.*, 40, 6077-6086.
5. Volkert W.A., Hoffman T.J., Therapeutic radiopharmaceuticals, 1999, *Chem. Rev.*, 99, 2269-2292.
6. Neves M., Kling A., Oliveira A., Radionuclides used for therapy and suggestion for new candidates, 2005, *J. Radioanal. Nucl. Chem.*, 266(3), 377–384.
7. Majkowska A., Neves M., Antunes I., Bilewicz A., Complexes of low energy beta emitters ^{47}Sc and ^{177}Lu with zoledronic acid for bone pain therapy., 2009, *Appl. Radiat. Isot.,* 67, 11-13.
8. Dilworth J. R., Parrott S. J., The biomedical chemistry of technetium and rhenium, 1998, *Chem. Soc. Rev.*, 27, 43-55.
9. (a) Harper P. V., Beck R., Charleston D., Lathrop K. A., Optimalization of a scanning method using ^{99m}Tc, *Nucleonics*, 1964, 22(1), 50-54; (b) Banerjee S., Pillai M. R. A., Ramamoorthy N., Evolution of Tc-99m in diagnostic radiopharmaceuticals, *Semin. Nucl. Med.*, 2001, 31, 260-277; (c) Jain D., Technetium-99m labeled myocardial perfusion imaging agents, *Semin. Nucl. Med.*, 1999, 29, 221-236.
10. Alberto R., in: McCleverty J. A., Mayer T. J. (Eds.), Comprehensive Coordination Chemistry II, vol. 5, 2004, Elsevier, 2004, starting p. 127.
11. Bandoli G., Mazzi U., Roncari R., Deutsch E., Crystal structure of technetium compounds, 1982, *Coord. Chem. Rev.*, 44(2), 191-227.

12. Tisato F., Refosco F., Bandoli G., Structural survey of technetium complexes, 1994, *Coord. Chem. Rev.*, 135/136, 325-397.
13. Bandoli G., Dolmella A., Porchia M., Refosco F., Tisato F., Structural overview of technetium compounds (1993-1999), 2001, *Coord. Chem. Rev.*, 2001, 214, 43-90.
14. Bandoli G., Dolmella A., Tisato F., Agostini S., Structural overview of technetium compounds (2000-2004), *Coord. Chem. Rev.*, 2006, 250, 561-573.
15. Banerjee S. R., Maresca K.P., Francesconi L., Vaillant J., Babich J. W., Zubieta J., New directions in the coordination chemistry of ^{99m}Tc: a reflection on technetium core structures and a strategy for new chelate design, 2005, *Nucl. Med. Biol.*, 32, 1-20.
16. Boschi A., Duatti A., Uccelli L., Development of technetium-99m and rhenium-188 radiopharmaceuticals containing a terminal metal-nitrido multiple bond for diagnosis and therapy, 2005, *Top. Curr. Chem.*, 252, 85-115.
17. Alberto R., Schibli R., Waibel R., Abram U., Schubiger A. P., . Basic aqueous chemistry of $[M(OH_2)_3(CO)_3]$+ (M=Re,Tc) directed towards radiopharmaceutical application, 1999, *Coord. Chem. Rev.* 190/192, 901-919.
18. Bigott H. M., Parent E., Luyt L. G., Katzenellenbogen J. A., Welch M. J., Design and Synthesis of Functionalized Cyclopentadienyl Tricarbonylmetal Complexes for Technetium-94m PET Imaging of Estrogen Receptors, *Bioconjug. Chem.*, 2005, 16, 255-264.
19. Abram U. and Alberto R., Technetium and Rhenium - Coordination Chemistry and Nuclear Medical Applications, 2006, *J. Braz. Chem. Soc.,* 17, 8, 1486-1500.
20. Bolzati C., Refosco F., Marchiani A., Ruzza P.,^{99m}Tc-Radiolabelled Peptides for Tumour Imaging: Present and Future, 2010, *Curr. Med. Chem.*, 2010, 17, 2656-2683.
21. Eckelman W. C., Richards, P., Meinken G., Chemical state of technetium-99m in biomedical products II. Chelation of reduced technetium with DTPA [penthanil], 1972, *J. Nucl. Med*. 13, 577-581.
22. (a) Pinkerton T. C., Heinemann W. R., Deutsch E., Separation of technetium hydroxyethylidene diphosphonate complexes by anion-exchange high performance liquid chromatography, 1980, *Anal. Chem.*, 52, 1106-1110; (b) Wilson G. M., Pinkerton T. C., Determination of charge and size of technetium diphosphonate complexes by anion-exchange liquid chromatography, *Anal. Chem.*, 1985, 57, 246-253.

23. Libson K., Deutsch, E., Barnett B.L., Structural characterization of a technetium-99-diphosphonate complex. Implications for the chemistry of technetium-99m skeletal imaging agents, 1980, *J. Am. Chem. Soc.*, 102, 2476-2478.
24. (a) Deutsch E., Glavan K. A., Sodd V. J., Nishiyama H., Ferguson D. L., Lukes S. J., Cationic Tc-99m complexes as potential myocardial imaging agents, 1981, *J. Nucl. Med.*, 22, 897-907; (b) Deutsch E., Bushong W., Glavan K. A., Elder R. C., Sodd V. J., Scholz K. L., Fortman D. L., Lukes S. J., Heart imaging with cationic complexes of technetium, 1981, *Science*, 214, 85-86; (c) Gerson M. C., Deutsch E., Nishiyama H., Libson K. F., Adolph R. J., Grossmann L. W., Sodd V. J., Fortman D. L., Vanderheyden J. L. E., Williams C. C., Saenger E. L., Myocardial perfusion imaging with ^{99m}Tc-DMPE in man, 1983, *Eur. J. Nucl. Med.*, 8, 371-374.
25. Abrams M. J., Davison A., Jones A. G., Costello C. E., Pang H., Synthesis and characterization of hexakis(alkylisocyanide) and hexakis(arylisocyanide) complexes of technetium(I), 1983, *Inorg. Chem.*, 22, 2798; (b) Jones A. G., Abrams M. J., Davison A., Brodack J. W., Toothaker A. K., Adelstein S. J., Kassis A. I., 1984, Biological studies of a new class of technetium complexes: the hexakis(alkylisonitrile)technetium(I) cations, *Nucl. Med. Biol*., 11, 225.
26. Treher E. N., Francesconi L. C., Gougoutas J. Z., Malley M. F., Nunn A. D., Monocapped tris(dioxime) complexes of technetium(III): synthesis and structural characterization of TcX(dioxime)$_3$B-R (X = Cl, Br; dioxime = dimethylglyoxime, cyclohexanedione dioxime; R = CH_3, C_4H_9), 1989, *Inorg. Chem.*, 28, 3411-2416.
27. (a) Pasqualini R., Duatti A., Synthesis and characterization of the new neutral myocardial imaging agent [^{99m}TcN(Hnoet)$_2$](Hnoet = N-ethyl-N-ethoxydithiocarbamato), 1992, *J. Chem. Soc. Chem. Commun.*, 18, 1354-1355; (b) Pasqualini R., Duatti A., Bellande E., Comazzi V., Brucato V., Hoffschir D., Fagret V., Comet M., Bis(dithiocarbamato) nitrido technetium-99m radiopharmaceuticals: a class of neutral myocardial imaging agents, 1994, *J. Nucl. Med.*, 35, 334-341.
28. (a) Boschi A., Bolzati C., Uccelli L., Duatti A., Benini E., Refosco F., Tisato F., Piffanelli A., A class of asymmetrical nitrido ^{99m}Tc heterocomplexes as heart imaging agents with improved biological properties, 2002, *Nucl. Med. Commun.*, 23, 689–693; (b) Boschi A., Uccelli L., Bolzati C., Duatti A., Sabba N., Moretti E., Di Domenico G., Zavattini G.,

Refosco F., Giganti M., Synthesis and biologic evaluation of monocationic asymmetrical ^{99m}Tc-nitride heterocomplexes showing high heart uptake and improved imaging properties, 2003, *J. Nucl. Med.*, 44, 806–814. (c) Bolzati C., Refosco F., Cagnolini A., Tisato F., Boschi A., Duatti A., Uccelli L., Dolmella A., Marotta E., Tubaro M., Synthesis, solution-state and solid-state structural characterization on monocationic nitrido heterocomplex $[M(N)(DTC)(PNP)]^+$ (M=^{99}Tc, Re; DTC=dithiocarbammate; PNP=heterodiphosphine), 2004, *Eur. J. Inorg. Chem. 9*, 1902–1913.

29. Bolzati C., Cavazza-Ceccato M., Agostini S., Tokunaga S., Casara D., Bandoli G., Subcellular distribution and metabolism studies of the potential myocardial imaging agent $[^{99m}Tc(N)(DBODC)(PNP5)]^+$, 2008, *J. Nucl. Med.*, 49, 1336–1344.
30. Sharp P. F., Smith F. W., Gemmell H. G., Lyall G., Evans N. T. S., Gvosdanovic D., Davidson J., Tyrrell D. A., Pickett R. D., Neirinckx R. D., Technetium-99m HM-PAO stereoisomers as potential agents for imaging regional cerebral blood flow: human volunteer studies, 1986, *J. Nucl. Med.*, 30, 171-177.
31. Edwards D. S., Cheesman E. H., Watson M. W., Maheu L. J., Nguyen S. H., Dimitre L., Nason T., Watson A. D., Walovitch R., in Technetium in Chemistry and Nuclear Medicine, Nicolini M., Bandoli G., Mazzi U. eds., Cortina International: Verona, Italy, 1990, vol. 3, p. 433.
32. (a) Fritzberg A. R., Kasina S., Eshima D., Johnson D. L., Synthesis and biological evaluation of technetium-99m MAG3 as a hippuran replacement, 1986, *J. Nucl. Med.*, 27, 111; (b) Eshima D., Taylor D., Fritzberg A. R., Kasina S., Hansen L., Sorensen J. F., Animal evaluation of technetium-99m triamide mercaptide complexes as potential renal imaging agents, 1987, *J. Nucl. Med.*, 28, 1180.
33. Despopoulos A., A definition of substrate specificity in renal transport of organic anions, 1965, *J. Theor. Biol.*, 8, 163-192.
34. (a) Kung M., Stevenson D. A., Plössl K., Meegalla S. K., Beckwith A., Essam W. D., Mu M., Lucki I., Kung H. F., [^{99m}Tc] TRODAT-1: a novel technetium-99m complex as a dopamine transporter imaging agent, 1997, *Eur. J. Nucl. Med.*, 24, 372-380; (b) Dresel S., Kung M., Plössl K., Meegalla S., Kung H., Pharmacological effects of dopaminergic drugs on in vivo binding of [^{99m}Tc]TRODAT-1 to the central dopamine transporters in rats, 1998, *Eur. J. Nucl. Med.*, 1998, 25, 31-39.

35. (a) Mozley P. D., Schneider J. S., Acton P. D., Plössl K., Stern M. B., Siderowf A., Leopold N. A., Li P. Y., Alavi A., Kung H. F., Binding of [^{99m}Tc]TRODAT-1 to Dopamine Transporters in Patients with Parkinson's Disease and in Healthy Volunteers, 2000, *J. Nucl. Med.*, 41, 584-589; (b) Felicio A. C., Godeiro-Junior C., Shih M. C., Borges V., Silva, S. M., Aguiar P. de C., Hoexter M. Q., Barsottini O. G., Andrade L. A., Bressan R. A., Ferraz H. B., Evaluation of patients with Clinically Unclear Parkinsonian Syndromes submitted to brain SPECT imaging using the technetium-99m labeled tracer TRODAT-1, 2010, *J. Neurol. Sci.*, 15, 64-68.
36. Baulieu F., Bourlier P., Scotto B., Mor C., Eder V., Picon L., De Calan L., Dorval E., Pottier J. M., Baulieu J. M., The value of inmunoscintigraphy in the detection of recurrent colorectal cancer, 2001, *Nucl. Med. Commun.*, 22, 1295-1304.
37. Moffat F., Pinsky C., Hammershaimb L., Petrelli N. J., Patt Y. Z., Whaley F. S., Goldenberg D. M., Clinical utility of external immunoscintigraphy with the IMMU-4 technetium-99m Fab' antibody fragment in patients undergoing surgery for carcinoma of the colon and rectum: results of a pivotal, phase III trial. The Immunomedics Study Group, 1996, *J. Clin. Oncol.*, 14, 2295-2305.
38. Tisato F., Porchia M., Bolzati C., Refosco F., Vittadini A., The preparation of substitution-inert ^{99}Tc metal-fragments: Promising candidates for the design of new ^{99m}Tc radiopharmaceuticals, 2006, *Coord. Chem. Rev.*, 250, 2034–2045.
39. (a) Mundwiler S., Candreia l., Hafliger P., Ortner K., Alberto R., Preparation of no-carrier-added technetium-99m complexes via metal-assisted cleavage from a solid phase, 2004, *Bioconjug. Chem.*, 15, 195–202. (b) Dunn-Dufault R., Pollak A., Fitzgerald J., Thornback J. R., Ballinger J. R., A solid-phase technique for preparation of no-carrier-added technetium-99m radiopharmaceuticals: Application to the streptavidin/biotin system, 2000, *Nucl. Med. Biol.*, 27, 803–807.
40. Deutsch E., Libson K., Vanderheyden J. L., Ketring A. R., Maxon H. R., The chemistry of rhenium and technetium as related to the use of isotopes of these elements in therapeutic and diagnostic nuclear medicine, 1986, *Int. J. Rad. Appl. Instrum.*, B 13, 465–477.

41. A. Duatti, Advances in the chemistry of technetium and rhenium: from ligands and cores to biocomplexes, in: M. Nicolini, U. Mazzi (Eds.), Technetium and rhenium and other metals in chemistry and nuclear medicine, SGE Editorial: Padua, Italy, 1999, pp. 3–17.
42. Seifert S., Heinrich T., Jentschel C., Smuda C., Bergmann R., Pietzsch H. J., Preparation and biological characterization of isomeric Re-188(V) oxocomplexes with tetradentate S-4 ligands derived from meso-dimercaptosuccinic acid for labeling of biomolecules, 2006, *Bioconjug. Chem.*, 17, 1601-1606.
43. Seifert S., Pietzsch H. J., The Re-188(III)-EDTA complex - a multipurpose starting material for the preparation of relevant Re-188 complexes under mild conditions, 2006, *Appl. Radiat. Isotopes*, 64, 223-227.
44. Bolzati C., Boschi A., Uccelli L., Duatti A., Franceschini R., Piffanelli A., An alternative approach to the preparation of Re-188 radiopharmaceuticals from generator produced [(ReO4)-Re-188]-: Efficient synthesis of Re-188(V)-meso-2,3-dimercaptosuccinic acid, 2000, *Nucl. Med. Biol.*, 27, 309-314.
45. Seifert S., Jentschel C., Bergmann R., Pietzsch H. J., Wunderlich G., Kotzerke J., Steinbach J., Very stable Re-188-S4 chelates for labeling biomolecules, 2007, *Nuklearmedizin-Nuclear Medicine*, 46, 181-184.
46. Seifert S., Kunstler J. U., Schiller E., Pietzsch H. J., Pawelke B., Bergmann R., Spies H., Novel procedures for preparing Tc-99m(III) complexes with tetradentate/monodentate coordination of varying lipophilicity and adaptation to Re-188 analogues, 2004, *Bioconjug. Chem*., 2004, 15, 856-863.
47. Boschi A., Bolzati C., Uccelli L., Duatti A., High-yield synthesis of the terminal Re-188-N multiple bond from generator-produced [(ReO4)-Re-188]$^{-}$, 2003, *Nucl. Med. Biol.*, 30, 381-387.
48. Savio E., Gaudiano J., Robles A. M., Balter H., Paolino A., López A. Hermida J. C., De Marco E.; Martinez G., Osinaga E., Knapp Jr. F. F., Re-HEDP: pharmacokinetic characterization, clinical and dosimetric evaluation in osseous metastatic patients with two levels of radiopharmaceutical dose, 2001, *BMC Nucl. Med.*, 2001, 1.
49. Lam M. G., de Klerk J. M., van Rijk P. P., ^{186}Re-HEDP for metastatic bone pain in breast cancer patients, 2004, *Eur. J. Nucl. Med. Mol. Imaging*, 31, S162-S170.

50. Lam M. G.; de Klerk, J. M., van Rijk P. P., Zonnenberg B. A., Bone seeking radiopharmaceuticals for palliation of pain in cancer patients with osseous metastases, 2007, *Anticancer Agents Med. Chem.*, 7(4), 381-97.
51. Paes F. M., Serafini A. N., Systemic metabolic radiopharmaceutical therapy in the treatment of metastatic bone pain, 2010, *Semin. Nucl. Med.*, 40(2), 89-104.
52. Wang S. J., Lin W. Y., Chen M. N.; Hsieh B. T., Shen L. H., Tsai Z. T., Ting G., Knapp Jr. F. F., Radiolabelling of lipiodol with generator-produced ^{188}Re for hepatic tumour therapy, 1996, *Appl. Radiat. Isotop.*, 47, 267-271.
53. (a) Garin E., Denizot B., Noiret N. Lepareur N., Roux J., Moreau M., Herry J. Y., Bourguet P., Benoit J. P., Lejeune J. J., Re-188-SSS lipiodol: radiolabelling and biodistribution following injection into the hepatic artery of rats bearing hepatoma, 2004, *Nucl. Med. Commun*, 25, 1007–1013; (b) Garin E., Noiret N., Malbert C., Lepareur N., Roucoux A., Caulet-Maugendre S., Moisan A., Lecloirec J., Herry J. Y., Bourguet P., Development and biodistribution of ^{188}Re-SSS lipiodol following injection into the hepatic artery of healthy pigs, 2004, *Eur. J. Nucl. Med. Mol. Imaging*, 31, 542-546; (c) Lepareur N., Garin E., Noiret N., Herry J. Y., A kit formulation for the labelling of lipiodol with generator-produced ^{188}Re, 2004, *J Label Compd Radiopharm*, 47, 857–867; (d) Automation of labeling of Lipiodol with high-activity generator-produced ^{188}Re, 2011, *Appl. Radiat. and Isotop.*, 69, 426–430.
54. Sundram F., Chau T. C. M., Onkhuudai P., Bernal P., Padhy, A. K., Preliminary results of transarterial rhenium-188 HDD lipiodol in the treatment of inoperable primary hepatocellular carcinoma, 2004, *Eur. J. Nucl. Med. Mol. Imaging*, 31, 250–257.
55. (a) Lambert B., Bacher K., Defreyne L., Van Vlierberghe H., Jeong J. M., Wang R. F., van Meerbeeck J., Smeets P., Troisi R., Thierens H., De Vos F., Van de Wiele C., Re-188-HDD/lipiodol therapy for hepatocellular carcinoma: an activity escalation study, *Eur. J. Nucl. Med. Mol. Imaging*, 2006, 33**,** 344–352; (b) Lambert B., Bacher K., De Keukeleire K., Smeets P., Colle I., Jeong J. M., Thierens H., Troisi R., De Vos F., Van de Wiele C., Re-188-HDD/lipiodol for treatment of hepatocellular carcinoma: A feasibility study in patients with advanced cirrhosis, 2005, *J. Nucl. Med.*, 46, 1326–1332; (c) Yoon C. J., Chung J. W., Park J. H., Kim Y. I., Lee K. H., Jeong J. M., Paeng J. C., Transcatheter arterial

embolization with ^{188}Rhenium-HDD-labeled iodized oil in rabbit VX2 liver tumor, 2004, *J. Vasc. Interv. Radiol*, 15, 1121–1128.

56. Boschi A., Uccelli. L, Duatti A., Colamussi P., Cittanti C., Filice A., Rose A. H., Martindale A. A., Claringbold P. G., Kearney D., A kit formulation for the preparation of Re-188-lipiodol: preclinical studies and preliminary therapeutic evaluation in patients with unresectable hepatocellular carcinoma, 2003, *Nucl. Med. Commun.*, 25, 691–699.
57. (a) Mevellec F., Roucoux, A., Noiret N., Patin H., Tisato F., Bandoli G., Synthesis and characterization of the bis(trithioperoxybenzoate)(dithiobenzoate)rhenium(III) hetero complex, 1999, *Inorg. Chem. Commun.*, 2, 230–233; (b) Mevellec F., Tisato F., Refosco F., Roucoux, A., Noiret N., Patin H., Bandoli G., Synthesis and Characterization of the "Sulfur-Rich" Bis(perthiobenzoato)(dithiobenzoato)technetium(III) Heterocomplex, 2002, *inorg. Chem.*, 41, 598-601; (c) Lepareur N., Mevellec F., Noiret N., Refosco F., Tisato F., Porchia M., Bandoli G., Synthesis and reactivity of "sulfur rich" Re(III) and Tc(III) complexes containing trithioperoxybenzoate, dithiobenzoate and dithiocarbamate ligands, 2005, *Dalton Trans.*, N 2866-2875.
58. Mevellec F., Roucoux A., Noiret N., Moisan A., Patin H., Duatti A., Synthesis and characterization of new ^{99m}Tc- radiopharmaceuticals with dithiobenzoate derivatives for the study of septic inflammatory processes, *J. Label. Compd. Radiopharm.*, 2003, 46, 319–331.
59. Bolzati C., Refosco F., Tisato F., Bandoli G., Dolmella A., Novel TcP_3X_3 (X = S, O) cores in Tc(III) chemistry, 1992, *Inorg. Chimica Acta*, 7-10.
60. Refosco F., Bolzati C., Moresco A., Bandoli G., Dolmella A., Mazzi U., Nicolini M., Synthesis of Tecnethium Complexes with a P,N Bidentate Phosphine Amine Ligand. Crystal Structure of Bis[(o-amido-phenyl)diphenylphosphine-kN,P]technetium(III) Perchlorate, 1991, *J. Chem. Soc. Dalton Trans.*, 11, 3043-3048.
61. Maina T., Pecorale A., Dolmella A., Bandoli G., Mazzi U., Synthesis and Characterization of 5-Coordinate Rhenium (III) Complexes with 2-(diphenylphosphino)ethanethiolate and Monothiolate Ligands - Crystal Structure of $[Re(Ph_2PCH_2CH_2S)_2(PHCH_2S)]$, 1994, *J. Chem. Soc. Dalton Trans.*, 16, 2437-2443.
62. Tisato F., Refosco F., Bandoli G., Bolzati C., Moresco A., Synthesis and Characterization of Neutral Technetium(III) Complexes with Mixed S, P-Bidentate Phospine-Thiolate Ligands.

Crystal Structure of [Tc(SCH2CH2PPh2)2-(SCH2CH2PPh2O)], 1994, *J. Chem. Soc. Dalton Trans.*, 9, 1453-1461.

63. Dilworth J. R., Griffiths D. V., Parrott S. J., Zheng Y., Synthesis and Characterisation of Rhenium dithiocarbamate complexes. Crystal structure of $[ReO\{O(OH)C_6H_4\}(S_2CNEt_2)_2]$, $[Re\{PPh_2(C_6H_4S\text{-}2)_2\}(S_2CNEt_2)]\cdot Me_2CO$, $[ReO\{PPh\text{-}(C_6H_4S\text{-}2)_2\}(S_2CNEt_2)]$, 1997, *J. Chem. Soc. Dalton Trans.*, 17, 2931-2936.
64. Bolzati C., Salvarese N., Carta D., Refosco F., Dolmella A., Pietzsch H.J., Bergmann R., Bandoli G., Synthesis and biological evaluation of new [Tc(N)(PS)]-based mixed-ligand compounds useful in the design of target-specific radiopharmaceuticals: the 2-methoxyphenylpiperazine dithiocarbamate derivatives as an example, 2010, *J. Biol. Inorg. Chem.*, 16, 1, 137-155.
65. (a) Rouschias G., Wilkinson G., The Preparation and Reaction of Trihalogeno(alkanonitrile)bis(triphenyl-phosphine)rhenium(III) Complexes, 1967, *Inorg. Phys. Theor.*, 993-1000. (b) Archer C. M., Dilworth J. R., Thompson R. M., McPartlin M., Povey D. C., Kelly J. D., The synthesis and reactivity of a new technetium(III) precursor. The crystal structures of (acetonitrile)trichlorobis(tri-m-tolylphosphine)technetium and $[Tc(bipy)_3]^{2+}$ (bipy = 2,2'-bipyridine), 1993, *J. Chem. Soc. Dalton Transactions*., 3, 461-466.
66. Rowbottom J., Wilkinson G., Dithiocarbamate Complexes of Rhenium(V) and (III), 1972, *J. Chem. Soc. Dalton Trans.*, 7, 826-830.
67. Joris S. J., Aspila K. I., Chakrabarti C. L., Decomposition of Monoalkyl Dithiocarbamates, Anal. Chem., 1970, 42, 6, 647-651.
68. Macrae C. F., Bruno I. J., Chisholm J. A., Edgington P. R., McCabe P., Pidcock E., Rodriguez-Monge L.; Taylor R., van de Streek J., Wood P. A., Mercury CSD 2.0 - new features for the visualization and investigation of crystal structures, 2008, *J. Appl. Cryst.*, 41, 466-470.